AFRICA CENTER OF EXCELLENCE FOR WATER MANAGEMENT
ADDIS ABABA UNIVERSITY SCHOOL OF GRADUATE STUDIES
COLLEGE OF NATURAL AND COMPUTATIONAL SCIENCES

PHILOSOPHIAE DOCTOR (Ph.D.) DISSERTATION

ENHANCED CADMIUM REMOVAL FROM AQUEOUS SOLUTIONS BY IMMOBILIZED ACTIVATED CARBON ON TEXTILE-COATED INCLINED PLATES

BY

GILBERT CHIFUNDO THOTHO CHINTOKOMA

A Ph.D. dissertation submitted to the Africa Center of Excellence for Water Management, the School of Graduate Studies of Addis Ababa University, in partial fulfillment of the requirements for the Degree of Doctor of Philosophy in WaterManagement (Water Science and Technology)

September, 2024

Addis Ababa, Ethiopia

Africa Center of Excellence for Water Management
Addis Ababa University
School of Graduate Studies

PHILOSOPHIAE DOCTOR (Ph.D.) DISSERTATION

ENHANCED CADMIUM REMOVAL FROM AQUEOUS SOLUTIONS BY IMMOBILIZED ACTIVATED CARBON ON TEXTILE-COATED INCLINED PLATES

BY

GILBERT CHIFUNDO THOTHO CHINTOKOMA

A Ph.D. dissertation submitted to the Africa Center of Excellence for Water Management, the School of Graduate Studies of Addis Ababa University, in partial fulfillment of the requirements for the Degree of Doctor of Philosophy in Water Management (Water Science and Technology)

DECLARATION

I, Gilbert Chifundo Thotho CHINTOKOMA, (GSR/7765/13), hereby declare that this research dissertation titled "Enhanced Cadmium Removal from Aqueous Solutions by Immobilized Activated Carbon on Textile-coated Inclined Plates" has been developed by myself and has not been submitted to this university or any other institution for the award of any academic qualification. The contents of this dissertation have not been plagiarized, and where the works of other researchers have been used, they have been appropriately cited.

Candidate Name	**Signature**	**Date**
GILBERT CHIFUNDO THOTHO CHINTOKOMA	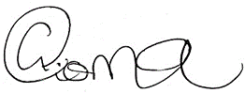	***30 September 2024***

AFRICA CENTER OF EXCELLENCE FOR WATER MANAGEMENT

ADDIS ABABA UNIVERSITY SCHOOL OF GRADUATE STUDIES

ENHANCED CADMIUM REMOVAL FROM AQUEOUS SOLUTIONS BY IMMOBILIZED ACTIVATED CARBON ON TEXTILE-COATED INCLINED PLATES

BY

GILBERT CHIFUNDO THOTHO CHINTOKOMA

A Ph.D. DISSERTATION SUBMITTED

TO

AFRICA CENTER OF EXCELLENCE FOR WATER MANAGEMENT

ADDIS ABABA UNIVERSITY

APPROVED BY BOARD OF EXAMINERS

This is to certify that we have read this PhD research dissertation and that in our opinion; it is fully adequate, in scope and quality, as a PhD dissertation for The Degree of Doctor of Philosophy in Water Management (Water Science and Technology)

Advisor
Name: **Prof. Yonas Chebude** Signature yonaschebude Date: ***30 September 2024***

Co-Advisor
Name: **Dr. Shimelis Kebede** Signature _____ Date: ***30 September 2024***

Examiner
Name: **Prof., Dr.-Ing Esayas Alemayehu** Signature _____ Date: ***30 September 2024***

Examiner
Name: **Prof. Feleke Zwege** Signature _____ Date: _____

Chairperson
Name: **Dr. Beteley Tekola** Signature _____ Date: _____

ABSTRACT

The rapid increase in population and industrial growth has led to the generation of large amounts of wastewater, which in turn has an impact on the water quality. Studies have shown that global increase in industrialization is one of the major contributors of heavy metals in wastewater. Common heavy metals found in wastewater include cadmium, chromium, arsenic, lead, mercury and nickel among others. These metals pose risks to aquatic ecosystems and human health, with potential effects including neurological, cancer and developmental issues. The strict regulations governing wastewater discharge require effective treatment techniques.

Adsorption has gained popularity as one of the methods for water and wastewater treatment owing to its relative simplicity, efficiency and cost effectiveness. Adsorption for water and wastewater treatment has been widely studied over the past decade, and has mainly focused on the use of low-cost renewable adsorbents for pollutants removal. Activated carbon is considered as one of the favorable adsorbents for use in adsorption process due to its enhanced surface area. The use of activated carbon (AC) as an adsorbent in water and wastewater treatment has been limited to laboratory scale due to among other things the powdery form of most activated carbons which pose a number of limitations for industrial application. The use of powdered activated carbon (PAC) is hindered by such challenges as adsorbent-adsorbate separation after adsorption process leading to secondary pollution, and regeneration of the spent adsorbent material which leads to loss of the valuable adsorbent through leaching. Even though granular activated carbon is used to overcome these challenges, its use is only limited to batch and column adsorption configurations. These challenges, along with others discussed in this study have hindered the large-scale implementation of the adsorption technique in wastewater treatment systems.

This study aimed at developing an innovative wastewater treatment process that integrates the inclined plate settlers (IPS) and Composite Adsorbent Coating (CAC) for heavy metal removal from aqueous solutions in a continuous set-up in an effort to boost the use of adsorption for large-scale industrial applications. The first part of this study focuses on the preparation of activated carbon from *Prosopis juliflora* (PJAC) wood by pyrolysis and chemical activation. The objective was to assess its effectiveness as an adsorbent for synthesizing CAC for heavy metal removal. The influence of impregnation ratio (IR), carbonization time (t), and carbonization temperature (T) on the Cd^{2+} percent (%) removal was evaluated using the Box-Behnken Design (BBD) of the Response Surface Methodology (RSM) (Design Expert software version 11).

The results indicated that all the variable preparation factors were significant ($p< 0.05$) in the Cd^{2+} removal by PJAC with T being the most significant ($p < 0.0001$). At the optimum conditions of IR=1.8, T=595 ºC and t=174 min, the model predicted a 99.9% Cd^{2+} removal efficiency while the adsorption experiment obtained a 96.7% removal efficiency, respectively. The SEM images of the optimized PJAC revealed a rough and porous morphological surface with an S_{BET} of 600.4m^2/g and a near neutral pH_{PZC} of 6.92. These findings highlighted the potential of utilising invasive plants like *Prosopis Juliflora* as effective adsorbents for removing heavy metals.

Later the prepared PJAC was then used to prepare the CAC to overcome the challenges associated with powdered activated carbon (PAC) in water and wastewater treatment. CAC was synthesized using a simple sol-gel method for the simultaneous reduction of Cd^{2+} and $Cr_2O_7^{2-}$. The CAC was also characterized by various techniques. Statistical analysis confirmed that pH and contact time significantly ($p < 0.0001$) affected both metal ions removal. Using the optimized conditions (pH=8.5, CAC dosage=0.25, adsorbate concentration=5mg/L, contact time=30 min and temperature=23.73°), the predicted and experimental ion removal efficiencies were 86.86 and 83.98% for Cd^{2+} and 94.26 and 58.08% for $Cr_2O_7^{2-}$, respectively. The Langmuir adsorption isotherm was the best-suited model ($R^2 > 0.99$), while the metal ions removal was regulated by the PSO kinetic model ($R^2 > 0.999$). The batch adsorption process was endothermic and spontaneous, as indicated by thermodynamic values (− ΔG°, +ΔH°, +ΔS°). The study only observed a 10% decline in the Cd^{2+} removal effectiveness of the CAC after three adsorption-regeneration cycles (with 0.1 M HCl of pH 0.3 as the eluent), indicating its stability for heavy metal removal.

The final part of the research aimed at developing an innovative method for treating wastewater, an Inclined Plate Adsorber (IPA). The effects of angle of plate inclination (θ_p), influent flow rate (Q) and adsorbate initial concentration (C_i) on Cd^{2+} percent removal efficiency (%) were studied. At optimized operating parameters (θ=45°, Q=5 ml/min and C_i=1.87 mg/L) the IPA Cd^{2+} predicted (R^2=0.9926) and experimental removal efficiencies were 75.8% and 69.7±4.67%, respectively. The adsorption capacity (mg/g) of IPA calculated using the breakthrough curve analysis (BTCA) was 9.6 mg/g. Comparing IPA performance with a tank without plates and a tank with plain plates, the Cd^{2+} removal efficiencies were 2.4±0.1% and 4.6±1.1%, respectively, confirming that the dominant pollutant removal mechanism in an IPA system is adsorption. Additionally, breakthrough curves were acquired for various Q, C_i, and θ_p. The results underpin the potential of using IPA for industrial wastewater treatment and enhancing the use of adsorption on a larger scale.

Keywords: Adsorption, Breakthrough curve analysis, Composite Adsorbent Coating, Inclined Plate Settler, Optimization, *Prosopis Juliflora,* Synergistic integration

DEDICATION

To the memory of my beloved mother, Mary Nthambala Chintokoma, who died just days before she could witness the completion of this project. However, it is comforting to know that she persevered until just the end, providing the necessary support and encouragement. Until we meet again, may you rest in eternal peace dear *Amama*. I will always miss you.

ACKNOWLEDGEMENT

First and foremost, I thank the Almighty God for His benevolence in bringing me thus far.

I also thank the World Bank for the PhD study scholarship and the Addis Ababa University through the Africa Centre of Excellence for Water Management (ACEWM) for the PhD. study admission.

I would like to express my heartfelt and sincere appreciation to my supervisors Professor Yonas Chebude and Dr. Shimelis Kebede for the endless supervision, guidance, moral support and mentorship throughout the study period. A particular mention goes to Prof. Yonas for being a father figure also, especially when things became rough.

I also thank the Centre for Development Management (CDM) for the opportunity to gain the necessary experience which was a prerequisite for this PhD and for all the support rendered throughout the study period.

I want to thank my family for their prayers, especially my parents, brothers, and sisters. A special thank you to my wonderful daughter for her love and prayers and her endurance during the time I was away.

I would also like to thank my family for their prayers and support throughout the study period. A special feeling of gratitude to my loving parents, Oxford and late Mary, for their words of encouragement and prayers throughout the years. A very special thank you to my wonderful daughter, Elsa, for being a lovely friend and for enduring all the years I was missing for my doctoral program. I love you dearly. *"See what the Lord has done!"*

Finally, I thank my colleagues and friends, too numerous to mention, without whom this work would not have been possible, for their support, counsel, inspiration, unwavering love, and emotional support.

LIST OF PUBLISHED PAPERS

Published papers that form the Ph.D. dissertation

Chintokoma, G.C., Chebude. Y., & Kassahun, S.K (2024). Cd^{2+} removal efficiency of activated carbon from *Prosopis Juliflora*: Optimization of preparation parameters by the Box-Behnken Design of Response Surface Methodology. *Heliyon.* 10(10). https://doi.org/10.1016/j.heliyon.2024.e31357 **(Elsevier)**.

Chintokoma, G.C., Chebude. Y., & Kassahun, S.K., Demesa, A. G., & Koiranen, T. (2024). Sol-gel synthesis of composite adsorbent coating from Prosopis juliflora –activated carbon for simultaneous adsorptive removal of Cd^{2+} and $Cr_2O_7^{2-}$ from wastewater. *AQUA — Water Infrastructure, Ecosystems and Society*, *73*(5), 945–968. https://doi.org/10.2166/aqua.2024.335 **(IWA Publishing)**.

Chintokoma, G.C., Chebude. Y., & Kassahun, S.K., Demesa, A. G., & Koiranen, T. (2024). Synergistic Integration of Inclined Plate Settler (IPS) and Composite Adsorbent Coating (CAC) for the enhanced removal of Cd^{2+} from wastewater. *Applied Water Science*. https://doi.org/10.1007/s13201-024-02292-2 **(Springer Nature)**.

LIST OF TABLES

LIST OF FIGURES

Table of Contents

LIST OF ABBREVIATIONS

AAU	Addis Ababa University
AC	Activated Carbon
ACEWM	Africa Center of Excellence for Water Management
ANOVA	Analysis of Variance
APE	Acrylic Polymer Emulsion
BBD	Box Behnken Design
BET	Brunauer-Emmett-Teller
CAC	Composite Adsorbent Coating
CCF	Cotton Cellulosic Fiber
CNCS	College of Natural and Computational Sciences
DI	Deionized water
DoE	Design of Experiments
DR	Dubinin-Radushkevich
EDX	Energy-dispersive X-ray spectroscopy
EIZ	Eastern Industrial Zone
EM	Elovich Model
FTIR	Fourier Transform Infrared spectroscopy
HCl	Hydrochloric acid
ICP-OES	Inductively Coupled Plasma- Optical Emission Spectroscopy
IP	Intra-Particle diffusion model
IPA	Inclined Plate Adsorber
IPS	Inclined Plate Settler
MCP	Mallard Creek Polymers
NF	Nano-Filtration
PFO	Pseudo-First-Order
$pH_{PZC,}$	Point of Zero Charge
PJAC	*Prosopis Juliflora* Activated Carbon
PSD	Particle Size Distribution
PSO	Pseudo-Second-Order
RO	Reverse Osmosis
RSM	Response Surface Methodology
SEM	Scanning Electron Microscopy
UF	Ultra-Filtration
XRD	X-ray powder diffraction

1. CHAPTER ONE: INTRODUCTION

Chapter Summary

This chapter provides a comprehensive overview of the study. The primary chapter emphasis is on providing the background information of the research by introducing the research area and outlining the rationale for the study. The chapter also outlines the study objectives, research questions, scope, and limitations of the study.

1.1. BACKGROUND INFORMATION

The discharge of substantial quantities of valuable heavy metals into global wastewater systems remains a pressing industrial concern. Industry effluents are the primary source of water pollution issues, mainly because the industrial sector utilizes a tremendous quantity of water while concurrently producing a substantial amount of highly polluted wastewater (Kurkura et al., 2012). The growth of industry has resulted in the increasing availability of heavy metals in industrial effluent (Hussain et al., 2012). The issue of heavy metal pollution has become a major global environmental concern, primarily because of its substantial toxicity and ability to accumulate in the food chain, even at trace amounts (Bahiru, 2020). Toxic heavy metals are a hazard to both animals and people and the environment in general due to their non-biodegradability, extended biological half-lives, and ability to collect in various body regions (Genchi et al., 2020).

Chromium (Cd) and cadmium (Cr) are among the hazardous heavy metals as they both tend to accumulate in the environment and can be found in natural deposits (A. Gupta et al., 2021). The primary sources of toxic Cd and Cr in the aquatic environment are natural, but human activities have caused an increase in their concentrations (M. F. Ahmed & Mokhtar, 2020).

Cd serves as a key constituent in various industrial sectors, including plating, battery manufacturing (specifically for cadmium-nickel batteries), phosphate-based fertilizer manufacture, stabilizer formulation, and alloy development (Demim et al., 2013). According to Genchi et al., (2020), exposure to Cd occurs through a number of pathways including consumption of contaminated water and food, inhalation and smoking. These exposures have been linked to the development of chronic renal failure, cancer, as well as bone demineralization

and fragility in both human and animal populations (Mahdi et al., 2021). Moreover, Cd exposure has been associated with several symptoms, including vitamin D deficiency, respiratory-related ailments, and gastrointestinal disorders that result in the loss of red blood cells. These conditions can impede the proper functioning of calcium in both human and animal bodies (Genchi et al., 2020).

Similarly, Cr is used in such industries as tanneries, electroplating, production of stainless steel and preservatives of wood (Nur-E-Alam et al., 2020). The most common forms of Cr found in wastewaters and the aquatic environment are Cr(III) and Cr(VI), with the latter being more harmful than Cr(III) compounds (Kinuthia et al., 2020), even though the degree to which chromium is mobile and toxic is predominantly determined by its physicochemical speciation (Tian et al., 2022). It is therefore imperative to eliminate these metals from industrial effluent prior to their introduction into aquatic environments, as their detrimental impacts on human health have been unequivocally demonstrated.

Among the available wastewater treatment techniques, adsorption is currently the most frequently utilized method for water purification, because of its high pollutant removal efficiency, simplicity and its potential to treat a large quantity of water in semi-continuous system with acceptable costs (Somma et al., 2021). Over the past decade research on the utilization of low-cost activated carbon prepared using locally available biomass has gained enormous attention in water and wastewater treatment (Tian et al., 2022; Hussain et al., 2021; Somma et al., 2021).

Recent research on adsorption has concentrated on utilizing affordable readily available eco-adsorbents, mainly because the extensive utilization of commercial activated carbon for water and waste treatment is not economically viable, primarily due to its exorbitant initial purchase and operational expenses. One such low cost adsorbent is the invasive *Prosopis Juliflora* (Patnaik et al., 2017). Originally from Peru, *Prosopis Juliflora,* was initially introduced in arid and semi-arid Africa and other regions primarily for land reclamation (Abdulahi et al., 2017). Regrettably, due to its invasive character attributed to several factors, the fast spread of *Prosopis Juliflora* is now regarded as a danger to pastoralist livelihoods in the environment (Sintayehu et al., 2020). Studies undertaken in Ethiopia and other areas has consistently found that the disadvantages of the *Prosopis Juliflora* plant outweigh its benefits (Shiferaw et al., 2019; Patnaik

et al., 2017). Research and policy makers have recommended its effective utilization so as to manage it sustainably.

1.2. RESEARCH PROBLEM AND JUSTIFICATION

Despite having a wide surface area that favors its capacity to adsorb a variety of water contaminants, powdered activated carbon (PAC) typically presents handling challenges, because it generally occurs in powder form (Shamsudin & Shahadat, 2019). Specifically, the direct application of activated carbon in fine particle powdery size causes leaching-related adsorbent loss and also leads to the development of secondary pollutants in treated water/wastewater complicating the separation of pollutant loaded adsorbent from the treated water or wastewater (Azha and Ismail 2017a) including challenges in regeneration, difficulties in recyclability (Gul et al., 2022).

For easy phase separation, the adsorbent material must be coated or immobilized onto a substrate or supporting material. After all the use of supporting materials for adsorption is said to enhance the mechanical strength and binding efficiency of obtained adsorbent (Arifin et al., 2013). As much as Granular Activated Carbon (GAC) has been used to overcome the challenges associated with PAC, however its use is limited to batch and column adsorption configuration only. The bottlenecks inherent in both batch and column adsorption configurations have impeded the implementation of the adsorption technique in large-scale wastewater treatment systems. This has necessitated the need for innovative wastewater treatment systems that enhance the use of adsorption technique for large-scale applications.

Prior researches have examined the use of adsorbents immobilized on a substrate (Azha et al., 2019, 2021; Shamsudin & Shahadat, 2019). These investigations successfully avoided the need for separation techniques, such as centrifugation and filtering, to obtain the final treated effluent. As much as the immobilizing of the adsorbent on a substrate was successful, however, none of these previously cited works have investigated the use of such composite adsorbent material specifically prepared from low-cost adsorbent (e.g. *Prosopis Juliflora*) wood for cadmium removal from aqueous solutions more so using a modified Inclined Plate Settler (IPS) i.e. Inclined Plate Adsorber (IPA).

The use of IPS for turbidity removal or as a pretreatment for other treatments techniques is well documented in the literature (Hu et al., 2022; Kasenene et al., 2021; Chintokoma et al., 2015). Recently IPS has been used in combination with other water and wastewater treatment techniques.

For example, IPS has been used in combination with constructed wetland (Kasenene et al., 2021), electrocoagulation (Hu et al., 2022) and activated carbon sponge tubes (Hyun & Kang, 2023) for turbidity and fecal coliform removal, oil and heavy metal removal and for the treatment of urban stormwater runoff.

However, all these recent studies had the combinations of the techniques in series configurations i.e. one treatment technique after the other in separate treatment units. The current study is unique as it aims at integrating IPS and adsorption in one treatment unit so as to decrease the treatment footprint. Hence, we postulate that the immobilization of activated carbon on inclined plate settlers to make an inclined plate adsorber (IPA) will considerably decrease adsorbent leaching, improve adsorbent recyclability, increase surface area for adsorbent-adsorbate contact and consequently enhance the effectiveness of Cadmium removal. *Prosopis juliflora* is selected in this study as a precursor for preparing activated carbon because it is readily available and is considered an invasive species that is spreading rapidly in many sub-Saharan countries including Ethiopia.

To the best of the author's knowledge, there has been no prior reported work of a heavy metal removal system that integrates IPS and adsorption to make an IPA. By leveraging the synergistic effect of IPS and CAC, this combination may have the following benefits: (a) enhancing the removal efficiency of Cd^{2+} by the synergistic effect of IPS and CAC; (b) reducing the footprint needed for individual adsorption apparatus and settler under the same flow rate; and (c) enhancing the potential of scaling up the system for large-scale wastewater treatment.

To this end, this work was aimed at developing an innovative method for treating wastewater influent by combining the strengths of both IPS and adsorption techniques in one treatment unit termed Inclined Plate Adsorber (IPA). The effects of angle of plate inclination (θ_p), influent flow rate (Q) and adsorbate initial concentration (C_i) on Cd^{2+} percent removal efficiency (%) was studied by employing the Box-Behnken Design (BBD) of the Response Surface Methodology (RSM).

1.3. OBJECTIVES OF THE STUDY

The aim of the study was to develop a novel heavy metal removal system utilising *Prosopis Juliflora* delivered adsorbent immobilized on an inclined plate settler.

1.3.1. General objective

The main objective of the study was to design and optimize an inclined plate settler coupled with adsorption for heavy metal removal from industrial wastewater.

1.3.2. Specific objectives

The following were the specific objectives of the research;

1. To prepare and characterize composite adsorbent coating (CAC) utilizing activated carbon prepared from *Prosopis juliflora* wood for Cd^{2+} removal;
2. To evaluate and optimize Cd^{2+} and $Cr_2O_7^{2-}$ removal efficiency using composite adsorbent coating batch adsorption setup;
3. To design and optimize an inclined plate adsorber for Cd^{2+} removal under continuous adsorption setup;
4. To examine the regenerative properties of the Cd^{2+}-loaded composite adsorbent coating (CAC).

1.3.3. Research questions

The study aimed to address the following research questions:

1. What is the optimum impregnation ratio (IR), carbonization time (t) and carbonization temperature (T) for the pyrolysis of activated carbon from *Prosopis Juliflora* wood (PJAC)?
2. What are the optimum operating conditions for simultaneous removal of chromium and cadmium from wastewater using Composite Adsorbent Coating (CAC)?
3. What is the optimal design parameter in inclined plate settler coupled with CAC (IPA) for the effective removal of Cd^{2+} from wastewater?
4. What are regenerative properties of the Cd^{2+} loaded composite adsorbent coating (CAC).
5. What is the dominant removal mechanism associated with Cd^{2+} removal from wastewater using the IPA?

1.4. SCOPE OF THE STUDY

This study aimed at developing an innovative wastewater treatment prototype that integrates an inclined plate system and adsorption to enhance heavy metal removal from aqueous solutions in a continuous set-up so as to enhance its practicality for large-scale application. The main objective of the study was to design and optimize an inclined plate settler coupled with adsorbent coated plates for heavy metal removal from aqueous media.

The study utilized simulated wastewater, to optimize and prepare PJAC for Cd^{2+} removal as a way of utilizing the invasive *Prosopis Juliflora* wood plant. The prepared PJAC was later used for the preparation of CAC of which its efficiency in heavy metal removal was tested on Cd^{2+} and $Cr_2O_7^{2-}$ metals. These were specifically selected because of their different ionic states so as to evaluate the efficacy of the prepared CAC on both. To this end the CAC Cd^{2+} and $Cr_2O_7^{2-}$ removal adsorption isotherms, kinetics and thermodynamics were evaluated.

The later part of the research aimed at designing and fabricating an innovative IPA system for the removal of Cd^{2+} only due to time constraint. The optimum geometric and operational parameters for Cd^{2+} removal was determined together with CAC adsorption capacity at both breakthrough and saturation time. Additionally, breakthrough curves were acquired for various flow rates (Q), cadmium influent concentrations (C_o), and plate inclination angles (θ). A comparison of the IPA performance with the performance of a tank without plates and an IPS with plain plates was also conducted whose findings were useful in the proposition of IPAPA dominant Cd^{2+} removal mechanism. Adsorption-desorption studies were also conducted to ascertain the stability and the reusability of the spent CAC.

1.5. SIGNIFICANCE OF THE STUDY

Cadmium and chromium are recognized as among the hazardous heavy metals in wastewater worldwide. The World Health Organization has set 0.1 mg/L as the limit for wastewater discharge into the environment for both Cd and Cr (WHO, 2011). Wastewater discharge containing elevated amounts of Cd and Cr above the permissible limits have been reported in Ethiopia and beyond. Industry use various other methods for removing these contaminants often which is limited in terms of high cost of treatment and complex design. Adsorption is one of the popular wastewater treatment techniques due to its simplicity, cost effectiveness and ability to remove a wide range of contaminants. However, the use of adsorption has so far been restricted to batch and column adsorption configurations. Some of the challenges associated with the use of activated carbon for water and wastewater treatment in both batch and column setups include limitations in its synthesis process, challenges in regeneration due to adsorbent leaching, difficulties in recyclability, and limitations in selectivity towards contaminants. These challenges have impeded the implementation of the adsorption technique in large-scale wastewater treatment systems.

Therefore, this study aimed at developing an innovative wastewater treatment prototype that integrates an inclined plate settlers (IPS) and adsorption (Inclined Plate Adsorber (IPA) to enable heavy removal from aqueous solutions in a continuous set-up so as to enhance its practicality for large-scale application. Due to time and resource limitation, Cd^{2+} was used as the model contaminant. The IPA system was optimized at various angle of inclination (θ), influent flow rate (Q) and adsorbate initial concentration (C_o) using the Box-Behnken Design (BBD) of the Response Surface Methodology (RSM). *Prosopis Juliflora* activated carbon was also used as an adsorbent for this study in an effort to effectively manage and utilize this harmful invasive species.

This study is particularly significant because It focuses on the development of the technologies and infrastructure for the treatment of waste water using the IPA system. The IPA is an innovative approach to wastewater treatment and places significant emphasis on the practical implementation of engineering principles to enhance pollutant's removal under continuous flow and the potential for its application on a larger industrial scale.

1.6. METHODOLOGICAL RESEARCH FRAMEWORK

The methodological framework adopted and followed for this study is vividly presented below.

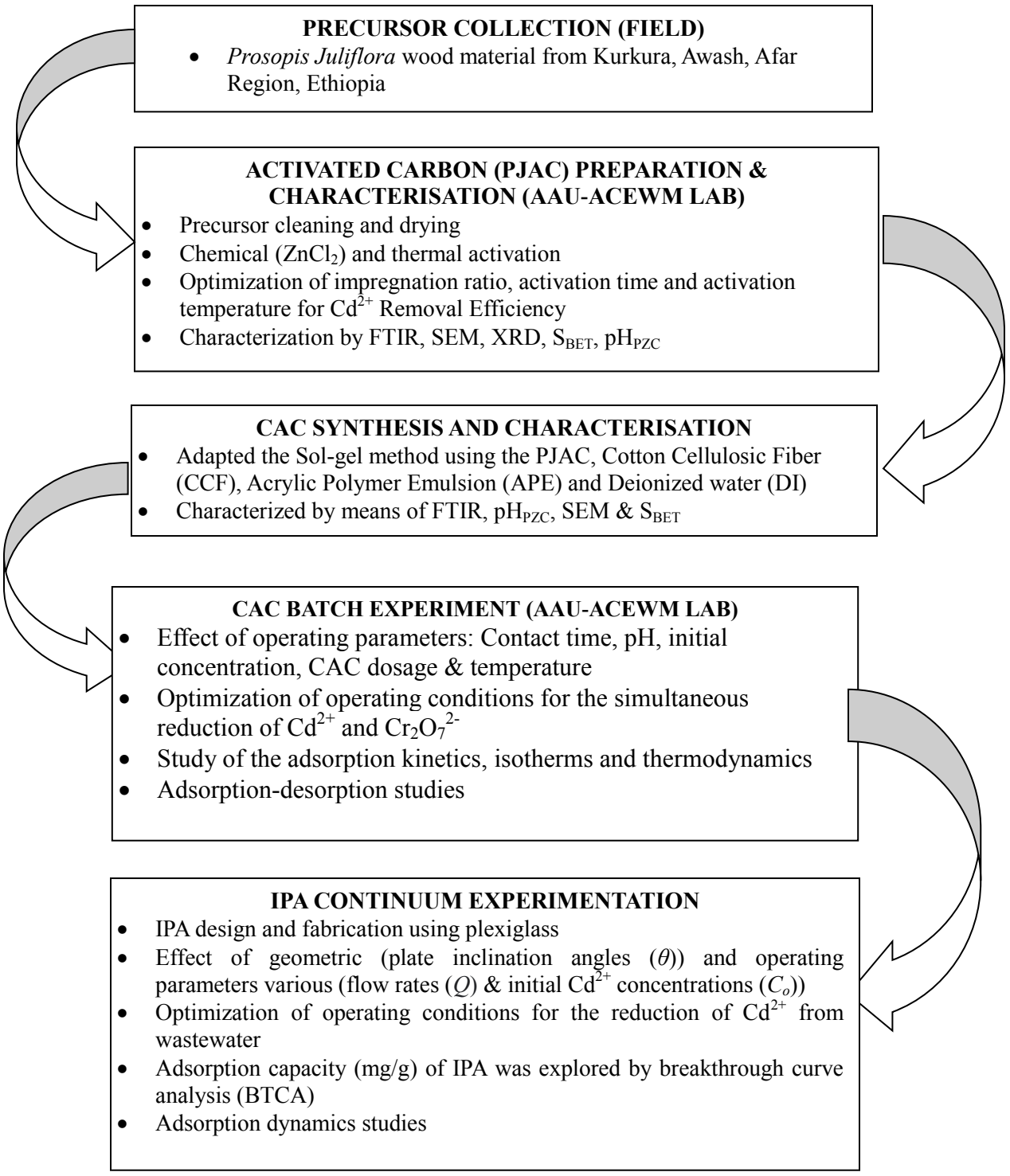

2. CHAPTER TWO: LITERATURE REVIEW

Chapter summary

This chapter provides an overview of previous research on heavy metals in wastewater. It introduces the heavy metals under study and then outlines the available remediation techniques. The chapter mainly highlights the relative advantage of coupling adsorption and inclined plate settler which is the nobility or the main focus of the research described in this thesis.

2.1. HEAVY METAL OCCURANCE IN WASTEWATER

Ehis-Eriakha and Akemu, (2022) defined heavy metals as metallic elements with at least 5 g cm^{-3} relative density that are harmful even at low levels. Examples of heavy metals include; Arsenic (As), chromium (Cr), lead (Pb), cadmium (Cd), mercury (Hg), and nickel (Ni) (Ali et al., 2017). They occur in the environment through both natural processes (geogenic and atmospheric deposits) and anthropogenic activities (P. Saha & Paul, 2019). However, their occurrence in waste water is mainly attributed to anthropogenic activities (Du et al., 2020). Studies have shown that global increase in industrialization is the major contributors of heavy metals in waste water (Shrestha et al., 2021). For instance hexavalent cadmium, chromium, and lead are toxic heavy metal ions that come into the waste water through industrial processes like tanning, coal mining, electroplating and the steel industry (Kerur et al., 2020). The wood processing industry, which uses a chromated copper-arsenate wood treatment to produce wastes containing arsenic; the inorganic pigment manufacturing industry, which creates pigments containing cadmium sulphide and chromium compounds; the petroleum refining industry, which produces conversion catalysts contaminated with chromium, nickel, and vanadium, and photographic operations, which create film with high concentrations of ferrocyanide and silver are also some other reported industrial heavy metal sources (Barakat, 2011).

Domestic household level activities are also contributing heavy metals into the waste water streams. Recent research has shown that waste water generated from households contains heavy metals such as cadmium, Lead, chromium and mercury (Drozdova et al., 2019). The heavy metals in the household waste are reported to be generated from personal care products, laundry detergents, medicine, food and kitchen utensils (Kalinowska et al., 2020). The majority of waste water contains heavy metals over the typical or allowable values established by the World Health Organization (Table 1) (Agoro et al., 2020; WHO, 2011).

Table 1: WHO permissible levels of heavy metal in drinking water and discharged Wastewater

Heavy Metal	Drinking Water (μg/L)	Discharged Wastewater (mg/L)
Arsenic (As)	10	0.1
Cadmium (Cd)	3	0.1
Copper (Cu)	2000	2.0
Chromium (Cr)	50	0.1
Lead (Pb)	10	0.1
Mercury (Hg)	6	0.01
Nickel (Ni)	70	0.1
Zinc (Zn)	3000	5.0

The waste water with high levels of heavy metal ends up in water bodies (ground water and surface water) which later causes serious problems to human beings, aquatic ecosystem and the environment (Ukah et al., 2019). In order to mitigate the environmental hazard posed by heavy metals like cadmium and chromium in water and wastewater, it is imperative to implement more effective and technologically advanced methods for their removal. To achieve this, it is important to first comprehend the chemistry of each heavy metal of concern as well as the working principles along with the merits and demerits of the various available remediation techniques. Subsequently, a synthesis of these various heavy metal removal techniques from effluent water can be conducted to determine the most effective method.

2.2. THE CHEMISTRY OF CADMIUM AND CHROMIUM

The chemistry of cadmium (Cd) and chromium (Cr) in waste water is a significant environmental concern due to the toxic and carcinogenic properties that these heavy metals poses (Lega Muhammd, 2018). Understanding their chemical behavior in waste water is pivotal in deriving the best method of removing them from the waste water. Their behavior in waste water is influenced by several factors, including pH, redox potential, presence of complexing agents, and the overall chemical composition of the water.

2.2.1. Cadmium

Cadmium (Cd) is highly toxic transitional metal (G. Ahmad et al., 2020). In wastewater, cadmium can exist in several forms including cadmium ion (Cd^{2+}), cadmium hydroxide ($Cd(OH)_2$, cadmium sulfide (CdS) and other cadmium complexes (Irshad et al., 2023). Cadmium in wastewater typically originates from industrial processes such as electroplating, battery manufacturing, pigment production, and alloy industries (Abdelmonem et al., 2024). In

nature, cadmium is only found in compounds like carbon dioxide, cadmium sulphide, carbonate and zinc ores, and never found in elemental form as such it is commonly obtained from Carbon Sulphide, which is also referred to as the mineral Greenockit ($Cd^{2+}S^{2-}$) through a process known as Zinc refinement (Shiel et al., 2010).

Research has shown that cadmium undergoes precipitation reaction in waste water (Luo et al., 2022). For example, it reacts with water to produce insoluble precipitate of cadmium hydroxide Cd $(OH)_2$ in alkaline conditions, while cadmium reaction with sulphide ions produces an insoluble cadmium sulphide (CdS) (Luo et al., 2022). These reactions are very important in waste water treatment since the insoluble precipitates of cadmium is readily eliminated from the waste water by either sedimentation or filtration. Cadmium ions can be adsorbed onto surfaces of solid particles, including activated carbon, bio sorbents, and certain types of clays (Salam et al., 2021). This is also important in waste water treatment since the concentration of cadmium in the waste water can be decreased by removing the organic matter and clay particle from the waste water (Aziz et al., 2020).

2.2.2. Chromium

Chromium is often found in 0, +2, +3 and +6 state despite that it can theoretically be found in all state from -2 to +6. The divalent chromium (Cr^{2+}) is readily oxidized in air to form trivalent chromium (Cr^{3+}). For this reason divalent chromium is rarely found in biological system Trivalent Chromium (Cr^{3+}) is the state which chromium naturally occurs and it is the most stable state of chromium (Kotaś & Stasicka, 2000). Trivalent chromium has low reactivity and does not have the ability to easily cross the cell membranes and makes it less of concern in the environment unlike Hexavalent chromium (Cr^{6+}). The hexavalent chromium is often industrial state of chromium and it is most oxidizing agent in acidic conditions (Kerur et al., 2021). When hexavalent chromium binds to oxygen as chromate (CrO_4^{2-}) or dichromate ($Cr_2O_7^{2-}$) it crosses cell membranes reacting with proteins and nucleic acid inside the cell as it is reduced to trivalent chromium (Cr^{3+}), damaging the cell (Eqn. 1; Chromate reduction inside cell) (Wise et al., 2008) and later forming complex protein complex (Eqn. 2: Formation of protein complex) (R. Saha et al., 2011).

$$CrO_4^{2-} + 8H^+ + 3e- \rightarrow Cr^{3+} + 4H_2O \quad (1)$$

$$Cr^{3+} + \text{Protein-SH} \rightarrow Cr\ (\text{Protein-S}) + 3H^{+} \quad (2)$$

To produce unadulterated chromium, a molten alkali and oxygen are applied to a chromate which turns chromium to alkali chromate. Water is then used to dissolve the alkali chromate, forming sodium dichromate in the process. Sodium dichromate is reduced by carbon to sesquioxide (Cr_2O_3) which is then converted by Aluminum to form chromium metal (Habashi, 2015)**.** Chromium and its related compounds have several uses across the global. For example, it is used to electroplate other metals due to its shiny properties and does not undergo rusting. It is also used to produce emeralds, stainless steel metals and making paints and dyes (Lunk, 2015).

As already mentioned, chromium does exist in multiple oxidation states, with Hexavalent Chromium and Trivalent chromium being the most significant in wastewater contexts. For example Chromium hydroxide ($Cr(OH)_3$) precipitate is formed when chromium ions react with hydroxide ions in basic conditions (Mitsui et al., 2019); Chromic Oxide (Cr_2O_3) is formed when chromium ions react with oxygen in the presence of water. Other studies show that hexavalent chromium is converted to less hazardous trivalent chromium by some bacteria present in the waste water (Zahoor & Rehman, 2009). Just like cadmium, chromium is also adsorbed by clay particles and organic matter present in the waste water (Mohamed et al., 2019).

2.3. CADMIUM AND CHROMIUM TOXICITY AND HEALTH IMPLICATIONS

Both cadmium and chromium can interact with other components in wastewater, such as sulfides, carbonates, and organic matter. These interactions may influence their solubility and transport. For example, cadmium can form insoluble sulfide compounds in the presence of sulfide ions, reducing its mobility. Chromium can form complexes with humic substances, affecting its speciation and toxicity (Gunatilake, 2015a).

2.3.1. Cadmium

The World Health Organization (WHO) has set a recommendation value of 0.003 mg/L (3 µg/L) for cadmium in drinking water and 0.1mg/L for wastewater discharge into the environment (Table 1) (WHO, 2011). Cadmium is toxic when found in the body above permissible levels. The toxicity of cadmium is primarily due to its ability to interfere with essential biological functions, such as enzyme activity and nutrient absorption (R. Gupta et al., 2024). Cadmium can replace

zinc in various enzymes, disrupting their normal function and leading to cellular damage (Genchi et al., 2020).

Other mechanism includes inhibition of heme synthesis where cadmium reduces the availability of functional heme molecules which are responsible for transporting oxygen and cellular metabolism. This results in cellular damage in tissues such as kidney and liver (Thévenod & Lee, 2013). According to Hernandez-Cruz et al., (2022), cadmium hinders functioning of mitochondria, leading to increased production of reactive oxygen species (ROS) and bioenergetic malfunction. Oxidative stress caused by cadmium and mitochondrial damage activate apoptotic pathways, including the mitochondrial-mediated pathway characterized by the release of cytochrome c and activation of caspases.

Chronic exposure to cadmium is reported to cause general weakening of bones and general loss in weight and density of bones leading to conditions known *osteomalacia* and *osteoporosis* respectively (Youness et al., 2012). This is due to the ability of cadmium to lower the availability of calcium (elements responsible for bone formation) thereby depriving the cells enough formation of strong bones leading to formation weak bones which are prone to fractures (Dermience et al., 2015).

Studies have also revealed that cadmium has the ability to impact development and reproduction in a number of species of mammals. Under conditions of cadmium toxicity, steroidogenesis is decreased, and ovarian haemorrhages and necrosis may co-occur (Rahimzadeh et al., 2017). It has been observed that exposure to cadmium above the permissible limits causes a drop in the incidence of live births and an increase in the incidence of impromptu miscarriage and time of pregnancy (S. Kumar & Sharma, 2019). It is alleged that cadmium reduces sperm count, density and volume while increasing occurrence of undeveloped sperm cells; this follows malfunction in spermatogenesis, low sperm quality, and accessory gland secretory functions(Massányi et al., 2020). Furthermore, research indicates that cadmium lowers serum testosterone levels, sex drive, and fertility (S. Kumar & Sharma, 2019). Other reported healthy issues due to exposure cadmium toxicity include cancer (prostate, kidney and Pancreatic cancer), nephrotoxicity, cardiovascular diseases hypertension and pulmonary diseases like emphysema (Charkiewicz et al., 2023).

2.3.2. Chromium

In contrast to trivalent chromium (Cr^{3+}), hexavalent chromium (Cr^{6+}) is thought to be poisonous and carcinogenic, having an impact on an organism's health, both immediately and over time (Mishra & Bharagava, 2016). Cr^{3}□ is less mobile and generally less toxic, but can still pose health risks if ingested in large amounts(Genchi et al., 2020). On the other hand, the toxic effects of Cr□□ are due to its high solubility and ability to generatereactive oxygen species, which can cause oxidative stress and DNA damage.

Cr□□ easily crosses cell membrane because it readily dissolves in water and once in the cell, it undergoes several reductions to form trivalent chromium (Cr^{3+}) (Poljsak et al., 2011). In the process of reducing Cr□□ to Cr^{3}□ highly chemically active oxygen molecules are produced. The extreme chemically active oxygen molecules initiate oxidative stress which harms biological constituents such as lipids, proteins, and DNA (Monga et al., 2022) leading to cell mutations and carcinogenicity conditions (Costa & Klein, 2006).

The WHO guideline value for total chromium in drinking water is 0.05 mg/L (50 µg/L) and for waste water discharge is 0.1 mg/L (Table 1) (WHO, 2011). Exposure to hexavalent chromium has different health effects. For instance, research on the prevalence of cancer in workers exposed to chromium (VI) shows a 7% greater risk of cancer when compared to the general population with similar demographics. Common cancers affecting workers exposed to chromium include; respiratory, oral, throat, prostate, and stomach cancers (Y. Deng et al., 2019). In addition, studies reveal that consuming significant quantities of chromium (VI) can result in serious harm to respiratory, gastrointestinal, cardiovascular, liver and kidney system and extreme cases are fatal (Hossini et al., 2022). Chromium (VI) is also reported to cause occupational asthma in sensitized individuals, dermatitis, skin ulcers and affects reproductive systems leading to poor development of fetus in pregnant women (Teklay, 2016).

Table 2 presents sources and health impacts of cadmium and chromium along with other heavy metals of concern (Baby et al., 2019). The need for removing such heavy metals from industrial wastewaters before discharge cannot be stressed enough.

Table 2: Summary of some heavy metals and their impact on health systems

Metal	Source	Toxicity
Cadmium	smelting of its ores, electroplating, batteries, plasticizers, alloys, pigments, nuclear industry, and cigarette smoke	damage to the kidneys, respiratory systems, and skeleton and is carcinogenic to humans

Chromium VI	produced in environment matrices (air, water, and soil) from different sources, e.g., wastewater and air mainly released from metallurgical and chemical industries,	Carcinogenic, nasal irritation, nasal ulcer and hypersensitivity reactions like contact dermatitis and asthma.
Lead	Battery wastes, fertilizers, smelting, ceramic industries	Carcinogen, brain damage, kidney damage etc.
Arsenic	Pesticides, deposits of natural minerals, and inappropriate disposal of arsenic-based reagents or chemicals	Respiration problems and mitosis and cell enzyme functionality
Zinc	galvanization, paint, batteries, smelting, fertilizers and pesticides, fossil fuel combustion, pigment, polymer stabilizers	highly toxic to plants, vertebrate fishes, invertebrates

2.4. WASTEWATER HEAVY METAL POLLUTION REMEDIATION

There are different remedial technologies in use for removing toxic heavy elements like cadmium and chromium. In general, conventional wastewater treatment consists of a combination of physical, chemical and/or biological processes and operations to remove solids including colloids, organic matter, nutrients, soluble contaminants (metals, organics, etc.) from effluents (Crini & Lichtfouse, 2019). Some of these processes and operations include primary, secondary, and tertiary treatments (Rubalcaba et al., 2007). Each of these technologies have their own principle of operation, advantages and limitations basing on such factors as simplicity, adaptability, effectiveness, cost, technical issues, and maintenance requirements. However, in some cases multiple treatment methods are employed in combination with other treatments (Younas et al., 2021).

2.4.1. Membrane filtration

Membrane filtration has attained significant interest for treating waste water because it can effectively remove suspended solids, organic compounds, and inorganic contaminants like cadmium and chromium by passing the contaminants through a semi-permeable membrane (Azimi et al., 2017). A semi-permeable membrane, in theory, operates as a filter that blocks some constituents from passing through while allowing others to do so. The selectivity and flux rate of a membrane are usually what determines its performance. The repulsion between charges effect, steric obstruction or size-based exclusion and ability to adsorb certain contaminants are commonly governed by membrane separation removal mechanisms (Abdullah et al., 2019). Depending on the particle size that can be retained, many types of membrane filtration, including

electrodialysis, nanofiltration, reverse osmosis, and ultrafiltration, can be applied to wastewater to eliminate heavy metals (Subramani & Jacangelo, 2015).

Ultrafiltration (UF), for instance, uses semi-permeable membrane to segregate heavy metals, macromolecules and suspended particles from inorganic solution based on the separating chemicals' molecular mass and pore diameter (Bodzek, 2015). These distinct characteristics of ultrafiltration (UF) enable it to permit the passage of water and small-molecule solutes, while retaining larger macromolecules that exceed the membrane's pore size (Mahmoud & Mostafa, 2023). Studies have shown that ultrafiltration membranes with low molecular weight cut-off (MWCO) are effective in removing cadmium, with higher removal rates observed at higher pH levels and lower ionic strengths (Meng et al., 2019). On the other hand, polymer-enhanced ultrafiltration (PEUF) using chitosan or quaternized hydroxyethyl cellulose ethoxylate (QHECE) as extracting agents has demonstrated high retention efficiencies for chromium ions (Cr (VI)) in water, achieving up to 92% removal efficiency (Akl et al., 2023). However, the major challenge with membrane technology which has affected its use and widespread adoption by developing countries and small-scale operations, is the high operations cost as the process is energy-intensive and requires significant cost for maintaining and replacing fouled and damaged membranes respectively (Elimelech et al., 2011). Membrane fouling occurs when there is deposition of suspended solids/particulate matter, organic compounds (grease and oils) and inorganic insoluble salts and minerals on the surface of the membranes which blocks the membrane pore and ends up reducing the efficiency and lifespan of the membranes (Crini & Lichtfouse, 2019).

2.4.2. Electro-coagulation

Electrocoagulation involves using electrical currents to remove contaminants by coagulating them into larger particles that can be easily removed (Touzani et al., 2024). During the electro-coagulation process the cathode is oxidized and water is reduced resulting in treated water and easy to settle floc (X. Zhao et al., 2010). The process removes suspended solids from waste water by using electricity to neutralise the negative particles by the formation of hydroxides in water to gather the suspended solids, help bridge, binds and strengthen the floc to sedimentation due to gravitational force (Fagnekar & Mane, 2015). The process gathers the suspended solids in water

without coagulation which happens when current is applied and it is capable of removing small particles and settling them into motion (Iwuozor, 2019).

Electro-coagulation is effective for a variety of pollutants, including cadmium and chromium.To remove cadmium (Cd^{2+}) from the waste water iron electrodes are used because iron hydroxide that form during the electrolysis process adsorb cadmium ions and enhance the extraction of cadmium ions from the solvent (C. Chen et al., 2014). On the other hand, trivalent chromium and hexavalent chromium are also removed from wastewater following the similar basic principle however their removal is highly affected by the reaction temperature, concentration of sulphuric acid and current density, with higher efficiency at optimal conditions (Peng et al., 2019)

Despite having high efficiency in removing heavy metals like cadmium and chromium, electro-coagulation process is challenged with high energy consumption for large scale operations as it requires constant supply of electricity (Nyangi et al., 2020). As such countries with poor electricity which is also expensive, finds it difficult to adopt the technology (C. Chen et al., 2014). Apart from high energy consumption, some research has shown that electro-coagulation process produces huge amount of secondary waste in form of sludge which requires further treatment and disposal (Khatun et al., 2024). The sludge confines removes heavy metals and other related coagulants which when they are disposed of, without being treated, they pause environmental concern and again further treating the sludge before disposing them off call for straining operational costs making the method expensive (Khatun et al., 2024).

Another reported limitation with electro-coagulation technique is that it requires optimizing different operational parameters such as type of electrode, type of electrolyte and density of electricity which may be very challenging in waste water system (Kobya et al., 2010). All these require constant adjustments of the electro-coagulation system in order to reach optimal conditions for contaminant effective removal from waste water which is very challenging in real practice. The variations in waste water chemical composition and flow rates affects the consistency of the electro-coagulation process demanding constant adjustment and monitoring which in turn reduces the efficiency of the system (Krystynik & Tito, 2017). The variations in composition of waste water brings other species of ions which form complex compound with the coagulants hindering the removal of the targeted metal ions (Heidmann & Calmano, 2008)). Other competing species turn to coat the electrode resulting in fouling of the electrode which

reduces the efficiency of the extraction of the targeted heavy metals found in waste water by increasing energy consumption and operational time (Peng et al., 2019).

2.4.3. Chemical precipitation

Chemical precipitation is among the most popular technique of eliminating chromium and cadmium found in waste water. The method involves adding of alkaline substances such as Calcium Hydroxide ($Ca(OH)_2$) into the waste water which increases the pH of the waste water, fostering formation of Metal hydroxide or insoluble (Azimi et al., 2017). The insoluble salts are called the precipitates which are removed by filtration or sedimentation. To remove cadmium from waste water; Calcium hydroxide is added and it dissociates to Ca^{2+} and $2OH^-$ (Eqn. 3); then the Cadmium (Cd^{2+}) reacts with hydroxide ion ($2OH^-$) forming Cadmium Hydroxide precipitate ($Cd(OH)_2$) (Eqn. 4) which is insoluble and can be removed by settling or filtration (M. Zhao et al., 2016).

$$\mathbf{Ca(OH)_2 \rightarrow Ca^{2+} + 2OH^-} \quad \mathbf{(3)}$$

$$\mathbf{Cd^{2+} + 2OH^- \rightarrow Cd(OH)_{2(s)}} \quad \mathbf{(4)}$$

While for chromium, hexavalent chromium (Cr (VI)) is first reacted with ferrous sulphate ($FeSO_4$) to produce trivalent chromium ion (Cr(III)) (Eqn. 5) which then reacts with hydroxide ions (OH^-) from calcium hydroxide which was added in the waste water to form chromium hydroxide precipitate (Eqn.6) (Islam et al., 2023);

Reduction of Cr (VI) to Cr (III) with ferrous Sulphate

$$\mathbf{3FeSO_4 + Cr_2O_7^{2-} + 8H^+ \rightarrow 3Fe^{3+} + 2Cr^{3+} + 4H_2O + 3SO_4^{2-}} \quad \mathbf{(5)}$$

Precipitation of Cr (III) as chromium hydroxide

$$\mathbf{Cr^{3+} + 3OH^- \rightarrow Cr(OH)_{3(S)}} \quad \mathbf{(6)}$$

Chromium hydroxide ($Cr(OH)_2$) which can be removed by sedimentation or filtration (Bashir et al., 2018). The efficiency of precipitation depends on factors such as pH, temperature, and the presence of interfering ions (Shanmugam & Arabi Mohammed Saleh, 2016). However, chemical precipitation is highly dependent on pH which may be difficult to maintain in large water system (BrbootI et al., 2011). It is also reported that the precipitates are difficult to remove at low

concentration while in large quantities they are linked to the production of a significant amount of sludge which can be difficult to manage and attracts additional operational costs (Meng et al., 2019). In addition, the approach uses chemicals which when not properly handled, they end up contaminating water system disrupting the aquatic ecosystem (Kurniawan et al., 2006). Chemical precipitation is also not cost effective in cases where space and infrastructure is required for handling chemicals, mixing and dumping of generated sludge (Fu & Wang, 2011).

2.4.4. Ion exchange

Ion exchange method involves the exchanging of heavy metal ions from waste water with ions on resins which have less or no toxic effect on biological system and environment such as Sodium ion (Na^+) and Potassium ion (K^+) (Tran et al., 2019). Sodium ion goes into the waste water while heavy metal ions are returned by the resin. To regenerate the resin for re-use, a solution of concentrated sodium (i.e. NaCl(aq)) is used which replaces the heavy metal ion from the resin (Korak et al., 2017). As these ion exchange resins can be regenerated and reused, it makes the process cost-effective for long-term operation, however, the initial investment in ion exchange systems can be high, and the process may be less effective in the presence of competing ions (Poustie et al., 2020).

The other advantage of ion exchange is that, the resin can be modified to remove specific heavy metals from the waste water increasing extraction efficiency (Taha et al., 2020). The method is very good at removing heavy metals at low concentration achieving highest level of purification while producing less sludge compared with other methods like chemical precipitation. However, ion exchange requires maintaining pH, flow rate and ion concentration optimal conditions which may be challenging for large waste water treatment (Abed et al., 2013). In case of high contaminant concentration of pollutants, larger quantity of resin is required with frequent regeneration as the capacity of the resin to return the pollutant ions is finite (Y. Bai, 2009). Proper disposal of the resin that has retained pollutant ions need be followed to avoid secondary contamination to the environment and this increases the operation cost of ion exchange method (M. Zhao et al., 2016).

2.4.5. Biological treatment

Bio-remediation uses biological organisms to remove contaminants from waste water and it works on the basis of techniques such as bioaccumulation, Phytoremediation and microbial

reduction (Saeed et al., 2022). Recent research has shown that bacteria (Pseudomonas aeruginosa, Bacillus spp) and Fungi (Aspergillus niger, Penicillium spp) when injected in waste water, heavy metals bio-accumulate in their bodies hence decreasing the levels of the metals in the waste water (Jeyakumar et al., 2023). Apart from bio-accumulation, some bacteria in waste water reduces heavy metals to less toxic form, for example, *Pseudomonas aeruginosa***,** in waste water converts the poisonous hexavalent chromium, to the less toxic trivalent chromium (Chatterjee, 2011).

On the other hand, heavy metals are also removed from waste water through bio-remediation method by growing plants in or around the contaminated water (constructed wetlands) which take up and store the metals in their biomass, for example, Water Hyacinth (*Eichhornia crassipes)* are reported to be efficient in taking up heavy metals and significantly reducing their levels from waste water (Murithi et al., 2014). Heavy metal removal from constructed wetlands is extensively reported to be through sediments adsorption and plant uptake (Alayu & Yirgu, 2018).

Bio-remediation is considered environmentally friendly due to its reliance on natural biological process that do not generate adverse by products (Gunatilake, 2015b). Other reports show that it is cost effective, provides in situ remediations, applicable to wide range of heavy metals and offers minimum disruption to the environment (Khan et al., 2009; Sharma et al., 2021). The major limitations with the method are; slow removal rates, dependent on specific environmental conditions and sequential bioaccumulation of the metals in the food chain (Filote et al., 2021; Saeed et al., 2022).

2.4.6. Inclined plate settlers

Inclined Plate Settlers (IPS) are high rate sedimentation devices consisting of a series of inclined parallel plates forming channels (plate stack) into which turbid waters can be fed for settling (Leung & Probsteln, 1983). Inclined plane settler consists of array of overlapping plates which aid the settling of suspended solids and heavy metals in a sedimentation tank (Takata & Kurose, 2017). Baffle plates on inclined plane settler reduces upward flow velocity, suppressing overflow of particulate matter and improving turbidity removal efficiency (Takata & Kurose, 2017). This process is facilitated by the extended retention time provided by the inclined plates, allowing for effective separation of the particulate and the water (Hu et al., 2022). An inclined plate settler

(IPS) has a lower hydraulic retention time (HRT) compared to a standard gravity settler, due to its shorter settling distance. In this situation, the available settling area depends on the total area of the plates projected onto a horizontal surface (Hyun & Kang, 2023). Of late IPS has been used as a pretreatment step in removing other contaminants including organic matter (OM), heavy metals, total suspended solids, (TSS), fecal coliform (FC) (Hyun & Kang, 2023; Kasenene et al., 2021).

2.4.7. Adsorption

In comparison to other wastewater treatment technologies, adsorption is thought to be a more effective and affordable way for removing heavy metals. The creation of high-quality effluent is the key benefit this approach offers. Adsorption has an advantage over other procedures since it is a cost-effective strategy for heavy metal remediation. Most of the time, the adsorbent may be recycled and utilized again (Ojedokun & Bello, 2016). Various literature has reported that adsorption is a technology that is good to the environment because it is simple to apply and produces no hazardous pollutants. Important adsorbent selection factors include, cost effectiveness, large surface area and porosity, distribution of functional groups, and polarity (Vunain et al., 2016). Adsorption working principle is well explained in Section 2.5.

Activated carbon, zeolites, graphene and fullerene and carbon nanotubes are all common and widely used adsorbents (Hussain et al., 2012, 2021). Because of their high adsorption effectiveness, carbons and their derivatives are the most widely utilized adsorbents due to their structural properties, which provide them a high surface area and allow for simple chemical alterations, they have extraordinary ability to withstand a variety of contaminants. The drawbacks in the activated carbons limit how often they may be used. They are expensive to produce, the used activated carbon is problematic to dispose of, and the regeneration process is time-consuming and inefficient. As a result, there is a lot of research done on low-cost adsorbents (Mariana et al., 2021).

The non-conventional adsorbents are cheap, abundantly available and have great complexing capacity due to their varied structure which binds the pollutant ions. They range from agricultural waste to industrial waste sludge and spent slurry (Rashid et al., 2021).

Table 3 summarizes the working principle, advantages and disadvantages of some of the available wastewater treatment techniques (Crini & Lichtfouse, 2019; Younas et al., 2021) .

Table 3:. Some of the recent available wastewater treatment techniques

Treatment	Process detail	Advantages	Disadvantages
Ion exchange	Metal ions from dilute solutions are exchanged with ions held by electrostatic forces on the exchange sites	Interesting and efficient technology for the recovery of valuable metals	High initial cost, partial removal of certain ions; resin disposal
Chemical precipitation	Precipitation of metal ions is achieved by the addition of chemicals, such as alum, lime, iron salts, and another organic polymer disposal	Both economically advantageous and efficient, adapted to high pollutant loads, very efficient for metals elimination, Not metal selective	Sludge generation, extra operational cost for sludge
Membrane Technology	Metal ions are separated by a semi-permeable membrane at a pressure greater than internal osmotic pressure that is cause by the dissolved solids	Simple, rapid and efficient, even at high Concentrations, produces a high-quality-treated effluent, no chemicals required, Low solid waste generation	High power consumption due to pumping pressure, high maintenance requirements due to fouling
Electrocoagulation	Electrical current plays an indirect role by generating coagulants by the dissolution of electrode materials.	Efficient elimination of dissolved inorganic matter	High capital and operational cost due to energy consumption and fouling maintenance requirements
Biological remediation	Bioaccumulation, Phytoremediation and microbial reduction of contaminants; Heavy metal removal is through sediments adsorption and plant uptake	Cost effective, provides in situ remediations, applicable to wide range of heavy metals and environmentally friendly	slow removal rates, dependent on specific environmental conditions and sequential bioaccumulation of heavy metals in the food chain
Adsorption	Molecules and ions from liquids or gases adhere to solid surfaces through functional group complexation, physical adsorption, ion exchange, and electrostatic attraction	Technologically simple equipment and adaptable to many treatment formats; Wide variety of target contaminants, effective process with fast kinetics	Chemical regeneration requirement, fouling, adsorbent leaching of activated carbon; challenges in disposal of exhausted adsorbent
Inclined Plate Settlers (IPS)	Uses the principle of gravity separation for suspended particles. Consists of a series of inclined plates or tubes at an angle (40-60˚)	Simple and compact design; small foot print, low energy requirements, Easy operation and maintenance	Not capable of effectively removing heavy metals without coupling with another technique

2.5. ADSORPTION

From the various recent water treatment technologies (Table 3), adsorption remains the most effective method for removing pollutants in wastewater and water with low costs, simple operation, and simple design (Sabzehmeidani et al., 2021).

2.5.1. Basic adsorption principle

The adsorption process is primarily driven by surface forces and involves the accumulation of molecules of adsorbate on the surface of the adsorbent. This phenomenon is extensively employed in wastewater treatment to remove pollutants, including heavy metals like cadmium (Cd) and chromium (Cr) (Gawande et al., 2017). Adsorption is classified into two based on interaction forces between the adsorbate and adsorbent and these are physisorption and chemisorption.

Physisorption, also known as physical adsorption, is a process where adsorbate adhere on the adsorbent surface as a result of electrostatic contact or weak Van der Waals forces without utilizing any chemical reactions (Gawande et al., 2017). Various adsorbent with high surface area such as Biochar, charcoal, Silica gel and Zeolite have proven to be efficient in physically adsorbing different type of adsorbate including heavy metals (S. Gupta et al., 2020). Physisorption is widely used because it deemed environmentally friendly as it does not involve use of any chemicals which may have negative impact to the natural system (Tony, 2022).

The adsorbent materials are often locally available and since no chemical reaction are involved, the process is reversible which gives a chance of re-using the adsorbent and these makes the physisorption cost effective. It is also reported that physisorption is specific to a particular adsorbate, a factor which offers wide range of adsorbate to be absorbed. However, failure of the physisorption to extract a specific adsorbate, weak binding forces, low adsorption capacity and temperature sensitivity are the limitations associated with physisorption (Habineza et al., 2017).

Chemisorption (Chemical adsorption) is a form of adsorption with the formation of robust chemical bonds between the adsorbate and adsorbent surface by ionic, covalent or through radical processes (A. Gupta et al., 2021). It occurs at temperature exceeding the adsorbate's threshold temperatures, requiring energy for its activation.

Chemisorption is preferable to physisorption due to its ability to particularly adsorb a specific adsorbate, high binding forces between adsorbent and adsorbate, and permanent adsorption performance (Schmickler & Santos, 2010). The challenge with chemisorption is that adsorbent materials used in chemisorption are often expensive as they are not locally available and it requires a lot of energy as a result more cost are incurred (Agboola & Benson, 2021). The chemical materials used in chemisorption may lead to discharge of toxic substance into the waste water end up negatively impacting the ecosystem (Biol Sci et al., 2018).

2.5.2. Adsorption theory

Adsorption theory encompasses the principles and models that define how molecules (adsorbates) follow to the surface of solids (adsorbents). It provides a framework to understand the mechanisms, kinetics, and equilibrium states of adsorption processes (Lv et al., 2024). Several adsorption theories have evolved across the global amongst which Langmuir adsorption theory, Freundlich adsorption theory and BET theory are fundamental (Swenson et al., 2019).

Langmuir adsorption theory

The theory was proposed by Irving Langmuir in 1916; it describes how the area occupied by adsorbate molecules on the solid adsorbent's surface varies with partial pressure or concentration at a constant temperature, under the following conditions: the adsorbent surface is uniform, molecules are adsorbed at specific active sites, each active site adsorbs only one molecule of adsorbate, and there is no interaction among the adsorbed molecules on the adsorbent surface (Swenson et al., 2019). According to the theory, the rate at which adsorbate molecules are adsorbed is proportional to the fraction of the surface area that remains uncovered, while the rate of desorption is proportional to the surface area covered by adsorbate molecules.

In relation to heavy metal extraction from waste water, the theory is applied to determine number of heavy metals that can be adsorbed at different concentrations and determination of maximum adsorption capacity of adsorbent for specific heavy metals. However, the theory is not applicable for heterogenous surface of adsorbent, the adsorbate that forms multilayer on adsorbent surface and where the adsorbate molecules interact on the surface of the adsorbent (Alafnan et al., 2021). Despite the limitations, the theory built a foundation for development of other improved adsorption theories.

Freundlich theory

The theory was proposed by Herbert Freundlich in 1909, which suggest that the amount of the adsorbate on a solid adsorbent's unit mass changes as a system's pressure changes at a specific temperature (Shaji & Zachariah, 2017). Unlike Langmuir adsorption theory, this theory is applied for adsorbent with heterogenous surface, the adsorbate that interact with each other on the surface of adsorbent and where the adsorbate forms multilayer on the adsorbent's surface (Quiñones & Guiochon, 1998). The theory is used to determined best adsorbent for specific heavy metal where different adsorbent can be subjected to Freundlich isotherm in order to characterize their performance on adsorbing the specific heavy metals (X. Chen et al., 2022). It is also applied in designing for removing heavy metals in waste water using absorbent with heterogenous surface in waste water with complex and varying heavy metal concentrations (X. Chen et al., 2022). The major setback with Freundlich theory is that it is more empirical such it fails to explicitly explain interaction at surface of the absorbent (Rangabhashiyam et al., 2014)

BET theory

The theory was put forth by Brunauer, Emmet and Teller in 1938, which presumes that the physisorption result in the multilayer adsorption creation (Cerofolini & Meda, 1998). It further presupposes that the adsorption sites on a solid surface are homogenous and that the adsorption at one site does not alter the adsorption at surrounding sites.Unlike Freundlich theory, this theory explains explicitly the surface area and porosity of adsorbents, interactions of adsorbate on the surface of the adsorbent and formation of layers of adsorbate on surface of adsorbent (Sattar Ali Khan, 2012). This is very important in waste water treatment as it helps in determining adsorption capacity of adsorbents to different adsorbate and this increases the efficiency of waste water treatment system. In addition, the ability of the theory to explain formation of monolayer and multilayer of adsorbate on homogenous and heterogenous surface of adsorbents can be applied in identifying right adsorbents and also adjusting their properties to improve adsorbent capacity (Scheufele et al., 2016).

2.5.3. Adsorption heavy metal removal mechanism

Adsorption uses different mechanisms in removing cadmium and chromium from waste including the following**;**

Electrostatic attraction: For example, Cadmium (Cd^{2+}) and chromium ions (Cr^{3+} & Cr^{6+}) get attracted and adsorbed by the oppositely charged adsorbent (Bandara et al., 2020) i.e. chromate is adsorbed to Chitosan due to electrostatic attraction between the net negative charge on Chromate and the positive charge of NH_4^+ on Chitosan (due to -OH and $-NH_3$ functional group on chitosan) (Bhavani et al., 2016).

Physical trapping/Pore filling mechanism: Adsorbate ions get physically trapped on the surface structure of the adsorbent as the waste passes through the column of the adsorbent (Gooty et al., 2022). Zeolite is an example of adsorbent that uses this mechanism which traps the cadmium and chromium ion in cavities (pores) within its crystalline structure as the waste passes through. The process removes the adsorbate ions from the waste water (Ugwu et al., 2022).

Reduction: For example, hexavalent chromium (Cr^{6+}) gets reduced to trivalent chromium ($Cr^{3+)}$ by adsorbents with electron donating function group (hydroxyl, phenolic, amino and carboxyl group), for instance, the $-CH_3$ from graphene oxide polymer adsorbent reduces the Cr^{6+} in form of chromate or dichromate to trivalent chromium by providing electron for the reduction process according to the Eqn (7) (Bandara et al., 2020);

R-CH-H + Cr (VI) → R-CH-OH +Cr (III) (7)

The reduced Cr^{3+} which is less toxic than Cr^{6+} is then adsorbed onto the adsorbent, hence removal from waste water (Bandara et al., 2020).

Hydrogen bonding: Adsorbents with functional groups like hydroxyl (-OH) or amino ($-NH_2$) groups form hydrogen bonds with cadmium and chromium ion in the waste water. For instance, biomass-derived adsorbents with hydroxyl groups can adsorb cadmium ions through hydrogen bonding interactions, enhancing removal efficiency (Pyrzynska, 2019).

Ion exchange: This mechanism is common in ion exchange resins, where functional groups on the resin surface replace ions in the water, for example, cation exchange resins can remove

cadmium ions by exchanging them with sodium or hydrogen ions initially present on the resin (Kumar Joshi et al., 2022).

Complexation: Adsorbents with chelating agents, such as iminodiacetic acid groups, form strong complexes with cadmium and chromium ion which are more stable, enhancing adsorption efficiency. This mechanism is particularly effective for specific target ions (Sud, 2012)

Surface Precipitation: Surface precipitation occurs when dissolved ions react to form a new solid phase atop the adsorbent (M. Zhao et al., 2016). The mechanism is common for metal hydroxides like chromium hydroxide ($Cr(OH)_3$), which form precipitates on adsorbent surfaces under suitable pH conditions (Bedemo et al., 2016). The precipitate is then adsorbed by adsorbents such as biochar and zeolite through other mechanism like sedimentation, pore filling and ion exchange (W. Ahmed et al., 2021).

2.5.4. Operation factors affecting adsorption

The efficiency of the adsorption of cadmium and chromium from waste water is influenced by a number of variables, including concentration, pH of the solution, temperature, adsorbent type and dosage, agitation speed and duration of contact, Ion strength, and the presence of competing ions (R. Kumar & Chawla, 2014).

Concentration: The adsorption capacity, per fixed adsorbent mass, increases with rise in concentration of chromium and cadmium ion present in the waste water (Abatan et al., 2020). At low concentration, the adsorption surface sites of adsorbent are readily available which leads to higher adsorption rates but, as the concentration is increasing the number of adsorption surface site decreases and adsorbate competition for the few sites slow down the process up until the equilibrium point where the adsorption rate becomes constant (de Borja Ojembarrena et al., 2022). The process can take time to reach equilibrium at high concentration due to increased mass transfer resistance (Xu et al., 2022).

pH of the solution: pH affects adsorption efficiency of heavy metals in the waste water differently (Padmavathy et al., 2016). For example, for Cr, at low pH Cr^{3+} exist in its ionic state which can be readily adsorbed while raising the pH, Cr^{3+} precipitates as $Cr(OH)_2$ a form which is less adsorbed relative to Cr^{3+} and this decreases the adsorption efficiency (Rzig et al., 2006). Hexavalent chromium (Cr^{6+}) is readily adsorbed at low pH because at high pH it exists as Cr_4^{2-} and HCr_4^- which

get electrostatically repelled by the negatively charged adsorbent hence decreasing the adsorption efficiency (Liu et al., 2023). On the other hand, optimal adsorption capacity of cadmium varies within neutral and slightly alkaline range depending on nature of the adsorbent used (Kavand et al., 2020). For instance, Thanh Nguyen et al., (2023) found that optimal pH of 6.54 for cadmium extraction from waste water; Wang et al., (2020) reported pH of 7 as ideal for cadmium adsorption using magnetic graphene oxide while a study by Joshi et al., (2022) indicated a pH of 8 as beneficial for biosorbent derived from *Acer oblongum* leaves in removing cadmium from waste water.

Temperature: The impact of temperature on adsorption of heavy metals depends on the thermal nature of the adsorption process. For exothermic adsorption, increasing temperature decreases adsorption capacity of the system as it changes and start favoring desorption while for endothermic adsorption increasing temperature favors adsorption (Shahid et al., 2021)

Adsorption dosage: The adsorption efficiency of heavy metals increases with increase in dose of adsorbent (Tran et al., 2019)**.** Increasing adsorbent increases adsorption sites onto which cadmium and chromium binds resulting in high removal rates, however, it important to note that different adsorbents have different optimal dose beyond which efficiency stops increasing and or starts decreasing (Mohamed et al., 2019)

Contact time: Adsorption efficiency increases during initial stage due to abundant availability of adsorption sites on adsorbent surface; and then adsorption continue to increase at decreasing rate as the adsorption sites becomes occupied with adsorbate up until equilibrium point is reached where the rate of adsorption equals rate of desorption (Ugwu et al., 2020).

Nature of adsorbent: Different adsorbent have different adsorption efficiency due to varying surface area, porosity and functional group (Yang et al., 2019). Porous adsorbents have large surface which increases available active adsorbent site for cadmium and chromium ion, for example, activated carbon has high adsorption efficiency because it is more porous and have high surface area (Kyzas & Kostoglou, 2014b). The same applies to functional group where adsorbents that forms strong bonds with adsorbate turn to have higher adsorption efficiency compared with their counterparts (Pathania & Srivastava, 2020).

3. CHAPTER THREE: MATERIALS AND METHODS

Chapter summary

This chapter presents the study's experimental research methodology. It describes the variables selection criteria, the experimental design and set-up used for each objective. The chapter also gives a thorough description of the data analysis methods applied for each objective in the study.

3.1. CAC SYTHESIS AND CHARACTERIZATION

This work was done at Addis Ababa University's (AAU) College of Natural and Computational Sciences' (CNCS) Core Water Laboratory. The activated carbon made from *Prosopis Juliflora* (PJAC) wood was prepared first in order to use it for synthesizing the Composite Adsorbent Coating (CAC).

3.1.1. Chemicals and materials

The wood from *Prosopis Juliflora* was collected at Kurkura, Awash, Afar Region in Ethiopia on 05-06th April 2022 (Fig. 1). Located at Latitude 9.0568777º and Longitude 40.2046295º, the area was chosen as there is a need to manage the problem of *Prosopis Juliflora* invasion amidst arable land scarcity in the region. All chemicals utilized in this investigation were of analytical grade and were employed without additional purification. These chemicals included zinc chloride ($ZnCl_2$), sodium hydroxide (NaOH), cadmium chloride hydrate ($CdCl_2 \cdot H_2O$), potassium dichromate (K_2Cr_2O7) and hydrochloric acid (HCl). Acrylic Polymer Emulsion (APE) (Ecronova ® RA 127) was supplied by Mallard Creek Polymers (Mallard Creek Polymers, 2019). Cotton Cellulosic Fiber (CCF) was sourced locally and deionized water (DI) was produced in the laboratory.

Figure 1: *Prosopis Juliflora* wood collection at Kurkura in Awash, Afar Region, Ethiopia

3.1.2. PJAC preparation

The activated carbon used for this objective was prepared using pyrolysis method utilizing both chemical and thermal activation. First a blade was employed to sever the spikes and outer branches. The biomass was extensively cleansed with tap-water to eliminate dirt which was followed by rinsing with DI water. The cleaned wood biomass was cut into smaller pieces (≤2 cm) and was then sun-dried for 7-days (Fig. 2).

Figure 2: *Prosopis Juliflora* wood pre-treatment

The desiccated precursor was saturated with a heated $ZnCl_2$ solution at various impregnation ratios[1] (IR) (1-2.0) for a duration of 2 hours, and subsequently immersed in the very same $ZnCl_2$ solution for 24 hours. After 24 hours, excess $ZnCl_2$ solution was poured out and the biomass was allowed to air dry after being thoroughly washed with deionized water. $ZnCl_2$ was used as a chemical activating agent in the preparation of the activated carbon as it enhances the pore formation during the activation process thereby accelerating the reaction rate and producing an activated carbon with a more porous structure. Subsequently, the impregnated biomass was introduced into a muffle furnace and subjected to different carbonization temperatures (T) (400-600 ºC) for varying carbonization time (t) (60-180 min) in order to remove the volatile components. The carbon was further cleansed with deionized water, dehydrated in a 40ºC oven for 24 hours, pulverized, and then subjected to a temperature of 800ºC in a muffle furnace for 120 minutes, with a consistent heating rate of 10ºC per minute to enhance its porosity and surface area. The prepared powdered activated carbon (PJAC) was then sieved using a 150-µm screen and at any point was stored in sealed containers for either optimization adsorption experiments (Section 3.1.4), characterization (Section 3.1.6) or CAC synthesis (Section 3.1.7).

[1] $M_z:m_p$ where m_z is the mass of $ZnCl_2$; and m_p is the mass of dried *Prosopis Juliflora*

3.1.3. DoE for PJAC preparation parameters optimization

The BBD of the RSM was employed in the Design of Experiments (DoE) for PJAC preparation parameters optimization. The initial step of the BBD's DoE consisted of identifying the independent variables (G. Kaur et al., 2021); thus the impregnation ratio (X_1), carbonization temperature (X_2), and carbonization time (X_3) and their respective ranges (limits). The parameters were coded at 3 levels: -1(low); 0(center); +1(high) (Table 4).

Table 4: Levels and experimental range of independent variables for the batch adsorption experiments

Variable	**Unit**	**Factors**	**Levels**		
			-1	**0**	**+1**
Impregnation Ratio (IR)	-	X_1	1	1.5	2
Carbonization Temperature (T)	°C	X_2	400	500	600
Carbonization Time (t)	Min	X_3	60	120	180

For this objective, a 3-factorial and a 3-level BBD with 3 replicas at the central point was used to conduct 15 trials for response surface modelling. The levels and limitations of the independent factors were established using values derived from a variety of sources, including previous literature and pilot/preliminary tests. Equation (8) was utilized to code the predetermined independent variables.

$$\boldsymbol{X_i = \frac{X_I - X_0}{\Delta X}} \quad (8)$$

X_i represents the dimensionless coded value of the of i^{th} variable, X_0 corresponds to the value of the variable in the center whereas ΔX denotes the step change. The model terms were generated and the experimental data was fitted using Eqn. (9). It is a model that is based on empirical data and uses a second-order polynomial equation (Montgomery, 2017).

$$\boldsymbol{Y = b_0 + \sum b_{ii}X_i + \sum b_{ii}X_i^{\,2} + \sum b_{ij}X_iX_j} \quad (9)$$

Where, the response variable $\boldsymbol{Y}$ represents Cd^{2+} reduction. The constant coefficients b_0 is the intercept whereas b_i, b_{ii} and b_{ij} correspond to the linear, quadratic and interaction terms respectively. The three independent variables (impregnation ratio (IR), carbonization time (t) and carbonization temperature (T)) are represented by X_i and X_j.

3.1.4. PJAC preliminary adsorption experiments and Cd^{2+} removal efficiency (%)

For this objective, Cd^{2+} percent removal efficiency (%) from aqueous solution was used to evaluate the effectiveness of the various PJAC prepared under different preparation parameters. Cd^{2+} stock solution with 1000 mg/L concentration was prepared by dissolving 17.9 g of the cadmium chloride

hydrate ($CdCl_2 \cdot H_2O$) in one litre of de-ionized water using a one litre volumetric flask. For all the batch adsorption experiments for this objective, 100 mg/L Cd^{2+} concentration (made by dissolving 100 ml of the prepared 1000mg/l stock solution into a 1L volumetric flask) was used.

For each of the 15 batch tests, 25 ml of a solution containing 100 mg/l of Cd^{2+} was placed into a 150 mL Erlenmeyer flask each containing 0.5 g of the prepared PJAC according to the DoE in Table 4. The pH of the solution was adjusted to 8.0. The mixtures were agitated concurrently using a mechanical shaker at a speed of 200 revolutions per minute and a temperature of 25 °C for duration of 30 minutes. Following adsorption, the samples underwent centrifugation at a speed of 3600 revolutions per minute for duration of 20 minutes. Inductively Coupled Plasma - Optical Emission Spectrometry (ICP-OES) (Agilent 5800) was used to measure the Cd^{2+} residual concentrations in the supernatant solutions. Equation 10 was utilized to calculate the Cd^{2+} percentage removal efficiency, R, (in %) while Eqn. 11 was used to determine the PJAC adsorption capacity, q, (in mg/g).

$$\boldsymbol{R = \frac{C_i - C_f}{C_i} \times 100} \tag{10}$$

$$\boldsymbol{q_e = \frac{(C_i - C_f)}{m} V} \tag{11}$$

Where $\boldsymbol{R}$ is the metal ion percent removal (%) efficiency, $\boldsymbol{q_e}$ is the adsorbent adsorption capacity (mgg^{-1}) at equilibrium, $\boldsymbol{C_i}$ and $\boldsymbol{C_f}$ are the initial and final metal ion concentrations (mg/L) respectively, $\boldsymbol{V}$ corresponds to adsorbate volume (L) and $\boldsymbol{m}$ corresponds to mass of adsorbent used (g).

3.1.5. Statistical Analysis and Model Fitting

To obtain the prediction models for the removal efficiencies the BBD was used. Using the optimal settings, the model's ability to predict the optimal response value for Cd^{2+} percent removal efficiency was assessed. Model suitability was examined and applied to the experimental data to describe whether or not the predicted model would generate incorrect or ambiguous results. The statistical tests performed for this objective included: sequential model (sum of squares) to measure the deviation of the data points away from the mean, lack of fit tests, and model summary, to verify the adequacy of the model in demonstrating the best Cd^{2+} percent removal efficiency (%). Using Design Expert version 11, regression analysis was conducted to fit mathematical models to the

experimental data in order to identify the best region for the responses under investigation. The statistical significance of the interactions was done using the Analysis of Variance (ANOVA).

3.1.6. PJAC characterization

The activated carbon produced under the optimized preparation parameters was subjected to both physical and chemical characterization. The physical-chemical characteristics examined on the synthesized activated carbon were; BET surface area (S_{BET}), surface charge (point of zero charge (pH_{PZC})), functional groups (Fourier-transform infrared spectroscopy (FTIR)), surface morphology (Scanning Electron Microscopy (SEM)), and the crystalline/amorphous structure (X-ray diffraction (XRD)) of the adsorbent. BET technique was used for PJAC surface area determination. To calculate the specific surface area of the PJAC (m^2/g), measurements of N_2 adsorption/desorption isotherms were conducted at temperature of -196 ºC using a Micromeritics equipment (ASAP 2420). Prior to registering the isotherms, the samples underwent outgassing at a temperature of 150 ºC for a duration of 16 hours under high vacuum. The PJAC morphology was measured using SEM (Hitachi TM 1000). The pH drift method was used for PJAC pH_{PZC} determination (Eutech Instruments PH 700 series pH meter). The initial pH values of the 0.1 M NaCl electrolyte were set from 3 to 12 while employing 0.1 M HCl and a 0.1 M NaOH solutions respectively for pH adjustment. The functional groups of the adsorbent's surface were analyzed using FT-IR measurements. The measurements were conducted at room temperature using a Spectrum 65 FT-IR instrument in KBr pellets (PerkinElmer). The FTIR spectrum was performed between the wavenumber range of 4000 to 400 cm^{-1}. The structural arrangement of the PJAC before and after Cd^{2+} adsorption was examined using XRD (Rigaku MiniFlex 600 Benchtop) which was carried out in scan range of 5° - 80° in 2 theta angles, 40 kV, 44 mA and of 10 deg/min scan speed.

On the other hand, chemical composition of *Prosopis Juliflora* in terms of ultimate (Carbon (C), Hydrogen (H), and Nitrogen (N) and other elements such as Sulphur (S) and Oxygen (O)) (the primary components), and proximate analysis (i.e. moisture, ash content and volatile material) respectively were sourced from various literature (Emirie, 2015; Keerthivasan et al., 2019; Mahajan et al., 2017).

3.1.7. Composite Adsorbent Coating synthesis

The Composite Adsorbent Coating (CAC) was synthesized using only the PJAC prepared under the determined optimized preparation parameters. A facile sol-gel method adapted from Azha & Ismail, (2019) was used for CAC synthesis using PJAC, CCF, APE and DI water (Figure 3 (a-e)). The synthesis of the PJAC/APE-CCF (CAC) adsorbent coating involved the blending of PJAC/APE/DI

through mixing 2 ml of APE and 4 ml of DI water with different quantities (0.25 g, 0.50 g and 0.75 g) of the PJAC. The resulting slurry was mixed with a magnetic agitator (Model RT Power) for approximately 3 hours to form a homogeneous solution. For every 15 cm by 5 cm (75 cm^2) of CCF per given adsorbent dosage, 2 ml of APE and 4 ml of DI were used. For example, to synthesize a 0.25 g CAC; 2 ml of APE and 4 ml of DI water were used per 0.25 g of PJAC on a 15 cm by 5 cm (75 cm^2) CCF.

A brush was employed to spread the homogeneous slurry of APE/PJAC on both sides of the 75 cm^2 CCF. To prevent detachment of the adsorbent coating, the prepared PJAC/APE/CCF strips were subjected to drying at 70 °C for 5 h. The dried CACs were then stored in air-tight bags for characterization and for use in further adsorption tests.

a) Clean CCF	b) PJAC/APE slurry	c) Strip coating	d) Oven drying	e) Dried CAC

Figure 3: *CAC synthesis*

3.1.8. CAC Physicochemical properties analysis

A CAC powdered sample was prepared for both BET Surface Area (S_{BET}) and particle size distribution (PSD) analysis. This involved mixing a known amount of APE, DI water and adsorbate (adsorbate dosage) for 180 minutes until a homogeneously blend. Then the homogeneous mixture was subjected to drying for 7 hours at 40°C in a vacuum oven (Townson + Mercer) under 300 mbar pressure. Subsequently, the desiccated material was pulverized into a fine powder and sieved through a 150 µm mesh for S_{BET} and PSD analyses.

Similarly, to the procedures for PJAC characterization in Section 3.1.6, the pore volume (cm^3/g), surface area (m^2/g), and pore size (125.3 Å) were determined through the utilization of the N_2 adsorption/desorption isotherm technique employing the BET method. The N_2 adsorption/desorption isotherms were obtained by conducting measurements at a temperature of 77.279 K using a BET surface analyzer (Micromeritics Instrument Flex Version 6.01).

Again, SEM (Hitachi TM 1000) was used to analyze surface morphology of the CAC. The elemental analysis of the CAC was performed using Scanning Electron Microscopy-Energy Dispersive X-Ray Analysis (SEM-EDX) (Hitachi TM 1000).

The alteration in the CAC's functional group prior to and following adsorption was examined by FTIR spectroscopy (PerkinElmer Spectrum 65) (spectral range; 4000 cm^{-1} - 400 cm^{-1}). The pH Point of Zero Charge (pH_{PZC}) of the CAC was also measured using a pH drift approach. For the CAC, 75 cm^2 (15 cm by 5 cm) of CAC coated with 0.25 g, 0.5 g and 0.75 g of adsorbent was each put in 10 flasks holding 80 mL of a 0.1 M NaCl solution but having ranges of pH values from 2-11. The pH adjustment was done using 0.1M HCl and O.1M NaOH. The final pH values were measured and compared to the initial pH values after 24 hours of equilibrium time. The pH_{PZC} was calculated by linear interpolation between two neighboring data points whose linear connections intersected with the bisector. The experiment was done in duplicate to confirm reproducibility.

3.2. CAC EVALUATION AND OPTIMIZATION

3.2.1. DoE for CAC operational parameters optimization

The RSM's BBD was also employed in the experimental design for CAC operational parameters optimization. For this objective Cd^{2+} and $Cr_2O_7^{2-}$ were selected as model contaminant heavy metals generally because of their toxicity in water but specifically because of their cationic and anionic forms respectively. The influence of initial concentration of metal ions, adsorbent dosage, pH, temperature and agitation time on Cd^{2+} and $Cr_2O_7^{2-}$ adsorption into the CAC in a binary component system was studied by employing the BBD of the RSM. Equation 8 was again used to code the predetermined independent variables.

Parameters were coded with three (3) levels: +1, 0, and -1, representing the high, center, and low levels, respectively. The independent parameters levels were based on values obtained from various literature as well as prior pilot experiments. The experimental design methodology for each independent variable is presented in Table 5. Again the empirical second-order polynomial model (Khedmati et al., 2017) was used for fitting the experimental data (Eqn. 9). A series of 45 experiments including five replications at the central points were conducted in a batch adsorption set-up for Cd (II) and Cr (VI) simultaneous removal.

Table 5: Levels of independent variables and experimental range for Cd^{2+} and $Cr_2O_7^{2-}$ adsorption experiments

Factor	Variables	Levels of the coded variables		
		-1	0	+1

A	pH	5	7	9
B	Metal ion concentration (initial) (mg/L)	5	27.5	50
C	Temperature	20	30	40
D	Adsorbent dosage (g)	0.25	0.5	0.75
E	Contact time (min)	15	60	105

3.2.2. Cd^{2+} and $Cr_2O_7^{2-}$ adsorption experiments and percent removal efficiency (%)

Standard 100 milligram per litre of Cd (II) and 100 milligram per litre of Cr (VI) solutions were prepared using the established protocol outlined in the APHA, (2005) standard procedure. For each given batch experiment, different required metal ion concentrations were diluted from the stock solutions accordingly.

For each of the 45 batch adsorption experiments, 100 ml of the adsorbate were carefully transferred into an Erlenmeyer flask (150 ml) and the required CAC dosage was added/put into the Erlenmeyer flask with pH adjustment made as needed. All the mixtures were simultaneously shaken in an automated water bath shaker at 150 rpm while varying the temperature and the contact time accordingly as presented in Table 4. A pH meter (Eutech instruments PH 700 series) was used to measure and adjust the adsorbate's pH before adsorption experiments. Again, the ICP-OES (Agilent 5800) was employed to quantify the concentration of adsorbate before and after adsorption experiment respectively. Equations 10 and 11 were again used in calculating the metal ion percent removal efficiency (%) and the CAC adsorption capacity (mg/g) respectively.

3.2.3. Model Fitting and Statistical Analysis

Regression analysis and ANOVA were performed on the experimental data using Design-Expert version 11 software. This analysis aimed at determining the relationship between the process variables and the experimental response (i.e. simultaneous metal ion removal). The interactions between factors and their effect on the simultaneous removal of Cd (II) and Cr (VI) were elucidated by the utilization of the same software program, which also facilitated the development of response surfaces as three-dimensional curves and two-dimensional contour plots. The models fit was assessed using the R-square (R^2). The model's statistical significance and its constituent components was evaluated using the F and p-values (95% confidence level).

3.2.4. Adsorption isotherm experiments

Adsorption isotherms were obtained by using a batch reactor in an automated water bath shaker to determine the key factors influencing Cd^{2+} and $Cr_2O_7^{2-}$ adsorption by CAC. Five different initial

doses of a mixture of Cd^{2+} and $Cr_2O_7^{2-}$ (i.e. 10 mg/L, 7 mg/L, 5 mg/L, 5 mg/L and 1 mg/L) were utilized to evaluate adsorption at optimized operating conditions, expect for the initial adsorbate concentration. In each experiment, 0.25 g of CAC was placed in 100ml of solute solution of pH 8.5 contained in 150 mL Erlenmeyer flasks. These flasks were then subjected to agitation in a water bath shaker for 105 minutes at 22.2°C. For quality control and data validity, all experiments were done in triplicates.

Following the determination of metal ion removal (%) and the quantity of metal ions adsorbed on CAC (q in mg g-1) using Eqn. 10 and 11, respectively, the obtained data were subjected to fitting with Langmuir, Freundlich, Dubinin-Radushkevich and the Temkin isotherm models in order to examine the adsorption mechanisms between CAC and the metal ions. Table 6 displays the isotherm model equations (Eqn. 12-15) and the types of plots employed in determining parameters of the model for data analysis.

Table 6: Isotherm models and their linear equations

Model	**Isotherm Linear form**	**Plot**	**Equation Number**
Langmuir	$\frac{1}{\mathrm{qe}} = \frac{1}{\mathrm{KL}qm\mathrm{Ce}} + \frac{1}{qm}$	$\frac{\mathrm{Ce}}{\mathrm{qe}}$ vs Ce	12
Freundlich	$\mathrm{Log\ qe} = \log \mathrm{K_F} + \frac{1}{\mathrm{n}} \log \mathrm{Ce}$	$\log$ qe vs $\log Ce$	13
Dubinin-Radushkevich	$\ln \mathrm{qe} = \ln q_{\mathrm{mDR}} - \log \mathrm{K_{DR}} \varepsilon^2$ *[$\varepsilon = RT\ ln\ (1 + 1/C_e)$]*	$\ln$ qe vs. ε^2	14
Temkin	$\mathrm{qe} = \frac{\mathrm{RT}}{B_T} \ln \mathrm{K}_T + \frac{\mathrm{RT}}{B_T} \ln \mathrm{Ce}$	qe vs $\ln Ce$	15

Where the K_L is the Langmuir equilibrium constants (L g^{-1}) and K_F is the Freundlich equilibrium constant (L g^{-1}). C_e is the metal ion concentration in the solution at equilibrium (mg L^{-1}); qe denotes the CAC adsorption capacity at equilibrium in solid phase (mg g^{-1}). q_m is related to the monolayer maximum adsorption capacity (mg g^{-1}) while 1/n is Freundlich adsorption intensity where 'n' is the Freundlich exponent. q_{mDR} (mg/g) denotes capacity of the saturation theory in the Dubinin-Radushkevich model equation whereby K_{DR} (mol^2/kJ) is the unit of energy and the Polanyi potential is given by ε. In the Temkin isotherm, B_T is the Temkin constant as it relates to the heat of sorption (J/mol), R is the common gas constant (8,314 J/mol K), T denotes the absolute temperature (K), and K_T denotes the Temkin equilibrium constant corresponding to the highest binding energy (L/g).

3.2.5. Adsorption kinetic experiments

Information on adsorption mechanism and potential rate-controlling actions is provided through kinetic modeling. Adsorption rate influences the selection of materials for use as adsorbents. As a rule of thumb, adsorbent materials should have relatively, a high adsorption affinity, a significant adsorption capacity, and a rapid adsorption rate (Nyangi et al., 2020). In this study, the rate of Cd^{2+} and $Cr_2O_7^{2-}$ adsorption on the CAC surface was evaluated by adsorption kinetic models: pseudo-first-order, pseudo-second-order, Elovich and the intra-particle diffusion models shortened as PFO, PSO, EM and IP respectively (J. Wang & Guo, 2020). The adsorption kinetic linear equations and the associated plots are presented in Eqns. 16-19 (Table 7).

Table 7: Linear forms and plots of the evaluated adsorption kinetic models

Model	Isotherm Linear form	Plot	Equation Number
PFO	$\ln(q_e - q_t) = \ln q_e - K_1 t$	$\ln(q_e - q_t)$ vs t	16
PSO	$\frac{t}{q_t} = \frac{1}{K_2 q_e^2} + \frac{t}{q_e}$	$\frac{t}{q_t}$ vs t	17
EM	qt= 1/βln (αβ) + 1/β ln (t)	qt vs. ln (t)	18
IP	$q_t = k_{id} t^{1/2} + C$	q_t vs $t^{1/2}$	19

For PFO, q_e denotes the equilibrium CAC adsorption capacity (g mg^{-1}), q_t denotes the amount of adsorbate adsorbed time t (g mg^{-1}) while K_1 denotes the PFO rate constant (min^{-1}). For PSO, q_e denotes the equilibrium CAC adsorption capacity (g mg^{-1}), q_t denotes the amount of adsorbate adsorbed time t (g mg^{-1}) whereas K_2 denotes the PSO rate constant ($g.mg^{-1}.min^{-1}$). For Elovich Model, α is the initial adsorption rate constant (mg g^{-1} min^{-1}) while β is the desorption process constant (g mg^{-1}). For IP, C denotes the film thickness, k_{id} denotes the IP kinetic rate constant, and q_t denotes the adsorption capacity of CAC at time t (g mg^{-1}) and t denotes the treatment time (min).

The adsorption kinetic study was conducted using initial metal ion concentration of 5mg/L at the optimized operating conditions (i.e. adsorbent dosage = 0.25 g; Temperature = 22.2 ºC; and pH = 8.5). Adsorbate solution of 200 ml was placed in 250 mL Erlenmeyer flask then the mixture underwent agitation using a mechanical shaker at 150 revolutions per minute (rpm) for different durations ranging from 30, 60, 90 and 120 minutes, upon which after a pre-determined agitation time, 20 mL of the supernatant was taken from the 250 mL Erlenmeyer flask for ICP-OES analysis.

Subsequently, metal ion removal efficiency and the quantification of adsorbed quantities of Cd (II) and Cr (VI) after a given treatment time (t) were calculated using Eqns. 10 and 11 respectively.

3.2.6. Adsorption thermodynamic experiments

The study also examined the effect of temperature and thermodynamic variables on Cd^{2+} and $Cr_2O_7^{2-}$ adsorption onto the CAC. Thermodynamic experiments were conducted by adding 0.1 L solution of 5 mg/L of both Cd^{2+} and $Cr_2O_7^{2-}$ into Erlenmeyer flasks (150 mL). Additionally, a 0.25 g dosage CAC was placed in each flask. While maintaining an agitation speed of 150 rpm for a duration of 105 minutes, the flasks temperatures were subsequently adjusted to 288.15 K, 303.15 K, and 318.13 K by adjusting the temperature of the automated water bath shaker. The thermodynamic parameters measured are ΔG°, the Gibbs free energy in J/mol, ΔS°, the entropy in kJ/mol, and ΔH°, the enthalpy variations in kJ/mol. Equations 20-22 were utilized to calculate the values of ΔG°, ΔH° and ΔS° respectively (Kwikima et al., 2022a).

$$\Delta G° = -RTlnKc \quad (20)$$

$$ln\ K_c = -\frac{\Delta H°}{RT} + \frac{\Delta S°}{R} \quad (21)$$

$$K_c = \frac{q_e}{C_e} \quad (22)$$

whereas ΔG° denotes the standard free energy change in J/mol, ΔH° denotes the standard enthalpy change in kJ/mol, ΔS° denotes the standard entropy change in J/(mol K, T denotes the solution absolute temperature (K), R denotes the universal gas constant (8.314 J/mol K), Kc denotes the equilibrium constant, q_e denotes the equilibrium adsorption capacity (mg/g), and C_e denotes the equilibrium concentration of metal ions in mg/L. Both ΔS° and ΔH° were computed from ln Kc vs. 1/T plot intercept and slope values.

3.3. IPA DESIGN, FABRICATION AND EVALUATION

3.3.1. IPA plate preparation and characterization

Similar procedure as reported in Sections 3.1.7 and 3.1.8 for CAC synthesis and characterization respectively was employed respectively when preparing the PJAC coated IPA plates. For the IPA plates, the substrate was made of 3 mm plexiglass and had different dimensions depending on the IPA angle of inclination as shown in Table 9. Specifically, the CCF was placed on same sized[2] plexiglass plate and then the homogeneous solution/slurry of APE/PJAC was applied on both the CCF and plate as already outline in Section 3.1.7. Similarly, the prepared PJAC/APE-CCF-Plate

[2] i.e. the CCF had the same size as the plexiglass plate while just leaving enough space e.g. ≤3mm on both ends of the plate to allow for plate insertion onto the IPS plate grooves.

was dried at 70 °C for 5 h. The flow diagram of IPA plate preparation as shown in Fig. 4 (a-e) shows a) CCF cutting to appropriate sizes, b) the plexiglass used as substrate, c) the CCF placed on same sized plexiglass, d) using brush to coat the PJAC/APE slurry onto the CCF placed on the plexiglass, e) PJAC/APE-CCF-Plate drying in an oven and f) final IPA plates product ready for use. The coated plates were then stored in airtight bags for characterization and use for the IPA experimentation (Fig. 7).

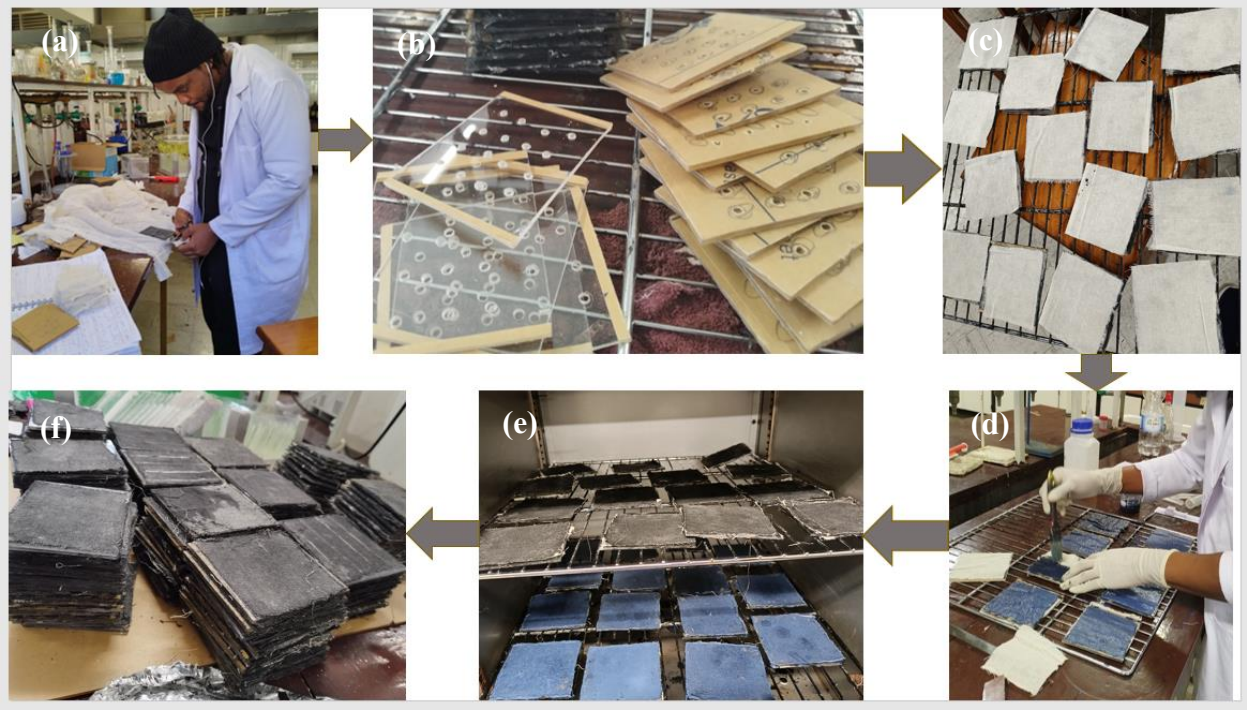

Figure 4: Flow diagram of the laboratory scale IPA plate adsorbent fabrication

3.3.2. Inclined Plate Settler Design Considerations

Table 8 shows the IPA design parameters that were considered before drawing and fabrication of the IPA system. These design parameters and their limits are based on experience of similar work (Chintokoma et al., 2015), resources and time constraints as well as from consultation of various previously published literature (Clark et al., 2007; Wisniewski, 2014; Zhang et al., 2020).

Table 8: Laboratory scale IPA design considerations

PARAMETERS	Unit	Inclined Plate Settler Coupled with Adsorbents		
Angle of Inclination	°	45	60	75
Plexiglass thickness	cm	0.3	0.3	0.3
Inlet Height	cm	11.00	11.00	10.50
Outlet Height	cm	9.00	10.00	9.50
Tank Height	cm	9.00	10.00	9.50

Tank Width	cm	10.00	10.00	10.00
Tank base, (base 1)	cm	14.00	14.00	16.00
Tank Top length, (bases 2)	cm	23.00	19.00	18.00
Effective IPA tank Height	cm	7.50	7.50	7.50
Big-inlet Plate length	cm	13.50	11.00	10.00
Big-inlet Plate width	cm	10.00	10.00	10.00
Plate Length	cm	10.50	9.10	8.03
Plate Width	cm	10.00	10.00	10.00
IPA effective length	cm	14.00	14.00	14.00
Number of Plates	Unit	13.00	15.00	17.00
Area per plate	cm^2	105	91	80.3
Adsorbent dosage per cm^2 of CCF (given 0.25g/75cm^2)	g	0.00333	0.00333	0.00333
Adsorbent per IPA plate per given IPA tank	g	0.3497	0.3030	0.2674
Total (effective) adsorbent dosage per given IPA tank	g	4.5455	4.5455	4.5458
Total Plate Area	cm^2	1365	1365	1365.1
Total Tank Volume	cm^3	1665	1650	1615
IPA effective volume with plates inside	cm^3	1050	1050	1050
Volume of the area occupied by plates without Spaces	cm^3	614.25	614.25	614.295
Tank Volume considering volume occupied by plates	cm^3	1050.75	1035.75	1000.705

3.3.3. Inclined Plate Settler Design

The design drawings of the IPA system were done using AutoCAD 2022 Version 24.1 (AC1032). Fig. 5 and 6 shows the 3D isometric view of the 45º angle inclined plate settler and the section view of the 60º angle inclined plate settler. The rest of the design drawings are presented as Annex 2.

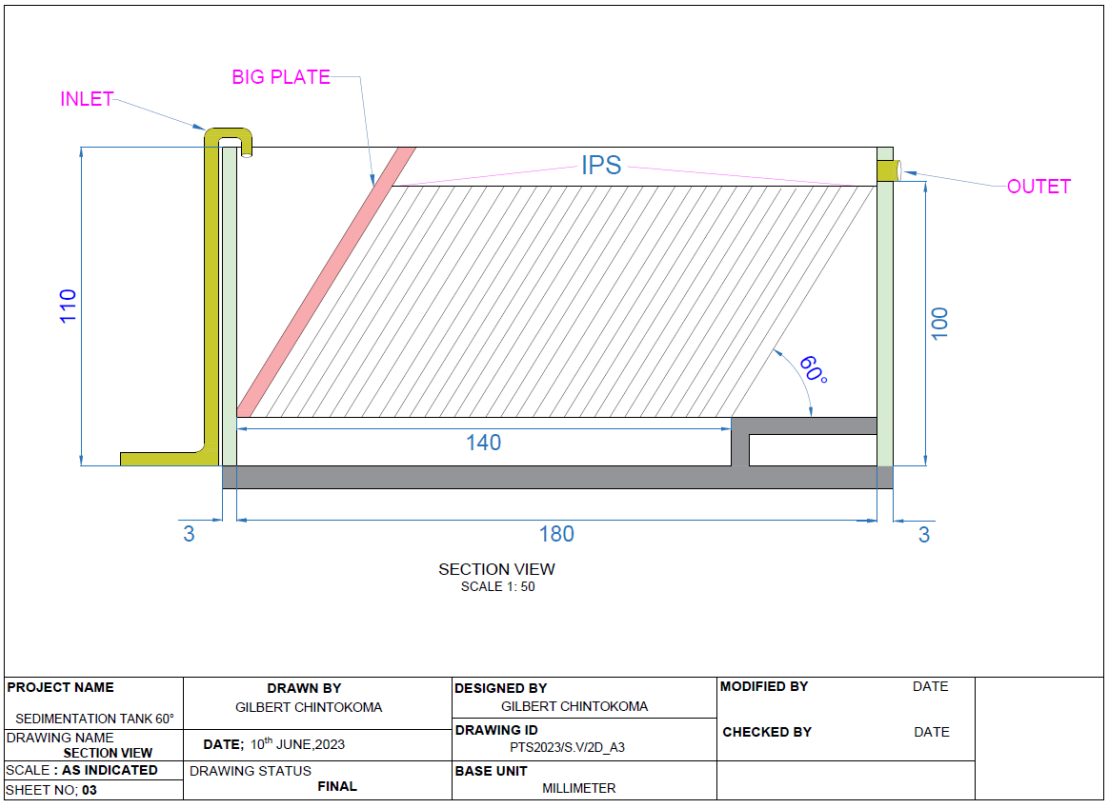

PROJECT NAME SEDIMENTATION TANK 60°	**DRAWN BY** GILBERT CHINTOKOMA	**DESIGNED BY** GILBERT CHINTOKOMA	**MODIFIED BY**	DATE
DRAWING NAME **SECTION VIEW**	**DATE;** 10th JUNE,2023	**DRAWING ID** PTS2023/S.V/2D_A3	**CHECKED BY**	DATE
SCALE : **AS INDICATED**	DRAWING STATUS **FINAL**	**BASE UNIT** MILLIMETER		
SHEET NO; **03**				

Figure 5: Section view of the 60º angle inclined plate settler

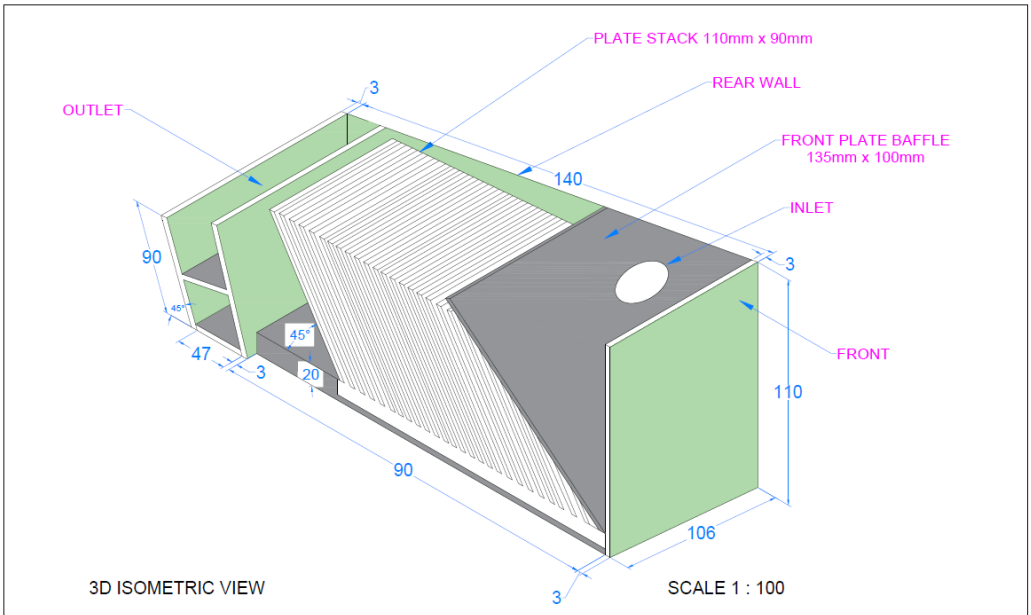

PROJECT NAME SEDIMENTATION TANK	**DRAWN BY** GILBERT CHINTOKOMA	**DESIGNED BY** GILBERT CHINTOKOMA	**MODIFIED BY**	DATE
DRAWING NAME **3D ISOMETRIC VIEW**	**DATE;** 30th MAY,2023	**DRAWING ID** PTS2023/3D.I/2D_A3	**CHECKED BY**	DATE
SCALE : **AS INDICATED**	DRAWING STATUS **FINAL**	**BASE UNIT** MILLIMETER		
SHEET NO; **04**				

Figure 6: 3D isometric view of the 45º angle inclined plate settler

3.3.4. IPA Fabrication

Based on the calculations and designs in sections 3.3.2 and 3.3.3, laboratory scale IPA tanks were fabricated using plexiglass of 3 mm thickness.

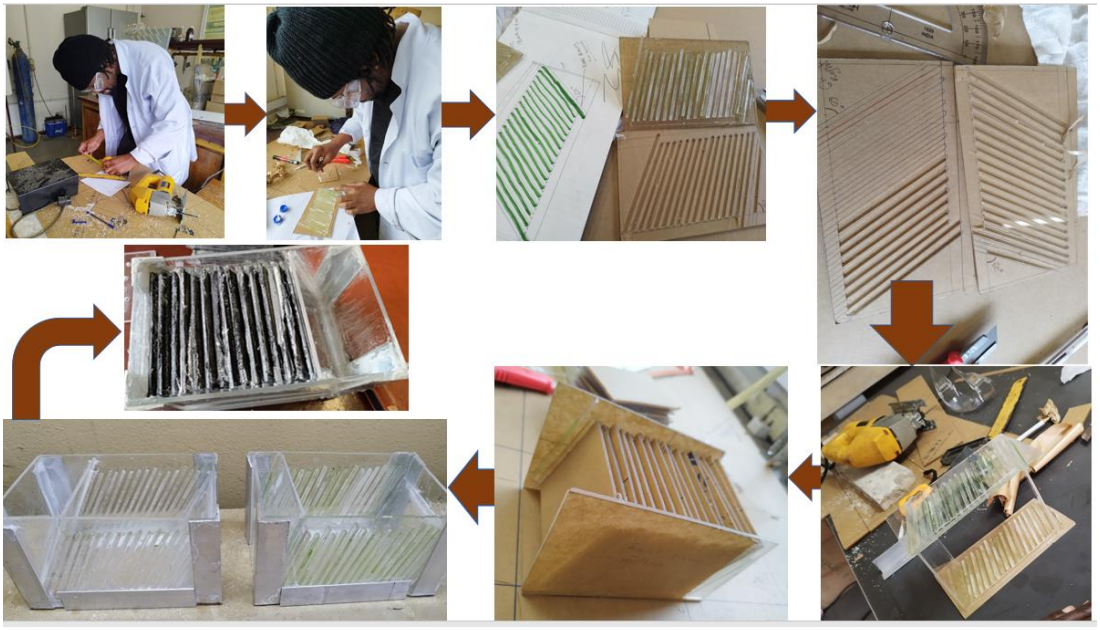

Figure 7: Flow diagram of the laboratory scale IPAfabrication process

3.3.5. IPA Heavy metal removal Design of Experiments

For objective three, cadmium was again used as the model heavy metal. The influence of angle of inclination (θ), influent flow rate (Q) and adsorbate initial concentration (C_i) on Cd^{2+} removal from aqueous solution using IPA was again studied by Box Behnken Design (BBD) of the Response Surface Methodology (RSM) (Singh Thakur et al., 2023). Equation 1 was again used to code the independent variables. Parameters were coded with three (3) levels: +1, 0, and -1, representing the high, center, and low levels, respectively based on values obtained from various literature as well as prior pilot experimentation (Table 9). The empirical second-order polynomial model (Eqn. 2) was used for fitting the experimental data.

Table 9: Levels of independent variables and experimental range for Cd^{2+} IPA experiments

Factor	Variables	Units	Levels of the coded variables		
			-1	0	+1
A	Angle of inclination (θ_p)	°	45	60	75
B	Influent flow rate (Q)	ml/min	5	12.5	20
C	Initial ion concentration (C_i)	mg/l	1	3	5

3.3.6. IPA continuous experiments and Cd^{2+} removal efficiency

The Standard 100 milligram per litre of Cd^{2+} solution was prepared using the established protocol outlined in the APHA, (2005) standard procedure. The required concentrations for each experiment of the IPA were attained by progressively diluting the original stock solution (1-5 mg/L). A pH meter (Eutech instruments PH 700 series) was used to measure and adjust the influent's pH to 8.5 before and during the IPA experimentation. The laboratory-scale IPA system comprised of 3mm thickness Plexiglass fabricated IPS, a peristaltic pump, and the CAC coated settler plates (Fig. 8).

Figure 8: Laboratory scale IPA experimental set up

For all the 15-IPA optimization experimentation, the peristatic pump continuously transferred influent of different concentration from the feed tank through the inlet to the tank with varying plate inclination angles (θ_p) at a controlled rate (Q) (Fig. 9). The influent from the inlet flow into the bottom of the IPS, raising steadily through the CAC coated plates and was finally discharged at the overflow weir through the outlet into the effluent tank. The shematic diagram of the lab-scale IPAexperimental set-up adapted from Chintokoma et al., (2015) is shown in Fig. 9. The ICP-OES (Agilent 5800) was again employed to quantify the concentration of adsorbate before and after

adsorption experiment, respectively. Similarly, Eqn. 6 was once more used to calculate the IPA Cd^{2+} percental removal efficiency (%).

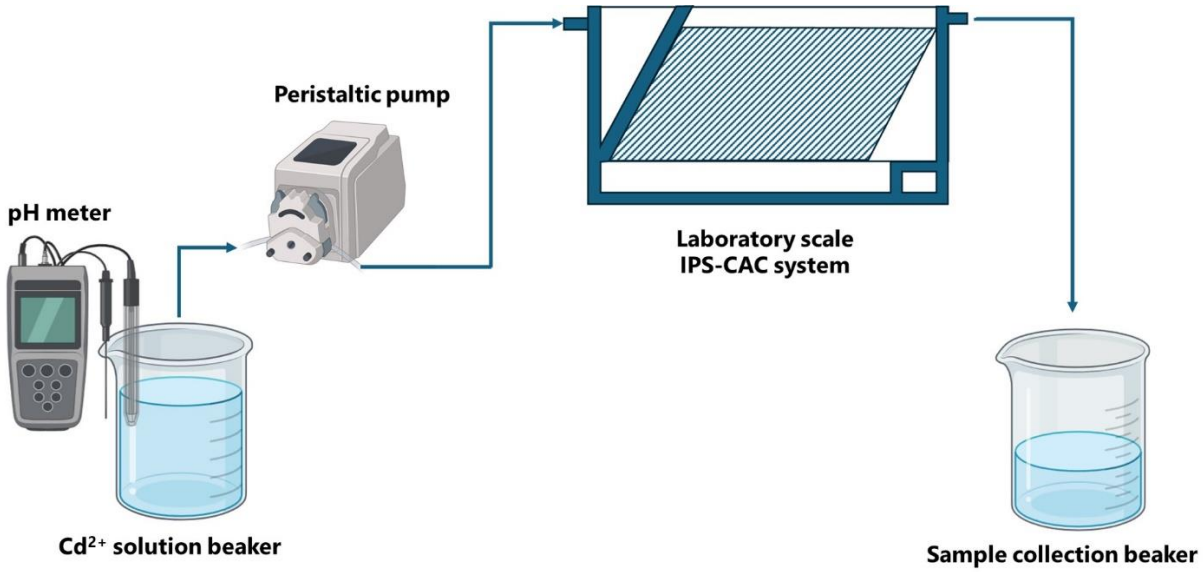

Figure 9: Schematic diagram of the lab-scale IPA experimental set-up

3.3.7. Breakthrough curve analysis and comparative tests

One goal of continuous or semi-continuous adsorption experiments is to produce a breakthrough curve and compute the maximum solid-phase concentration, which represents the adsorbent's maximal adsorption capacity. Breakthrough curves show how the pollutant concentration in the wastewater changes over time, mainly in a column experimental setup. They can be used to figure out how the continuous sorption process works. The findings may be utilized to develop and operate a full-scale treatment system. After optimization of the operating parameters in the IPA system, breakthrough experiments were conducted at the optimized conditions for a 14-day (336 hours) period.

The width and shape of the mass-transfer zone are determined by the adsorption isotherm, flow rate, mass transfer rate to the particles, and diffusion in the pores (Fernandez et al., 2023). Equation 23 can be used to estimate the stoichiometric/breakthrough time.

$$t_b = \int_0^{\infty} \left(1 + \frac{C_b}{C_o}\right) dt \qquad (23)$$

where C_b, is the breakthrough concentration (mg/L), C_o is the influent concentration and t_b is the breakthrough time (hrs.).

Equation 23 for breakthrough time or any time t, which represents the area above the curve between the limit t = 0 to t = t, can be written as Equation 24:

$$t_{st} = \int_0^t \left(1 + \frac{C_{st}}{C_o}\right) dt \tag{24}$$

Where t_{st} is the saturation time (hrs.) and C_{st} is the saturation concentration at time t_{st}.

Using the breakthrough curve analysis results, the IPA system overall breakthrough adsorption capacity, $\boldsymbol{Qe}$, (mg/g) of the CAC was calculated using Eqns. 25 and 26.

$$\boldsymbol{Qe} = \frac{(\boldsymbol{F}*\boldsymbol{C}*\boldsymbol{t}*\boldsymbol{D})}{\boldsymbol{m}} \tag{25}$$

$$\boldsymbol{D} = \left(\frac{\boldsymbol{C}}{\boldsymbol{C_o}}\right)_{\boldsymbol{final}} - \left(\frac{\boldsymbol{C}}{\boldsymbol{C_o}}\right)_{\boldsymbol{initial}} \tag{26}$$

Where $\boldsymbol{Qe}$ denotes the IPA overall breakthrough Cd^{2+} adsorption capacity (in mg/g), $\boldsymbol{F}$ denotes the optimized influent flow rate (in L/min), $\boldsymbol{C}$ and $\boldsymbol{C_o}$ are the breakthrough final and initial Cd^{2+} concentration (mg L^{-1}), respectively, $\boldsymbol{t}$ is the breakthrough time (in hours) $\boldsymbol{D}$ is the C/C_o displacement and $\boldsymbol{m}$ denotes the total mass of the CAC adsorbent dosage (in grams). Using Equation 25, the $\boldsymbol{t}$ was replaced with, $\boldsymbol{t_{ex}}$, exhaustion time (in hours) and similarly the $\boldsymbol{C}$ was replaced with $\boldsymbol{C_{ex}}$, the exhaustion concentration (in mg L^{-1}), to calculate the IPA adsorption capacity at exhaustion/saturation (in mg/g).

In addition, breakthrough curves were obtained by dynamic testing conducted in an IPA system, where the plate inclination angle, flow rates, and initial influent concentration were each varied at a time while the other factors were kept constant. The experiments were carried out at same pH, same total adsorbent dosage and same pump running time corresponding to same total volume of adsorbate per experiment except only for those experiments with varying flow rates. The total mass of adsorbent on CAC was always 45.5g (Table 8) with a total pump running time of 336 hours and adsorbate pH of 8.5. The IPA removal efficiency at the optimized conditions was also compared with the removal efficiency of a tank with no plates (IPS-NP) and tank with plain plates (IPS-PP). This experiment was also used to substantiate the argument on the Cd^{2+} removal mechanism by the IPA.

3.3.8. Evaluation of the IPA Cd^{2+} removal efficiency data

Regression analysis and ANOVA were performed on the experimental data using Design-Expert version 11 software. This analysis aimed at determining the relationship between the process variables and the Cd^{2+} removal. The interactions between factors and their effect on the IPA removal of Cd^{2+} were elucidated by the utilization of the same software program, which also facilitated the development of response surfaces as three-dimensional curves and two-dimensional contour plots. The models fit was assessed using the R-square (R^2). The model's statistical significance and its constituent components was evaluated using the F and p-values (95% confidence level). Microsoft Excel was used for calculating the mean 24-hour effluent concentration and for analyzing the breakthrough data. Both the mean effluent concentrations and the breakthrough graphs were plotted in OriginPro 2023 (Learning Edition) software.

3.4. CAC REGENERATION CAPACITY STUDY

3.4.1. CAC Adsorption-Desorption Experiments

The assessment of adsorption-desorption equilibrium is a key criterion for evaluating the full utilization of all active sites on an adsorbent (Ray et al., 2020, Aktar, 2021). Hence, after the assessment of the IPA Cd^{2+} removal efficiency (%) and overall CAC adsorption capacity (mg/g) under continuous set-up, the feasibility of reutilizing the adsorbent was as well examined using a batch adsorption configuration. Batch adsorption-desorption experiments were conducted with 5.34 mg/L adsorbate of pH of 8.5 and 70 mL of 0.1 M HCl of pH 0.3 as the eluent. Spent CAC was each placed in 70 mL desorption liquid in 250 mL flasks, which were subsequently agitated at 20°C and 200 rpm for 120 minutes. The adsorption-desorption studies were conducted in triplicates. The regenerated CAC was subjected to three cycles of application in order to analyze its adsorption behavior (Saini et al., 2019). After that, the supernatant was analyzed using ICP-OES to detect the Cd^{2+} concentrations in the samples. Equation 27 was used to calculate the Cd^{2+} quantity that was desorbed (Q_{de}):

$$\boldsymbol{Q_{de}(mg/g)} = \frac{\boldsymbol{C_i \times V}}{\boldsymbol{W_i}} \tag{27}$$

where $\boldsymbol{Q_{de}}$is the Cd^{2+} desorbed amount (mg/g), $\boldsymbol{V}$ is the HCl volume as desorption liquid (L), $\boldsymbol{C_i}$ denotes the concentration of Cd^{2+} in the desorption supernatant (mg/L), and $\boldsymbol{W_i}$ is the CAC mass (g). On the other hand, Cd^{2+} desorbed percentage (%) was calculated using Eqn. 28:

$$\boldsymbol{Cd^{2+}\ desorption}\ (\%) = \frac{\boldsymbol{Cd}_{\boldsymbol{desorbed}}}{\boldsymbol{Cd}_{\boldsymbol{adsorbed}}} \times \mathbf{100} \quad (28)$$

Where $\boldsymbol{Cd}_{\boldsymbol{desorbed}}$ and $\boldsymbol{Cd}_{\boldsymbol{adsorbed}}$ are the concentrations of desorbed and adsorbed Cd^{2+}, respectively

4. CHAPTER FOUR: RESULTS AND DISCUSSION

Chapter summary

This chapter provides an exposition of the research findings. The chapter comprises the empirical results and the subsequent analysis of the data, aimed at addressing the research objectives set-out in Chapter 1. The key research findings and analysis included in this chapter are 1) the optimum PJAC and CAC preparation parameters for Cd^{2+} *removal, 2) the optimized CAC and IPA* Cd^{2+} and $Cr_2O_7^{2-}$ *removal operation parameters, 3) the CAC* Cd^{2+} and $Cr_2O_7^{2-}$ *removal adsorption isotherms, kinetics and thermodynamics, 4) the proposed dominant IPA* Cd^{2+} *removal mechanism, 5) the adsorbent capacity at both breakthrough and saturation time and 6) reusability of the spent adsorbent.*

4.1. CAC SYTHESIS FROM PJAC AND ITS CHARACTERIZATION

The PJAC preparation and characterization section is mainly based on the following published papers:

Chintokoma, G.C., Chebude. Y., & Kassahun, S.K (2024). Cd^{2+} removal efficiency of activated carbon from *Prosopis Juliflora*: Optimization of preparation parameters by the Box-Behnken Design of Response Surface Methodology. *Heliyon.* 10(10). https://doi.org/10.1016/j.heliyon.2024.e31357 **(Elsevier)**.

While the CAC preparation and synthesis sections are partly based on the following published paper;

Chintokoma, G.C., Chebude. Y., & Kassahun, S.K., Demesa, A. G., & Koiranen, T. (2024). Sol-gel synthesis of composite adsorbent coating from Prosopis juliflora –activated carbon for simultaneous adsorptive removal of Cd^{2+} and $Cr_2O_7^{2-}$ from wastewater. *AQUA — Water Infrastructure, Ecosystems and Society*, *73*(5), 945–968. https://doi.org/10.2166/aqua.2024.335 **(IWA Publishing)**.

4.1.1. PJAC proximate and ultimate analysis

Carbon samples' proximate analysis provides information about the moisture and volatile matter, fixed carbon and ash content (Oke et al., 2022). On the other hand composition of C, H, N as well as other elements such as S and O (the primary components) in weight percentage is revealed upon doing an ultimate analysis of the carbon samples (Chowdhury, 2013). Table 10 summarizes the proximate and ultimate analysis of *Prosopis Juliflora* from previous studies (Emirie, 2015; Keerthivasan et al., 2019; Mahajan et al., 2017). The table demonstrates that the low ash and high carbon content of *Prosopis Juliflora* make it a promising candidate for usage as a raw material for activated carbon preparation for use as an adsorbent (A. Kumar & Jena, 2016; Ukanwa et al., 2020).

Table 10: *Prosopis juliflora* Proximate and ultimate analysis

Analysis type	**Biomass (weight %)**		**Activated carbon (weight %)**
Proximate analysis			
Reference	(Emirie, 2015)	(Mahajan et al., 2017)	
Moisture	11.5	10.85	2.98
Volatile matter	71	72.83	17.54
Fixed carbon	15.19	14.47	78.56
Ash	2.22	1.85	0.92
Ultimate analysis			
Reference	(Keerthivasan et al., 2019)	(Mahajan et al., 2017)	
Carbon	47.16	45.20	79.81
Hydrogen	5.81	5.58	2.48
Nitrogen	0.42	0.65	0.61
Oxygen	46.41	51.50	17.04
Sulphur	0.20	0.07	0.61

4.1.2. PJAC characterization

As already mentioned in Section 6.1.6, the characterization of the activated carbon was done only on the PJAC prepared under the determined optimized preparation parameters.

4.1.2.1. PJAC SEM-EDX and S_{BET} analysis

The PJAC morphology before and after Cd^{2+} adsorption is shown using SEM images under different magnification (Fig. 10(a-b)) and the PJAC elemental composition is shown in Fig. 10(c-d). As seen from Figures 10(a-b). The PJAC surface morphology was rough, porous and had a BET surface area (S_{BET}) of 600.4 m^2/g which provides a relatively substantial number of active sites for Cd^{2+} adsorption. The activated carbon's relative high surface area is because of the presence of many grooves and projections as depicted in figures 5(a-b) (Gopal et al., 2014). The EDX analysis shows the presence of ZnCl2 which affects Cd adsorption by improving the surface area and pore

distribution of the adsorbent, which may enhance the overall capacity for cadmium uptake (Mbarki et al., 2022).

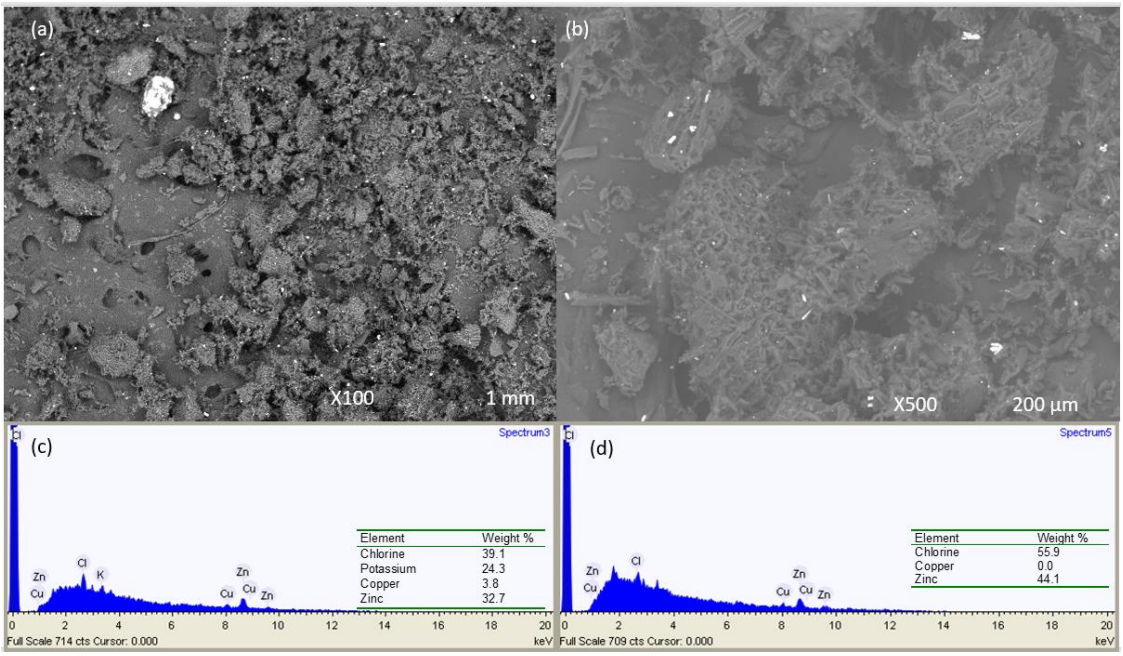

Figure 10: SEM image (a-b) and EDX spectrum (c-d) of the PAC prepared under optimized conditions

4.1.2.2. PJAC FTIR analysis

The characteristic pattern for the adsorption of Cd^{2+} onto both loaded and unloaded powdered activated carbon (PAC) was investigated by using FTIR spectroscopic analysis (Fig. 11). FTIR studies are employed to predict the types of functional groups contained in adsorbent materials (M. Kumar & Tamilarasan, 2017). The characteristic FTIR spectra of activated carbon pre and post adsorption provide the presence of preliminary functional groups present in them and which functional groups are engaged in the adsorption process respectively.

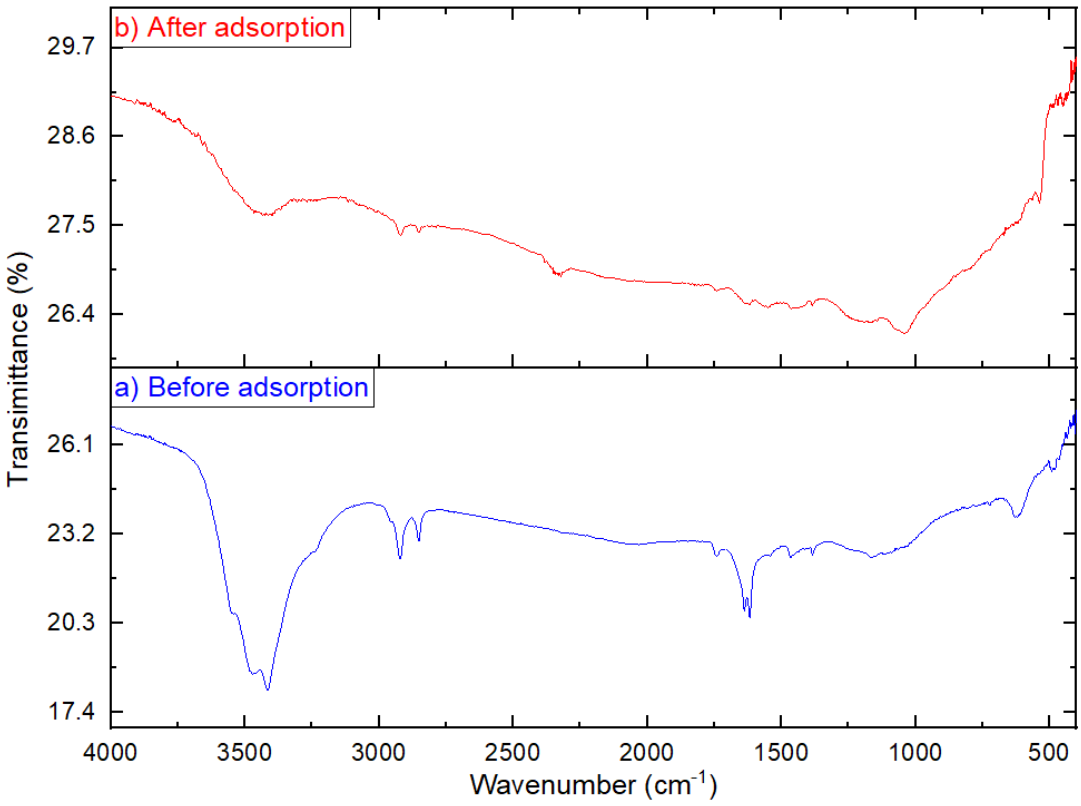

Figure 11: FT-IR spectra of the PJAC prepared under optimal conditions; a) before and b) after adsorption

Spectra of the sample before adsorption (Fig. 11a) display a wide band within frequency range 3600 to 3000 cm^{-1} which suggests presence of -NH stretching and -OH bonding of hydroxyl, carboxyl group, and phenol or alcohol groups (Najmi et al., 2020). Peaks of preliminary functional groups of the unloaded adsorbent show a relatively broad peak at 3472 and 3415 cm^{-1} (0-H stretching) (Somyanonthanakun et al., 2023), sharp peaks at 2921 cm^{-1} and a relatively small peak at 2851 cm^{-1} (C-H stretching alkane) (Reddy et al., 2014) and a presence of a sharp peak at 1618 cm^{-1} (C=C stretching). The study's observed peaks are consistent with those from results found by both (Emirie, 2015) and (Kaur et al., 2021).

After the adsorption of Cd^{2+}, the PAC shows there was reduction in the peak heights and disappearance of some peak heights including some changes in the peak positions of the FTIR spectrum (Fig 11b). There are significant changes in the position and intensity of peaks in the FTIR spectra after Cd^{2+} adsorption. After adsorption (Fig. 11b), the PJAC shows a significant reduction in peak bands, suggesting that the functional groups are fully engaged in the adsorption process.

The observed peak reduction reveals that there was a strong characteristic adsorption of Cd^{2+} onto the PJAC surface. The FTIR study of PJAC shows distinct peaks that indicate availability of

various functional groups. These functional groups i.e. methyl, methylene, alkanes, amide, and organo-halogens, are crucial to Cd^{2+} adsorption (Kaur et al., 2022). Cd^{2+} adsorption has been discovered to be related with interactions involving carboxylic, hydroxyl and amino acid groups (Kaur et al., 2022; Kwikima et al., 2022b). The hydroxyl (-OH) groups are involved in the formation of hydrogen bonds with Cd ions while the carboxyl (-COOH) groups can chelate Cd ions, forming stable complexes. These interactions between both functional groups enhances the overall adsorption of Cd ions (Vázquez-Guerrero et al., 2021). On the other hand amino acid groups can facilitate Cd2+ adsorption by providing active sites for interaction with Cd2+ ions through the "bridge effect" created by the protonated amino groups (Song et al., 2020).

4.1.2.3. PJAC pH_{PZC} determination

Based on precursor source and preparation method, the surface of any activated carbon might be neutral, acidic, or basic. This surface nature of the PJAC in this work was determined by the pH_{PZC} i.e. pH at which the adsorbent surface achieves electrical neutrality and is also referred to as the isoelectric point. (H. Deng et al., 2009). In addition, understanding the electrostatic interactions during the adsorption process is contingent upon the pH_{PZC} value. As shown from Fig. 12, the PJAC pH_{PZC} is slightly acidic at 6.92. Several previous studies on the preparation of zinc chloride modified carbons have shown similar slight acidic pH of point of zero charge: 6.85 (Farnane et al., 2020), 6.0 (Mbarki et al., 2022) and 5.92 (H. Deng et al., 2009).

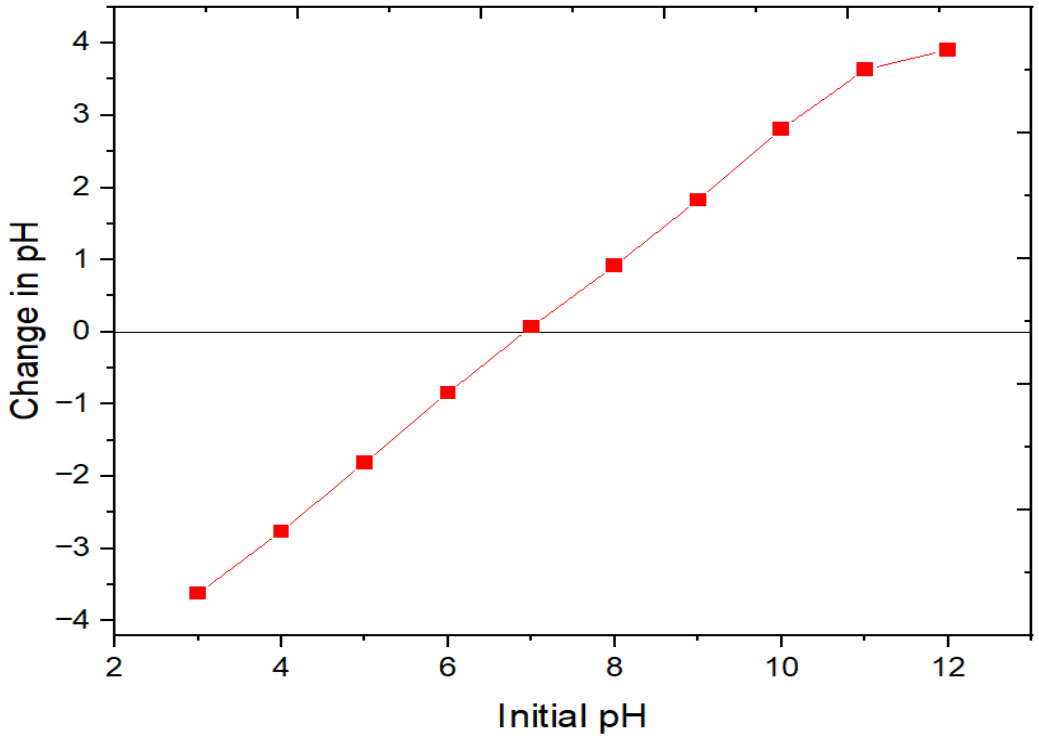

Figure 12: Point of Zero Charge (pH_{PZC}) of the prepared PJAC

4.1.2.4. PJAC XRD analysis

The XRD analysis investigated the amorphous or crystalline structure of the PJAC before (unloaded) and after (loaded) Cd^{2+} adsorption (Fig. 13). From the Fig. 13b, the presence of broad and diffuse peaks around 23° 2θ angle 44° 2θ angle respectively can be noted which signify the amorphous nature of the synthesized adsorbent. Evidently, the loaded PJAC (Fig. 13a) shows some variations in the intensity of peaks as compared to that of unloaded PJAC (Fig. 13b) due to the adsorption of Cd^{2+} onto the PJAC surface.

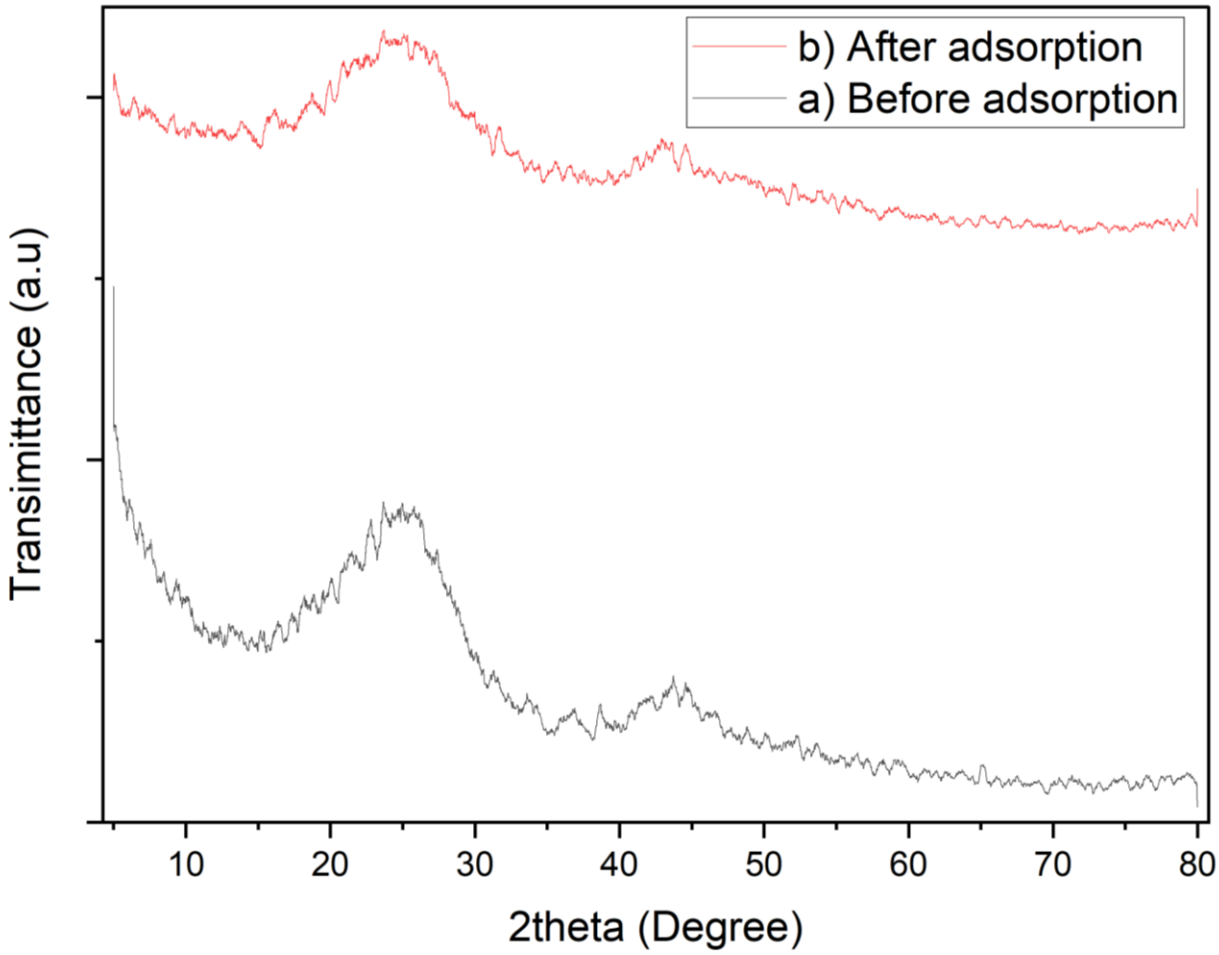

Figure 13: XRD profile for the prepared Prosopis Juliflora activated carbon (a)before and (b) after adsorption

4.1.3. CAC characterization

4.1.3.1. CAC SEM and BET Analysis

The SEM images of plain CCF and CAC (before and after adsorption of Cd^{2+} and $Cr_2O_7^{2}$) were captured at different magnifications as shown in Fig. 14. In the SEM micrograph of the plain CCF (Fig. 1a-b), the cotton fibers of the CCF are very evident but lack a rough structure. Clearly the cellulosic fibers are arranged in a loosely spiral network in the plain CCF sample. The presence of intra-fibrous holes in the CCF clearly contribute to its high surface area. According to Kumar et al., (P. Kumar et al., 2022), cotton fiber is predominantly composed of cellulose, accompanied by a limited number of non-cellulosic components that encompass the cellulose core. CCF's large surface area, low weight, ease of handling, and affordable pricing (Azha et al., 2017b), makes it a

good material as an ideal substrate. These characteristics make the use of CCF in wastewater treatment facilities practical and relatively cost effective.

The SEM images of CAC with different adsorbent dosages (Fig. 14(c-h)) is illustrates the porous, rough surface resulting from the coated adsorbent, consequently increasing the adsorbent capacity as compared with the plain CCF (Fig. 14(a-b)). The homogenous structure observed in the CAC morphology suggests that the APE-DI-adsorbent mixture was well blended during the preparation of the CAC. On the other hand, the bright spots in the after-adsorption SEM images indicate the adsorption of Cd^{2+} and $Cr_2O_7^{2}$ onto CAC (Fig. 14(i-j)) depicting the surfaces of particles after adsorption. The S_{BET} area of the prepared CAC was determined to be 10.6 m^2g^{-1}. In a study conducted by Azha et al., (Azha et al., 2017b) focusing on the removal of industrial dye utilizing a bentonite clay layer supported by an acrylic polymer emulsion, the S_{BET} of the prepared composite was found to be 5.55 m^2g^{-1}. Notably, the S_{BET} found in this study is comparatively higher than the value of 2.085 m^2/g reported by Shamsudin & Shahadat, (Shamsudin & Shahadat, 2019) in their synthesis of an composite adsorbent coating material. The relatively low specific surface areas found in all these studies could be attributed to the challenges with regards to preparing and the difficulty in getting a representative sample of the CAC as a powdered specimen for BET and porosity analyses.

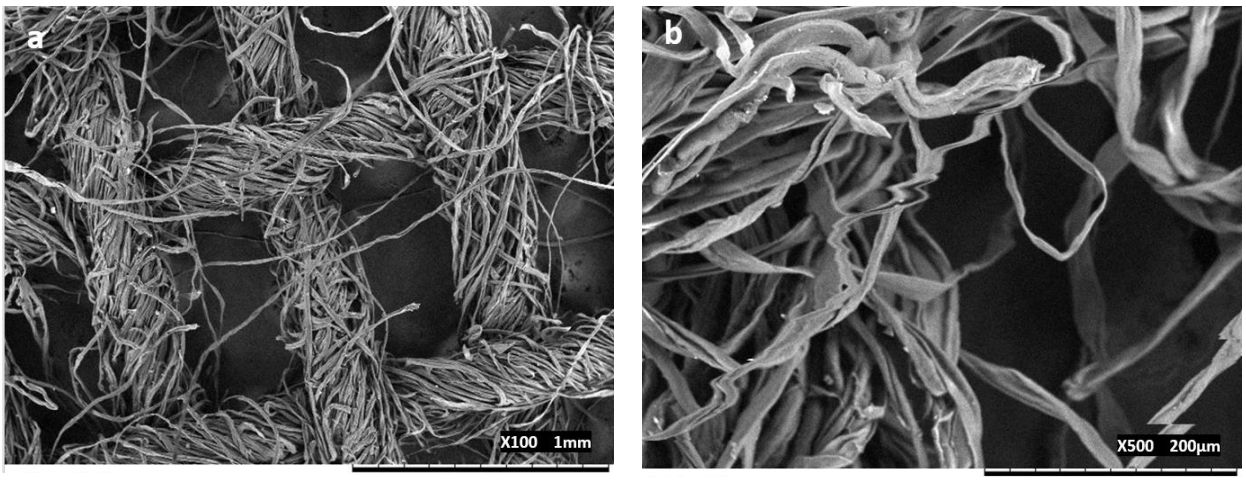

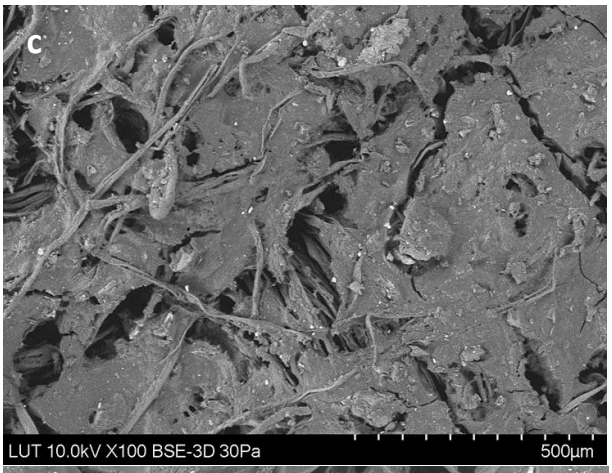
c
LUT 10.0kV X100 BSE-3D 30Pa
500µm

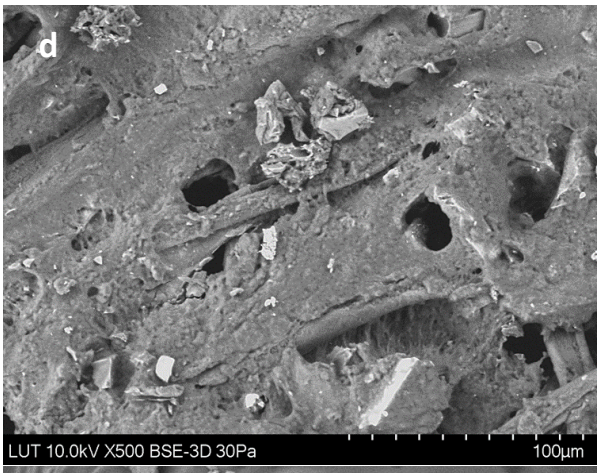
d
LUT 10.0kV X500 BSE-3D 30Pa
100µm

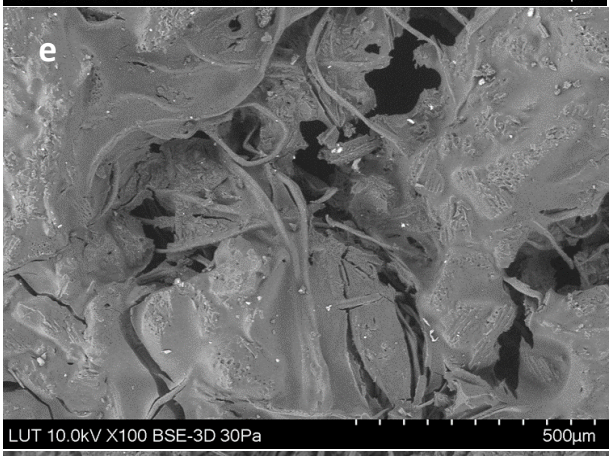
e
LUT 10.0kV X100 BSE-3D 30Pa
500µm

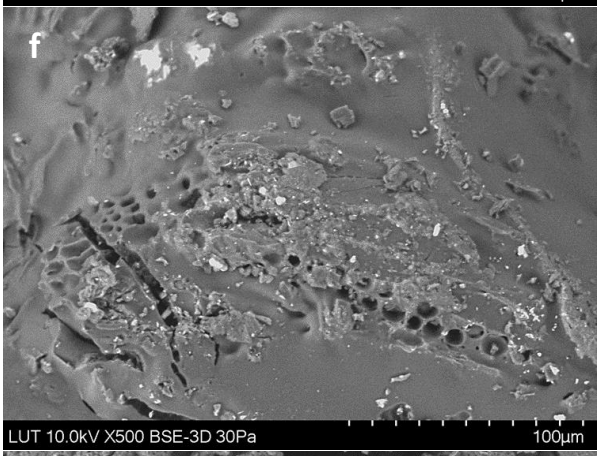
f
LUT 10.0kV X500 BSE-3D 30Pa
100µm

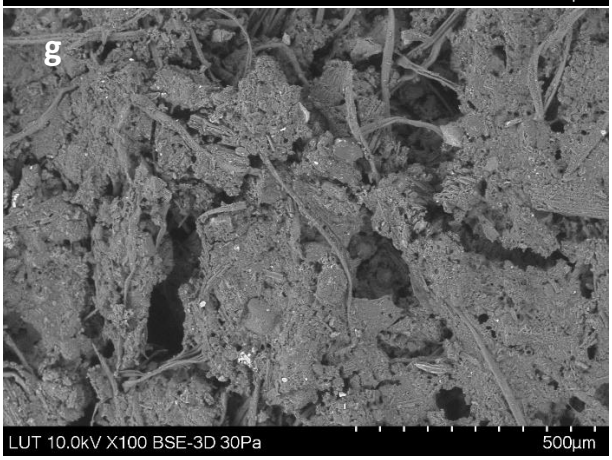
g
LUT 10.0kV X100 BSE-3D 30Pa
500µm

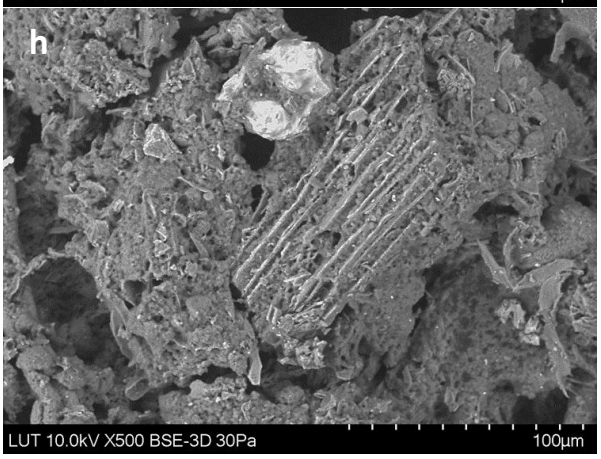
h
LUT 10.0kV X500 BSE-3D 30Pa
100µm

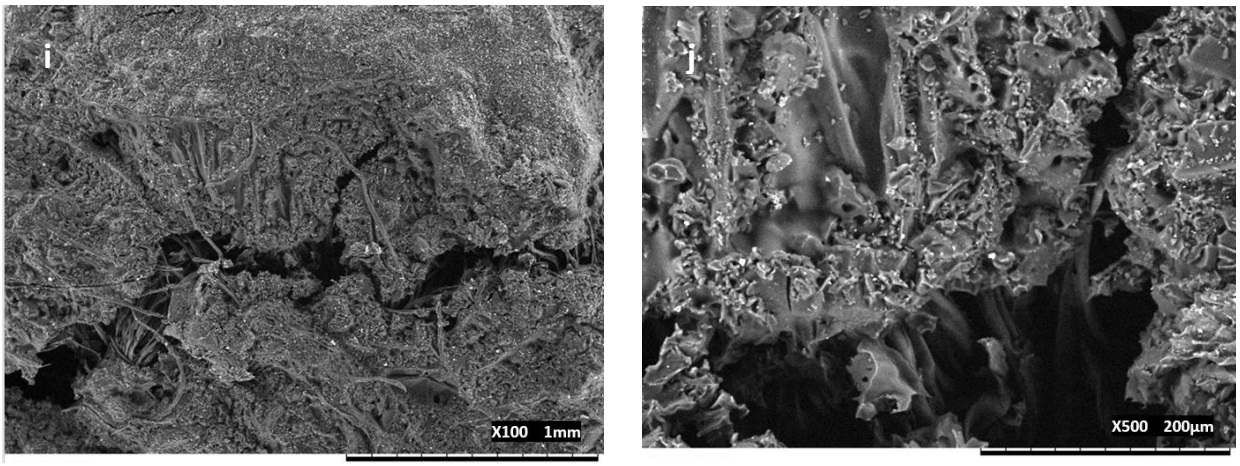

Figure 14: SEM images (with different magnifications) of plain uncoated CCF(a-b), PAC (c-d), 0.25g CAC(c-d), 0.5g CAC (e-f), 0.75g CAC (g-h) before adsorption and contaminated 0.25 CAC after adsorption of Cd^{2+} and $Cr_2O_7^{2-}$ (i-j)

4.1.3.2. CAC FTIR Analysis

The FTIR analysis was performed to ascertain the presence of functional groups on the surface of the CAC. Additionally, FTIR was utilized to evaluate any alterations in the functional groups of the clean and loaded CAC. The FTIR spectra of APE and the prepared CAC are presented in Fig. 15(a-e). The broad APE peak at 3000-2830 cm^{-1} together with a sharp APE spectra peak at 1780-1670 cm^{-1} corresponds to C-H and C=O group stretching. The appearance of both peaks confirms the presence of a carboxylic acid rather than an alcohol (Smith, 2011). On the other hand, the broad peak observed at 3700-3200 cm^{-1} in the CAC corresponds to O-H stretching. Vividly the intensity of this peak increased as the adsorbent dose on CAC also increased. After the adsorption of Cd^{2+} and $Cr_2O_7^{2-}$ the CAC shows an almost complete disappearance of the peak heights of the FTIR spectrum (Fig 2e).

The observed reduction in peak intensity in the FTIR spectra following Cd^{2+} and $Cr_2O_7^{2-}$ adsorption shows that the functional groups are fully involved in the adsorption process. Moreover, the disappearance of the peaks reveals that there was a strong characteristic adsorption of either Cd^{2+} or $Cr_2O_7^{2-}$ or both onto the surface of the CAC. The decrease in the intensities of the functional groups of on the CAC could be as a result of reduced vibration intensity or changes in peak positions due to altered bond strengths as a result of physical adsorption by electrostatic attraction and or pore filling onto the adsorbent surfaces.

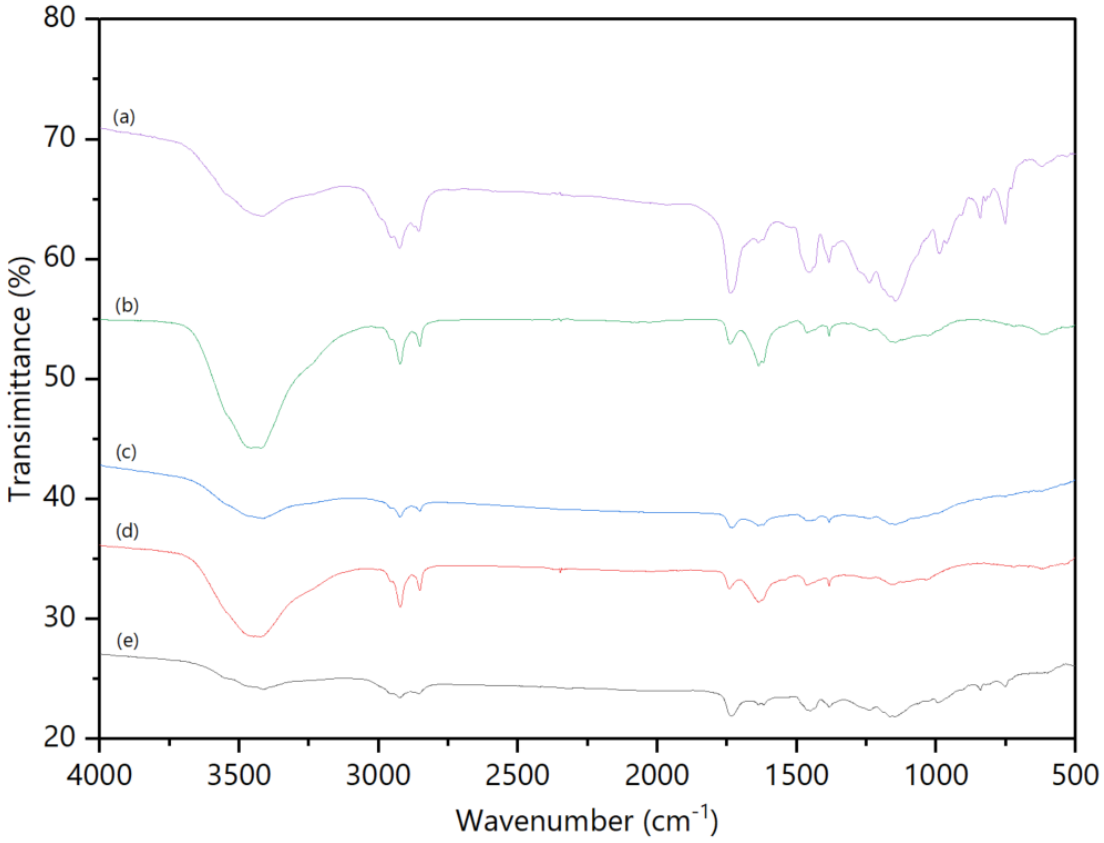

Figure 15: FTIR spectra of APE (a), 0.75g CAC (b), 0.5g CAC (c) 0.25g CAC before (d) after adsorption of Cd^{2+} and $Cr_2O_7^{2-}$ (e)

4.1.3.3. CAC pH_{PZC} determination

The surface property of the CAC in this study was determined by the Point of Zero Charge (pH_{PZC}) which represents the pH value at which the surface of the adsorbent attains overall electrical neutrality (H. Deng et al., 2009). As shown in Fig. 16, the pH_{PZC} of the prepared CAC is slightly acidic but increases with adsorbent dosage. It is shown that the 0.25 g CAC exhibited a pH_{PZC} of 6 while the 0.5 g CAC and 0.75g CAC both had a pH_{PZC} of 6.6. When comparing with the pH_{PZC} values among the CACs of different dosages, the relatively lower pH_{PZC} observed on the 0.25 g CAC (6.0) in comparison with the other CAC dosages (6.66) could be attributed to the basic nature of the APE which served as the binder of the adsorbent onto the substrate (MCP, 2012). Nevertheless, it was crucial to understand the adsorbent's point of zero charge because it affects the

electrostatic interactions occurring between the adsorbate and CAC. For instance, negatively charged adsorbent surface foster electrostatic interactions that facilitate the adsorption of positively charged ions, such as Cd^{2+}, when the solution pH is higher than pH_{PZC}. However, as the pH of the solution drops, the positively charged adsorbent surface facilitates the adsorption of negatively charged ions like $Cr_2O_7^{2-}$ (Renu et al., 2023).

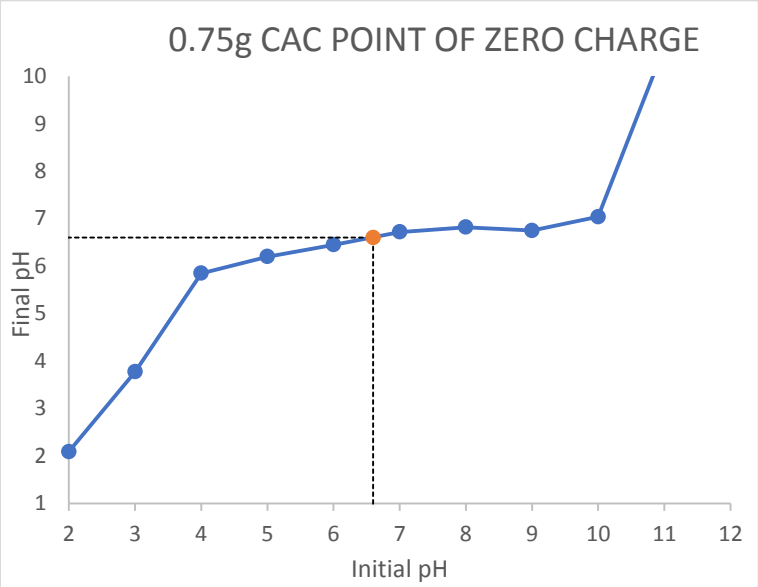

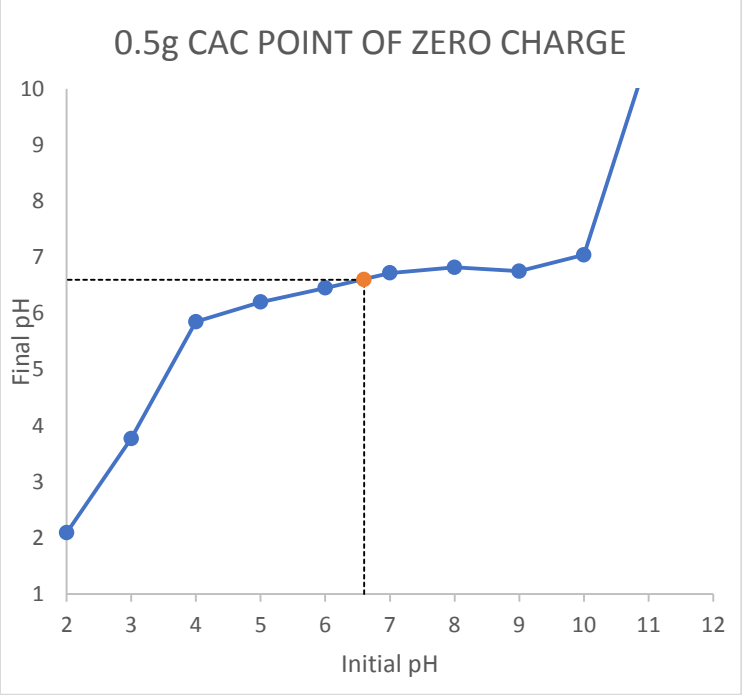

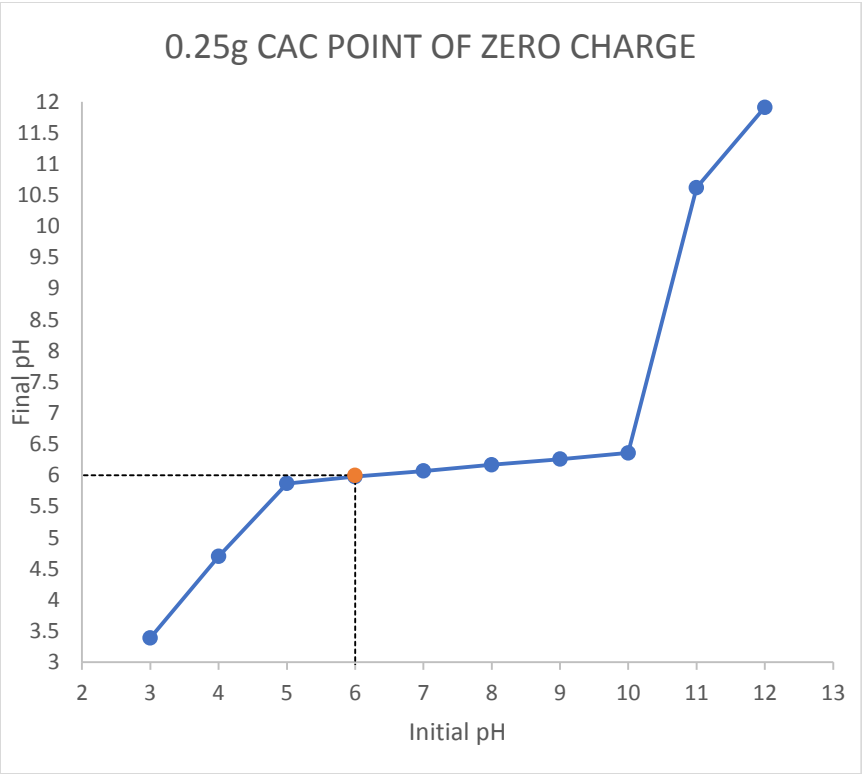

Figure 16: pH_{PZC} of the prepared CAC with different adsorbent dosages

4.1.4. Statistical analysis for PJAC preparation

4.1.4.1. ANOVA, Model Fitting and Model Diagnostic Model

The correlations between PJAC preparation variables and Cd^{2+} removal efficiency as the response values was developed by the BBD. Table 11 displays the comprehensive design matrices along with the response values gleaned from the experimental results. Runs 10-12 were undertaken at the center point to assess the experimental error and also check study results' repeatability. Using Eqn. 10, the Cd^{2+} percentage removal efficiency (%) ranged from 41.25% to 99.82%.

Table 11: BBD experimental design setup and results for the synthesis of the PJAC

Run	Impregnation Ratio, IR, (X_1)	Carbonization Temperature, T, (°C) (X_2)	Carbonization Time, t, (min) (X_3)	Initial Cd^{2+} Concentration (mg/L)	Final Cd^{2+} Concentration (mg/L)	Cd^{2+} Percent Removal Efficiency (%)
1	1.5	500	120	100	40.43	59.57
2	1.5	600	180	100	58.5	41.5
3	1	500	60	100	28	72
4	1	600	120	100	37.82	62.18
5	2	400	120	100	17.45	82.55
6	1.5	400	180	100	1.62	98.38
7	1	400	120	100	49.25	50.75
8	1	500	180	100	58.75	41.25
9	1.5	500	120	100	41.43	58.57
10	2	500	180	100	49.25	50.75

11	1.5	500	120	100	40.75	59.25
12	1.5	400	60	100	42.81	57.19
13	2	600	120	100	50.69	49.31
14	2	500	60	100	38.02	61.98
15	1.5	600	60	100	0.18	99.82

The study assessed the coefficients of the model for constant terms, quadratic effects, cubic effects, and interaction effects. ANOVA and regression analysis findings for the quadratic model of the response surface for Cd^{2+} removal efficiency using PJAC adsorption are displayed in Table 12. The P-value evaluates each coefficient's statistical significance and the intensity of the interaction among the factors, with effects below 0.05 being deemed significant (Montgomery, 2017). As the level of significance increases, the relationship between observed and predicted values also increases (A. Ahmad et al., 2020). The model's F-Value of 43.33 showed that the model was significant (*p=0.0003*) implying that at-least one of the variables in the model significantly influences Cd^{2+} adsorption by PJAC. For the Lack of Fit test, the F value of 0.32 and p-value of 0.8182 indicates that the Lack of Fit is not significant compared to pure error and also that it is not statistically significant for the experimental settings respectively. This suggests that the model is sufficient (Christensen, 2016).

Table 12 shows that of all the individual parameters under study, carbonization temperature (T) was the most significant preparation parameter (Sum of Squares (SS) =1323.8, *p-value=0.0001*), followed by carbonization time (SS=245.98, *p-value=0.0058*) and the least significant parameter was the impregnation ratio (SS=152.69, *p-value=0.015*).

Table 12: The ANOVA and regression analysis findings for the quadratic model's response surface for Cd^{2+} % removal efficiency by PJAC adsorption

Source	**Sum of Squares (SS)**	**Degree of Freedom (df)**	**Mean Square**	**F-value**	**p-value**	
Model	4516.53	9	501.84	43.33	0.0003	significant
A-Impregnation Ratio	152.69	1	152.69	13.18	0.0150	
B-Carbonization Temperature	1323.81	1	1323.81	114.31	0.0001	
C-Carbonization Time	245.98	1	245.98	21.24	0.0058	
AB	935.75	1	935.75	80.80	0.0003	
AC	0.0000	1	0.0000	2.159E-06	0.9989	
BC	8.44	1	8.44	0.7287	0.4323	
A^2	323.48	1	323.48	27.93	0.0032	
B^2	1380.34	1	1380.34	119.19	0.0001	
C^2	49.53	1	49.53	4.28	0.0935	
Residual	57.91	5	11.58			
Lack of Fit	18.58	3	6.19	0.3151	0.8182	not significant
Pure Error	39.32	2	19.66			
Corrected Total SS	4574.43	14				

$R^2 = 0.9873$; adjusted $R^2 = 0.9646$; predicted $R^2 = 0.9157$; adequate precision=21.0418

The high regression coefficient (R^2=0.9873) showcases the model's ability to forecast response in the experimental input data. The observed 21.04 adequate precision indicates an acceptable and adequate signal-to-noise ratio (i.e. >4). Again the adjusted R^2 of 0.9122 is lower than the R^2 value (0.9873), indicating that "the additional input variables are or could not add value to the model"(Mahmood et al., 2020). The Predicted R^2 (0.9157) and the adjusted R^2 (0.9646) exhibit a satisfactory level of concordance as the difference between them is less than 0.2. According to the measured R^2 values, the PJAC adsorption process was satisfactorily explained by the regression models. Consequently, the model developed in this work was deemed adequate for predicting Cd^{2+} removal efficiency from aqueous medium. Figure 17 depicts the standard probability curve of residues. The output may be inferred from the fact that the model is deemed acceptable due to the occurrence of a fairly linear relationship among the points in the graph.

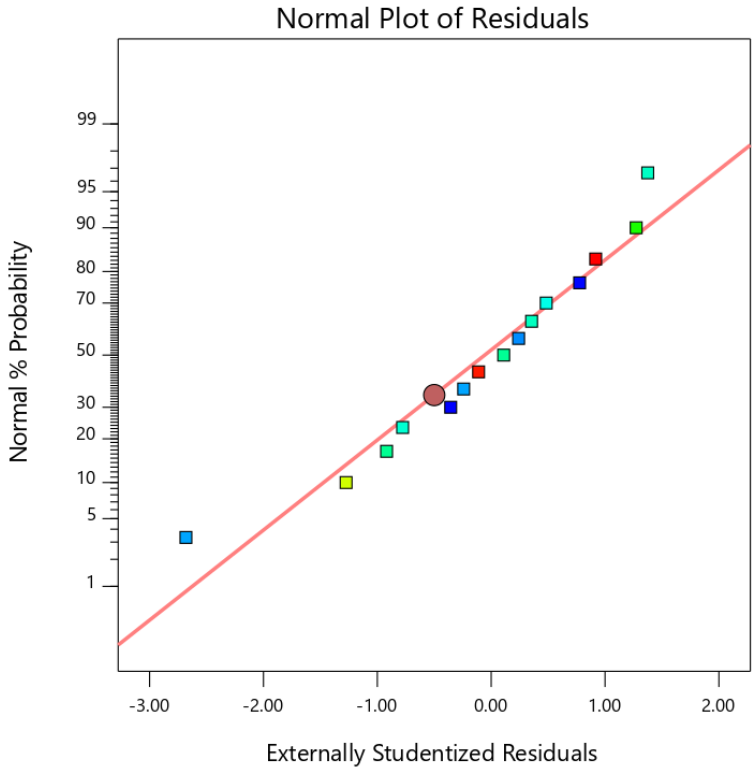

Figure 17: Normal probability plots PJAC adsorption process

The model's correctness was determined by examining the experimental diagnostic plots and outcomes of the model (Fig. 18(a-b)). With regards to actual residues against the fit plot, for a model to be reliable; a model must not exhibit any sequence of rising or falling point patterns in the real residues versus the fitted values (Montgomery, 2017; Nyangi et al., 2020). The close alignment

between residuals and predicted Cd^{2+} removal (Fig. 18a) corroborates with the ANOVA results presented in Table 12.

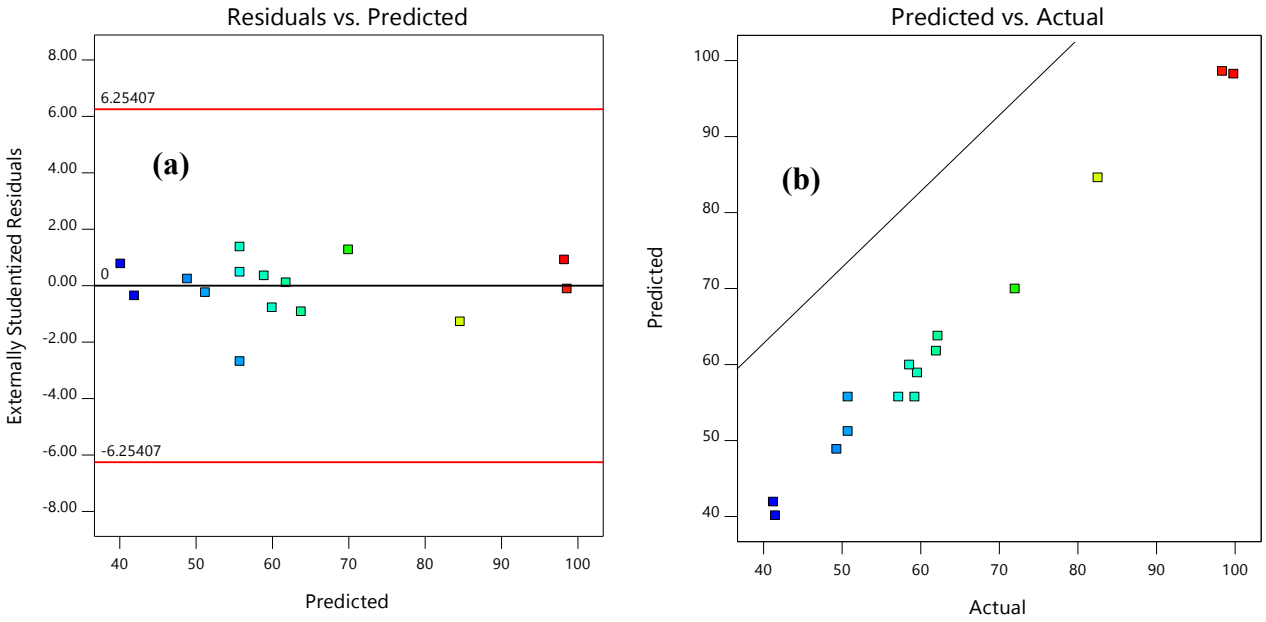

Figure 18: a) Residuals and predicted results plots for Cd^{2+} removal by PJAC adsorption process and b) Predicted and actual results plots for Cd^{2+} removal by PJAC adsorption process

The predicted and actual graphs in Fig. 18(b) further support the strong correlation between the projected and actual results. This indicates that the model was capable of making accurate predictions within the constraints of the set of the preparation parameters (Montgomery, 2017). It can, therefore, be concluded that the response surface's quadratic model developed in this work accurately describes the experimental data of Cd^{2+} removal efficiency with preparation factors in PJAC adsorption.

4.1.4.2. Model Equations based on coded and actual factors

A quadratic model was chosen based on the recommendation of BBD of Design Expert for the PJAC Cd^{2+} adsorption from an aqueous solution. Basing on the sequential model sum of squares (SS), the models were chosen by considering the highest order polynomials with significant additional terms and avoiding any model aliasing. The equations for the percentage removal efficiency of Cd (II) are expressed by second order polynomial Eqns. (29) and (30), representing the coded and actual factors, respectively.

$$\boldsymbol{Coded\ factors\ Cd(II) Removal\ Efficiency}\ (\%) = 55.73 + 4.37A + 12.86B + 5.55C + 15.3AB + 0.002AC + 1.45BC - 9.36A^2 + 19.34B^2 + 3.66C^2 \quad (29)$$

$$\boldsymbol{Actual\ factors\ Cd(II) Removal\ Efficiency}\ (\%) = 624.9650 - 31.9025IR - 2.2928T - 0.2729t + 0.3059IR * Temp + 0.0001IR * t + 0.0002T * t - 37.44IR^2 + 0.0019T^2 + 0.001t^2 \quad (30)$$

Where *A*, *B*, and *C* represent the coded values and *IR*, *T*, and *t* represent the actual values for impregnation ratio, the carbonization temperature (in degrees Celsius), and the carbonization time (in minutes) respectively.

4.1.5. Effect of PJAC preparation parameters

Fig. 19 depicts the 3-dimensional response surfaces showing the effect of PJAC preparation parameters on Cd^{2+} removal efficiency (%). The effect of varying impregnation ratio (IR) and carbonization temperature (T) on Cd^{2+} removal efficiency (%) by the PJAC was evaluated while keeping the carbonization time (t) constant at 120 minutes (Fig. 19 (a)). As shown in Fig. 19a Cd^{2+} removal efficiency increases as the impregnation increases. However, once the impregnation ratio exceeds 1.7, the removal efficiency begins to decline. Notably, as the proportion of chemicals increases, there is a gradual improvement in the metal ion removal efficiency (Prauchner & Rodríguez-Reinoso, 2012). The improvement in the removal efficiency as the IR increases up to 1.7 is due to an increase in the specific surface area as well as total pore volume (Olorundare et al., 2014).

Again, from the PJAC FTIR spectra (Fig.10), it is shown that the activated carbon contains phenol groups, which have acidic characteristics. Consequently, the Cl from $ZnCl_2$ interacts with the H from phenol. As a result, the oxygen from phenol which is now hydrogen atom free would introduce a pair of electrons into the vacant orbital of Zn (Pavia et al., 2009). As explained by both (Najmi et al., 2020) and (Teng & Yeh, 1998), $ZnCl_2$ possesses two Cl; therefore, it can react with two phenol-containing structures to create cross-links. Since the Zn (II) forms cross-links and creates a stiff matrix, raising the $ZnCl_2$ ratio would result in higher Cd^{2+} removal efficiency until IR 1.7 as shown in Fig. 19a. However, as the impregnation ratio is increased past 1.7, there is a decrease in the efficiency of Cd^{2+} removal. This is due to the excessive activation caused by the higher proportion of zinc chloride, which alters the structure of activated carbon. As a result, the pores may connect or disappear, (Z. Li et al., 2020), which lowers the efficiency of Cd^{2+} removal as observed.

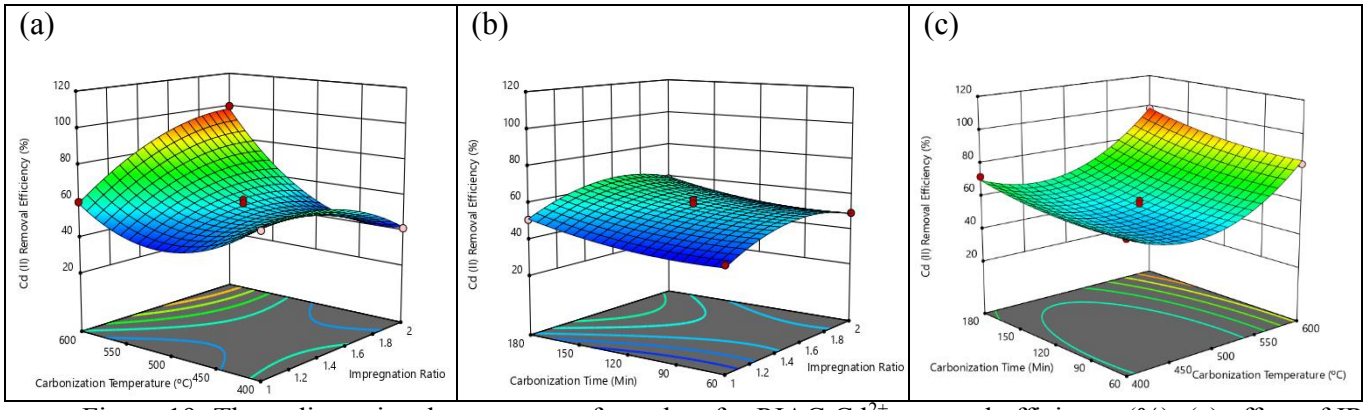

Figure 19: Three-dimensional response surface plots for PJAC Cd^{2+} removal efficiency (%); (a) effect of IR and T, (t=120 min); (b) effect of IR and t, (T=500ºC); (c) effect of t and T, (IR=1.5)

The high Cd^{2+} removal efficiencies with increasing carbonization temperature was attributed to increase in both micro and mesopores. A porous structure develops because at higher carbonization temperatures there is release of more volatile chemicals (Najmi et al., 2020). Temperatures above 450 °C can cause an increase in porosity due to the development of tar, which occurs when lignocellulosic material is treated with acid (Hsu & Teng, 2000). Olorundare et al., (2014) found that at temperatures exceeding 450 °C; an increase in IR also increases the micro and mesopore volume. The pore-widening process might be considerably accelerated by excess $ZnCl_2$, which would result in the development of a mesoporous structure (Qian et al., 2008).

The Fig. 19(b) displays the three-dimensional response surface that illustrates how the Cd^{2+} removal efficiency is affected by the impregnation ratio (IR) and carbonization time (t) (T=500ºC), while Fig. 4(c) shows the interactive influence of carbonization temperature (T) and carbonization time (t) on Cd^{2+} removal efficiency (IR=1.5). The Fig. 19(b) indicates that the effect of carbonization time (t) on Cd^{2+} removal efficiency was not significant ($p>0.05$), despite the varying impregnation ratios (IR). From Fig. 19c, it is evident that the Cd^{2+} removal efficiencies vary significantly ($p<0.05$) with carbonization time (t) at different carbonization temperatures (T). When the carbonization time (t) is short (≤1.5 hours) and the carbonization temperature (T) is low (≤500°C), the recorded Cd^{2+} removal efficiencies are relatively low. This is likely due to insufficient time for the complete development of porosity in the char structure (Teng & Yeh, 1998).

4.1.6. PJAC preparation process optimization

The process optimization was conducted using BBD of the RSM with the objective of maximizing the Cd^{2+} removal efficiency (%). The influencing preparation parameters were all set in range; impregnation ratio (1-2), carbonization temperature (400-600 °C) and carbonization time (60-180 minutes). Out of the 53 solutions suggested, optimum adsorption conditions (Desirability=1) were obtained and selected at Impregnation ratio 1.77, carbonization temperature 595°C and carbonization time 173.6 minutes for 99.9 % Cd^{2+} removal (Table 13). The function's strong desirability suggests that it may accurately describe the experimental model and conditions.

Table 13: Some of the solutions suggested and selected for preparation parameters optimization tests for Cd^{2+} removal by *PJAC*

Number	Impregnation Ratio	Carbonization Temperature (°C)	Carbonization Time (minutes)	Cd^{2+} Removal Efficiency (%)	Desirability	
1	**1.771**	**595.132**	**173.628**	**99.935**	**1.000**	**Selected**
2	1.618	598.577	177.291	99.134	1.000	
3	1.622	599.934	176.062	99.725	1.000	
4	1.698	594.349	174.096	98.125	0.971	
5	1.940	599.460	144.679	98.979	0.977	
6	1.726	598.102	169.944	98.986	0.989	
7	1.791	597.774	157.278	98.464	0.969	
8	1.967	599.164	178.218	98.659	0.986	
9	1.978	599.587	135.367	97.783	0.953	
10	1.948	599.904	146.795	99.676	1.000	

4.1.7. Predicted versus experimental Cd (II) removal efficiency

With the optimal preparation parameters as shown in Table 13 (i.e. IR=1.771, T=595°C and t=174 minutes), new additional activated carbon was freshly prepared and subsequent adsorption experiments in triplicate were run using the same operating conditions as reported in section 2.4 (i.e. Cd^{2+} concentration=100 mgL^{-1}, adsorbate volume=25ml, pH =8, temperature=25 °C, shaking time=30 minutes, PJAC dosage=0.5g and shaking speed=200 rpm) These batch adsorption experiment studies were run for the powdered activated carbon prepared under optimized conditions to compare the predicted against the experimental Cd^{2+} removal efficiencies. An average of 96.7% Cd^{2+} removal efficiency was experimentally obtained against the 99.9% removal efficiency that was predicted by the model. The experimental removal efficiency was relatively lower but not significantly different to the predicted Cd^{2+} removal efficiency by adsorption using *Prosopis Juliflora* powder prepared using both chemical and thermal activation.

4.1.8. PJAC Comparative studies

A literature review with other activated carbons prepared from *Prosopis Juliflora* biomass and synthesized in the same way (i.e. chemical and thermal activation) was undertaken to assess the comparative advantage of the synthesized material in this study (Table 14). The S_{BET} of the final PJAC synthesized under optimum conditions formed the basis of the comparison for the main reason that the other papers dealt with other pollutants other than cadmium used in this study. Table 6 compares the S_{BET} of activated carbon generated from *Prosopis Juliflora* from this study to those previously reported in the literature. The S_{BET} of the activated carbon synthesized in this study was relatively comparable to the S_{BET} of other activated carbon prepared from the same biomass material reported in previous studies (Table 14).

Table 14: S_{BET} of activated carbon prepared from *Prosopis Juliflora* reported in previous studies

Material	**Impregnation Ratio (IR)**		**Carbonization**		**Activation**		**S_{BET} (m^2/g)**	**Reference**
	Chemical	Ratio	Temp (°C)	Time (min)	Temp (°C)	Time (min)		
Seed / Polyaniline	$ZnCl_2$,	-	400	-	800	10	1028	(Gopal & Asaithambi, 2015)
Wood	KOH	1	600	-	800	-	748.91	(Mahajan et al., 2017)
Wood	H_2SO_4,	1	500	-	-	-	358.47	(Manjunath & Kumar, 2018)
Wood	H_3PO_4,	2.5	600	120	-	-	946.06	(Chandrasekaran et al., 2020)
Wood	H_2SO_4,	1	500	-	-	-	320.49	(G. Kaur et al., 2021)
Wood	$ZnCl_2$	1.8	595	174	800	120	600.4	This Paper

4.2. CAC PERFOMANCE EVALUATION AND OPTIMIZATION

This section is mainly based on the following published paper:

Chintokoma, G.C., Chebude. Y., & Kassahun, S.K., Demesa, A. G., & Koiranen, T. (2024). Sol-gel synthesis of composite adsorbent coating from Prosopis juliflora –activated carbon for simultaneous adsorptive removal of Cd^{2+} and $Cr_2O_7^{2-}$ from wastewater. *AQUA — Water Infrastructure, Ecosystems and Society*, *73*(5), 945–968. https://doi.org/10.2166/aqua.2024.335 **(IWA Publishing)**.

The graphical abstract of this paper is presented below:

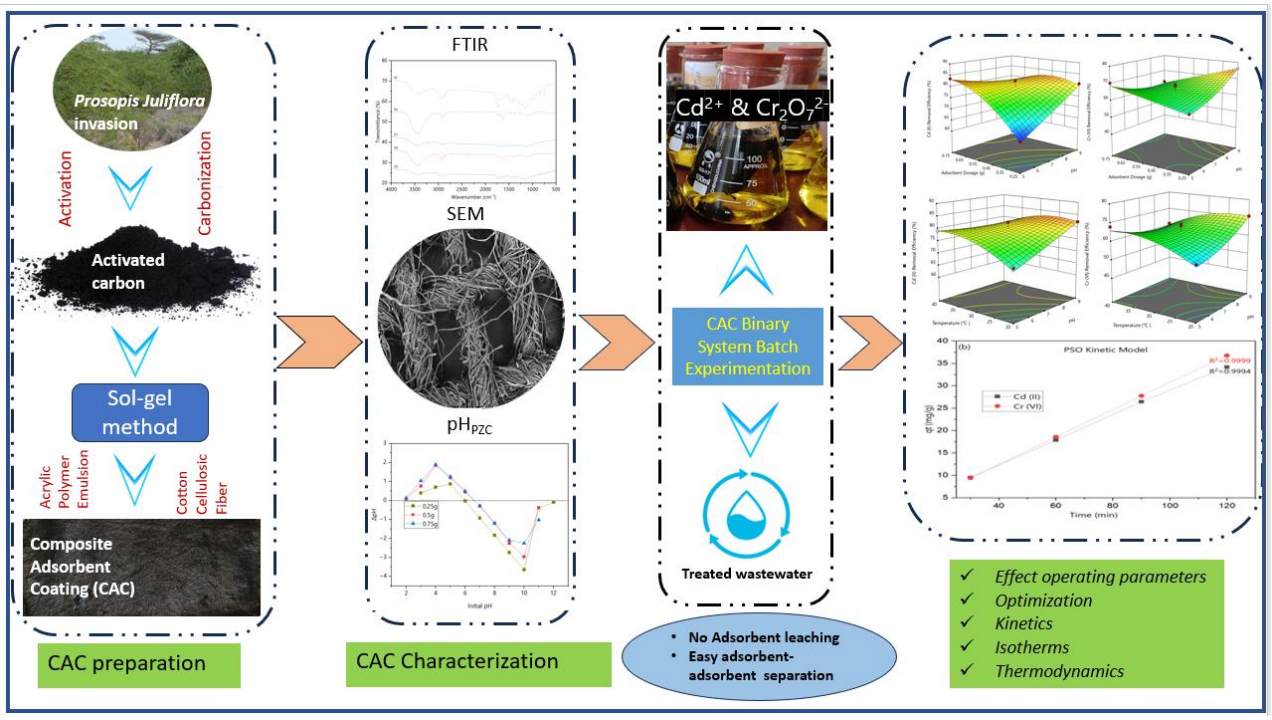

4.2.1. CAC Cd^{2+} and $Cr_2O_7^{2-}$ simultaneous removal from wastewater

Table 15 presents the experimental findings, which shows the actual reduction of Cd^{2+} and $Cr_2O_7^{2-}$ under different operating conditions using the prepared CAC with varying dosages. The actual values of the process variables and their variation limits were selected based on data from preliminary studies and various literature sources.

Table 15: The BBD showing actual Cd (II) and Cr (VI) percental reduction for CAC at different operation parameters

Run	pH	Adsorbent Dosage	Initial Concentration	Contact Time	Temperature	Removal Efficiency (%)	
						Cr (VI)	Cd (II)
		g	mg/L	Min	°C	%	%
1	7	0.25	27.5	60	40	57.67	65.60
2	7	0.25	50	60	30	54.56	67.14
3	7	0.5	50	15	30	79.06	78.16
4	7	0.5	27.5	60	30	60.49	76.65
5	7	0.75	5	60	30	49.40	78.20
6	5	0.25	27.5	60	30	59.86	62.98
7	7	0.5	27.5	60	30	57.16	77.96
8	5	0.5	5	60	30	52.60	74.02
9	9	0.5	27.5	15	30	67.40	75.29
10	7	0.5	5	60	20	50.00	74.80
11	7	0.75	27.5	105	30	57.82	79.09
12	5	0.5	27.5	60	20	56.00	70.58
13	7	0.75	27.5	60	40	60.11	79.13
14	7	0.5	27.5	105	40	58.69	81.02
15	7	0.75	27.5	60	20	58.55	75.51
16	9	0.5	27.5	60	40	61.09	75.56
17	7	0.5	27.5	105	20	60.00	74.95
18	7	0.5	5	60	40	53.80	78.20
19	9	0.75	27.5	60	30	62.84	77.20
20	7	0.25	27.5	15	30	69.09	65.31
21	7	0.5	27.5	15	20	62.18	69.38
22	7	0.75	27.5	15	30	69.49	76.04
23	7	0.5	50	105	30	64.90	78.70
24	7	0.5	50	60	20	64.82	76.44
25	7	0.25	27.5	60	20	66.29	70.26
26	7	0.25	5	60	30	65.80	69.40
27	7	0.5	27.5	60	30	67.46	82.29
28	7	0.5	27.5	60	30	68.00	82.22
29	5	0.5	27.5	60	40	67.89	78.91
30	5	0.5	27.5	15	30	72.40	73.09
31	5	0.5	50	60	30	68.50	76.16
32	7	0.5	27.5	15	40	66.18	76.40
33	7	0.5	27.5	60	30	67.16	79.38
34	7	0.5	50	60	40	65.14	76.62
35	9	0.5	27.5	60	20	70.98	82.15
36	7	0.5	5	15	30	60.00	75.60

37	7	0.5	5	105	30	67.00	85.80
38	9	0.5	50	60	30	70.32	85.82
39	5	0.5	27.5	105	30	60.31	82.29
40	5	0.75	27.5	60	30	70.36	83.56
41	9	0.5	5	60	30	67.20	82.00
42	7	0.75	50	60	30	73.10	80.42
43	9	0.25	27.5	60	30	76.25	80.69
44	9	0.5	27.5	105	30	72.84	84.84
45	7	0.25	27.5	105	30	72.87	79.13

Clearly Table 15 results indicate that Cd^{2+} removal was generally higher than that of $Cr_2O_7^{2-}$ at various operating conditions. The observed higher CAC uptake capacity of Cd^{2+} over $Cr_2O_7^{2-}$ could be due to several factors including surface charge of the adsorbent at the pH of interest and their ionic properties. As presented in section 4.1.3.3 on CAC pH_{PZC}, the o.25g CAC had 6 while both 0.5 and 0.75g CAC had 6.66 respectively as their pH $_{PZC}$. In this case Cd²□ can be adsorbed both below and above the pH_{PZC}, whereas Cr□O□ ²□ adsorption would be favored only below these pH_{PZC}. At pH above highest observed PZC, the CAC surface is negatively charged, enhancing Cd²□ adsorption through electrostatic attraction. Similarly, at pH below lowest observed pH_{PZC}, the CAC surface is positively charged, facilitating Cr□O□ ²□ adsorption through electrostatic attraction. However, at this pH below the lowest pH_{PZC} as much as the CAC is positively charged, but Cd²□ can still be adsorbed through ion exchange and surface complexation. On the other hand, at pH above the highest observed pH_{PZC}, the CAC surface, as already highlighted, is negatively charged, reducing Cr□O□ ²□ adsorption due to electrostatic repulsion.

With reference to the ionic properties (Table 16), Cd^{2+} is more adsorbed than $Cr_2O_7^{2-}$ probably because Cd^{2+} has smaller (4.260 A˚) hydrated radii than and $Cr_2O_7^{2-}$ (4.61A˚), making it more accessible to adsorbent pores. Again Mohan & Singh, (2002), assert that metals with higher standard reduction potential (as demonstrated by Cd^{2+} in Table 15) exhibit enhanced ionic interaction with the electron-rich surface of adsorbents. Furthermore, Cd^{2+} has a higher electronegativity value (1.69) than $Cr_2O_7^{2-}$ (1.66), making it exhibit a higher affinity for the adsorbent surface (Jain et al., 2016; Kadirvelu et al., 2008; Obayomi et al., 2020).

Table 16: Ionic properties of Cd^{2+} and $Cr2O_7^{2-}$

Property	**Cd^{2+}**	**$Cr_2O_7^{2-}$**	**Reference**
Molecular Weight	769.52	294.18	(Obayomi et al., 2020) (Jain et al., 2016)
Atomic Weight	112.41	51.01	
Electronic Configuration	$[Kr]4d^{10}5s^2$	$[Ar]3d^5 4s^1$	
Hydrated radii (A˚)	4.260	4.61	

Ionic radii (A˚)	0.95	0.52	(Kadirvelu et al., 2008)
Standard Reduction Potential (V)	$Cd^{2+} + 2e^- \rightarrow Cd$ (-0.403)	$Cr^{6+} + 3e^- \rightarrow Cr^{3+}$ (1.1) $Cr^{3+} + 3e^- \rightarrow Cr$ (-0.74)	
Coordination number	6 & 4	6 & 4	
Electronegativity	1.69	1.66	

4.2.2. Evaluation of the CAC $Cd^{2+}$and $Cr_2O_7^{2-}$ removal adsorption data

4.2.2.1. Regression model development and validation

Operating parameters like pH, adsorbent dosage, contact time, initial concentration, temperature and their interactions affect contaminants removal efficiency from aqueous solutions (Amrutha et al., 2023). As mentioned, batch adsorption experiments were performed to study the combined effect of the operating factors on simultaneous removal of Cd^{2+} and $Cr_2O_7^{2-}$ from aqueous media using CAC. Table 15 has summarized the results of the experiments on different combination of operating parameters. Equation 9 illustrates the response function's coefficients and Table 17 presents the p-values and F-values for assessing the validity of the model prediction for simultaneous removal efficiencies of Cd^{2+} and $Cr_2O_7^{2-}$. The actual second order polynomial equations describing the CAC Cd^{2+} and $Cr_2O_7^{2-}$ removal efficiencies are given by Eqns. 31 and 32, respectively:

Cd (II) removal % = *-69.0119 + 11.7802 * pH + 155.696AD + 0.133294C + 0.308463T + 2.97017 * Temp + -12.0368 * pH * AD + 0.00933333 * pH * C + 0.000962121 * pH * T + -0.186364 * pH * Temp + 0.199111AD * C + -0.239192AD * T + 0.827182AD * Temp + -0.00238519CT + -0.00357778C * Temp + -0.000525253T * Temp + 0.0589725 * pH^2+ -70.2161AD^2+ -0.000795249C^2+ -0.00029769T^2+ -0.0306782 * $Temp^2$*

(31)

Cr (VI) removal % = *-28.3383 + 5.22543 * pH + 27.3961AD + 0.528989C + -0.153651T + 3.9797 * Temp + -11.9636 * pH * AD + -0.071 * pH * C + 0.0486843 * pH * T + -0.272273 * pH * Temp + 1.55289AD * C + -0.343434AD * T + 1.01818AD * Temp + -0.00522469CT + -0.00386667C * Temp + -0.00294949T * Temp + 0.659806 * pH^2 + -1.47796AD^2+ -0.00312237C^2+ 0.00144301T^2+ -0.0381434 * $Temp^2$*

(32)

(where T=Contact Time, C=Initial Concentration, AD= Adsorbent Dosage, Temp= Temperature)

Table 17: Regression analysis and ANOVA results for quadratic model response surface for $Cd^{2+}$and $Cr_2O_7^{2-}$ removal by CAC

	Cd (II) response		Cr (VI) response		
Source	**F-value**	**p-value**	**F-value**	**p-value**	
Model	10.21	< 0.0001	8.74	< 0.0001	Significant
A-pH	19.72	0.0002	10.07	0.0041	
B-Adsorbent Dosage	52.82	< 0.0001	2.57	0.1217	

C-Initial Concentration	0.0232	0.8801	33.33	< 0.0001	
D-Contact Time	35.83	< 0.0001	5.90	0.0230	
E-Temperature	3.39	0.0782	0.0185	0.8930	
AB	25.98	< 0.0001	13.72	0.0011	
AC	0.1265	0.7252	3.91	0.0595	
AD	0.0054	0.9421	7.36	0.0121	
AE	9.97	0.0043	11.37	0.0025	
BC	0.8998	0.352	29.25	<0.0001	
BD	5.19	0.0318	5.72	0.0249	
BE	3.07	0.0926	2.448	0.1281	
CD	4.18	0.0519	10.73	0.0032	
CE	0.4648	0.5019	0.2901	0.5951	
DE	0.0401	0.8430	0.6753	0.4193	
Lack of Fit	0.8508	0.6485	0.3165	0.9636	Not significant
R^2	0.8948		0.8793		
Adjusted R^2	0.8072		0.7787		
Predicted R^2	0.6281		0.6311		
Adequate Precision	14.2322		13.4231		

The models used for the simultaneous removal of $Cd^{2+}$and $Cr_2O_7^{2-}$ show significant high F-values of 10.21 and 8.74, respectively and low p-values (≤0.0001) for both metal ions. This observation suggests that there is a notable influence on the response variable from at least one of the factors included in each model (Brereton, 2019). For Cd^{2+}, pH (A), adsorbent dosage (B) and contact time (D) were highly significant to the model, all showing low p-values ($p<0.05$). In the case of $Cr_2O_7^{2-}$ removal, pH (A), initial concentration (C) and contact time (D) were all highly significant ($p<0.05$) to the model. Table 17, shows that pH (A) and contact time (D) were significant ($p< 0.05$) for both metal ions removal while temperature was insignificant ($p>0.05$) for both metal ions removal. Meanwhile, several interaction terms were also found to be significant ($p< 0.05$) in both models including pH an adsorbent dosage (AB), pH and temperature (AE) and adsorbent dosage and contact time (BD). The square terms of adsorbent dosage (B^2, $p< 0.0001$) and temperature (E^2, $p=0.0011$) were highly significant to the Cd^{2+}removal model while the squares of pH (A^2), contact time (D^2) and temperature (E^2) were all significant model terms to $Cr_2O_7^{2-}$ removal ($p < 0.05$). The lack of fit F-values of 0.85 for Cd^{2+} and 0.32 for $Cr_2O_7^{2-}$ obtained, indicated that the lack of fit is not significant in both models.

The models' comparatively high regression coefficients (R^2) of 0.895 and 0.879 for Cd^{2+} and $Cr_2O_7^{2-}$ removal respectively indicate that both models are capable of accurately predicting the response. The models have also demonstrated a signal to noise ratio of 14.2 and 13.4, for the

removal of Cd^{2+} and $Cr_2O_7^{2-}$, respectively, indicating their appropriateness and adequacy. There is a good agreement between predicted and adjusted correlated coefficient as the difference between them is ≤ 0.2. The factors added to modify the models have improved the models because the adjusted R^2 (0.81 and 0.78) for both metals is more than the predicted R^2 (0.62 and 0.63) for Cd^{2+} and $Cr_2O_7^{2-}$ respectively. Hence, the response surface model developed in this research for predicting both of Cd^{2+} and $Cr_2O_7^{2-}$ removal efficiency from a binary component aqueous media can be considered satisfactory.

Figure 20 shows the normal percentage probability of residual against the normal plot of residuals for Cd^{2+} (Fig. 20a) and $Cr_2O_7^{2-}$ (Fig. 20b) removal, respectively. Both plots display an S-shaped pattern and form a fairly straight line, demonstrating a good correlation between probability and normal reduction, which confirms the assumption that both models are suitable for predicting the removal efficiencies of both metals (Brereton, 2019; Khoshraftar et al., 2023).

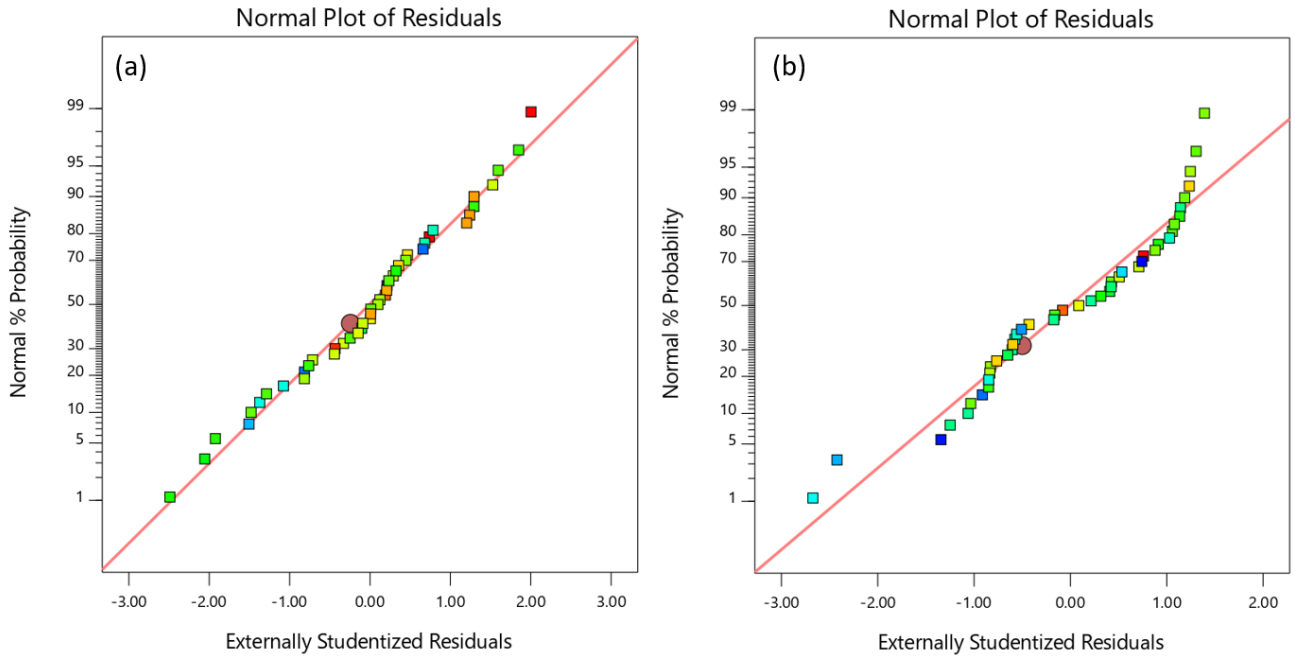

Figure 20: Normal probability plots for CAC on (a) cadmium removal (b) chromium removal

Figure 21 shows predicted and the actual plots confirming the correspondence between the residual and predicted simultaneous Cd^{2+} (Fig. 21a) and $Cr_2O_7^{2-}$ (Fig. 21b) reduction implying that the models could well predict within the range of operating parameters. Consequently, one can assert that the quadratic models of the response surface developed in this study that relate the reduction of

Cd^{2+} and $Cr_2O_7^{2-}$ with operating parameters are most suitable for describing the experimental outcomes of the composite adsorbent coating adsorption process in a binary component system.

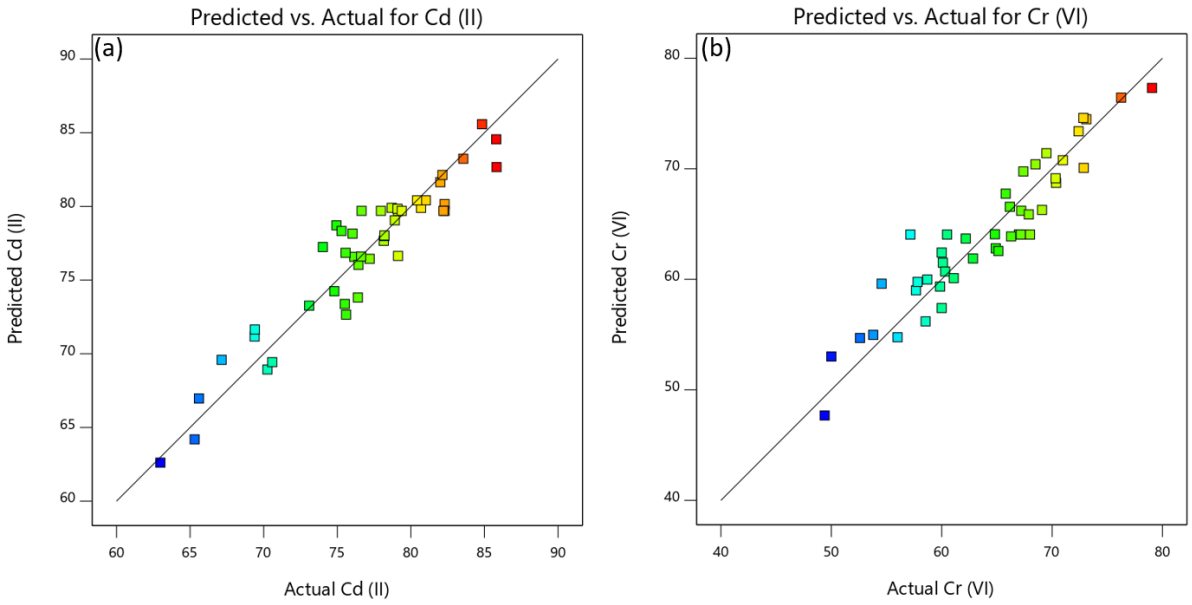

Figure 21: Plots for predicted against actual results for (a) Cd (II) (b) Cr (VI) reduction by CAC

4.2.3. Effect of operating parameters on CAC Cd^{2+} and $Cr_2O_7^{2-}$ simultaneous removal

Various studies have emphasized that the important operation parameters, affecting the performance of adsorption process, are initial pH of solution, initial concentration of pollutant, contact time, solution temperature and adsorbent dosage (Mandal et al., 2021; Qasem et al., 2021; Roy & Bharadvaja, 2021; Sreedhar & Reddy, 2019). Again, using BBD of the RSM, the effects of these parameters on Cd^{2+} and $Cr_2O_7^{2-}$ adsorption onto CAC was shown by the response surface plots while the rest of the operating conditions were set at their mid points (Fig. 22).

4.2.3.1. Effect of pH

The observations from Fig. 22(a-b) reveal distinct trends in the removal efficiency of the metal ions with Cd (II) removal increasing with pH and Cr (VI) removal decreasing with pH which is consistent with the CAC's pH_{PZC}. Vividly, when the pH of the solution is higher than the determined pH_{PZC}, the negatively charged surface of the adsorbent provides electrostatic interactions that promote the adsorption of positively charged Cd^{2+}. On the other hand, as the pH of the solution lowers below the pH_{PZC}, the surface of the adsorbent becomes positively charged,

hence promoting the adsorption of the negatively charged $Cr_2O_7^{2-}$ (Mandal et al., 2021; Roy & Bharadvaja, 2021; Singh et al., 2023).

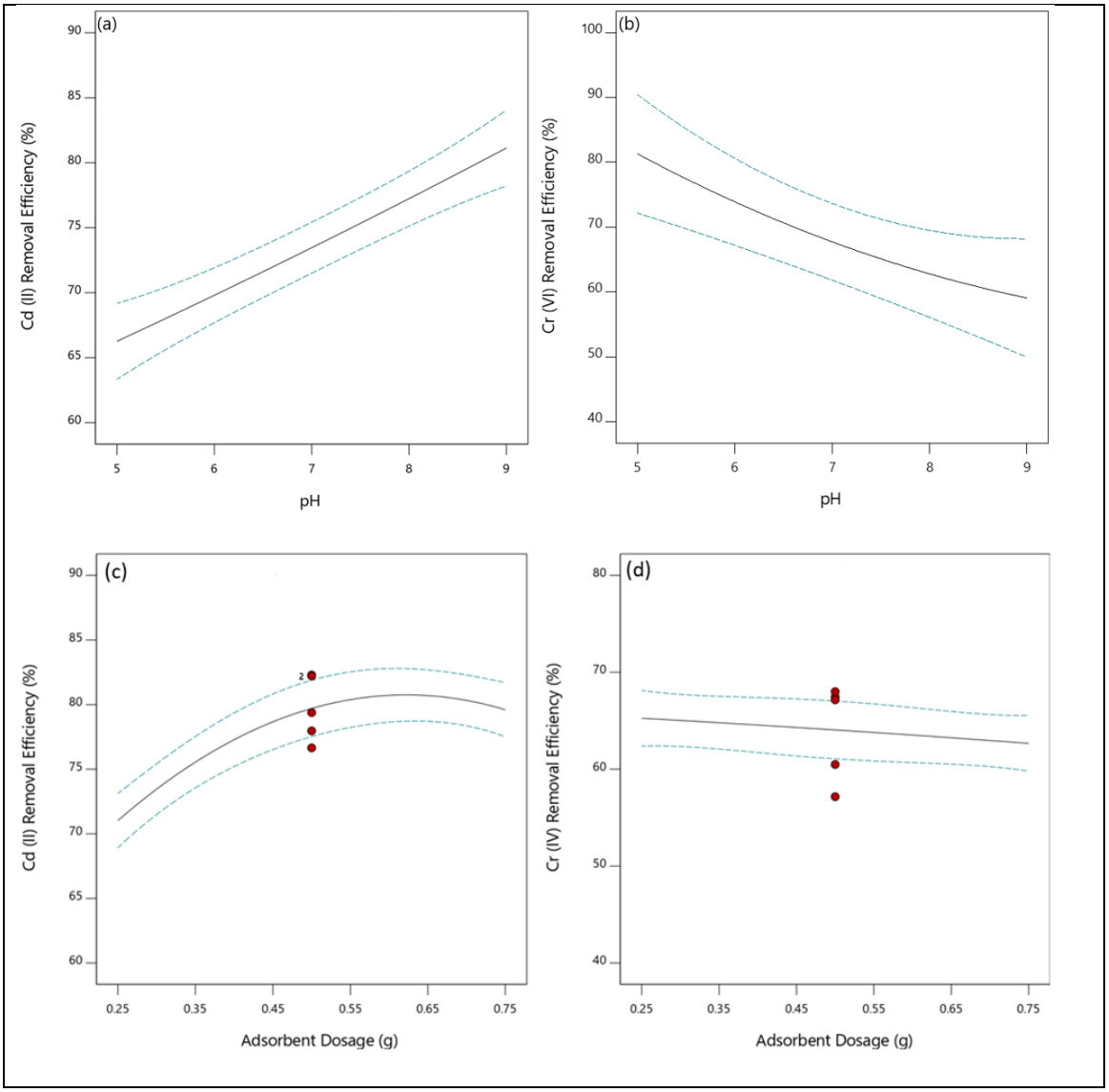

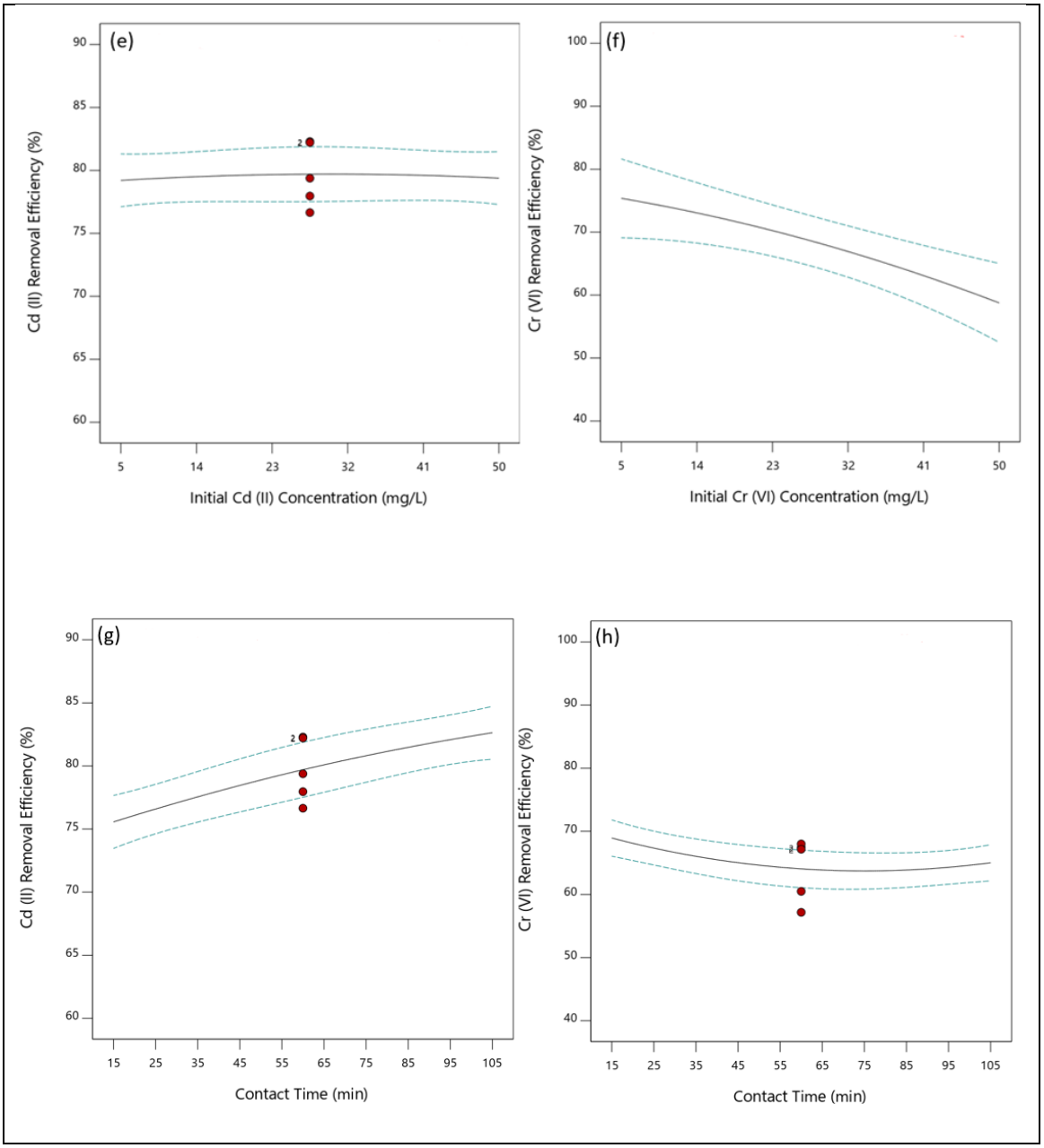
(e)
Cd (II) Removal Efficiency (%)
Initial Cd (II) Concentration (mg/L)
(f)
Cr (VI) Removal Efficiency (%)
Initial Cr (VI) Concentration (mg/L)
(g)
Cd (II) Removal Efficiency (%)
Contact Time (min)
(h)
Cr (VI) Removal Efficiency (%)
Contact Time (min)

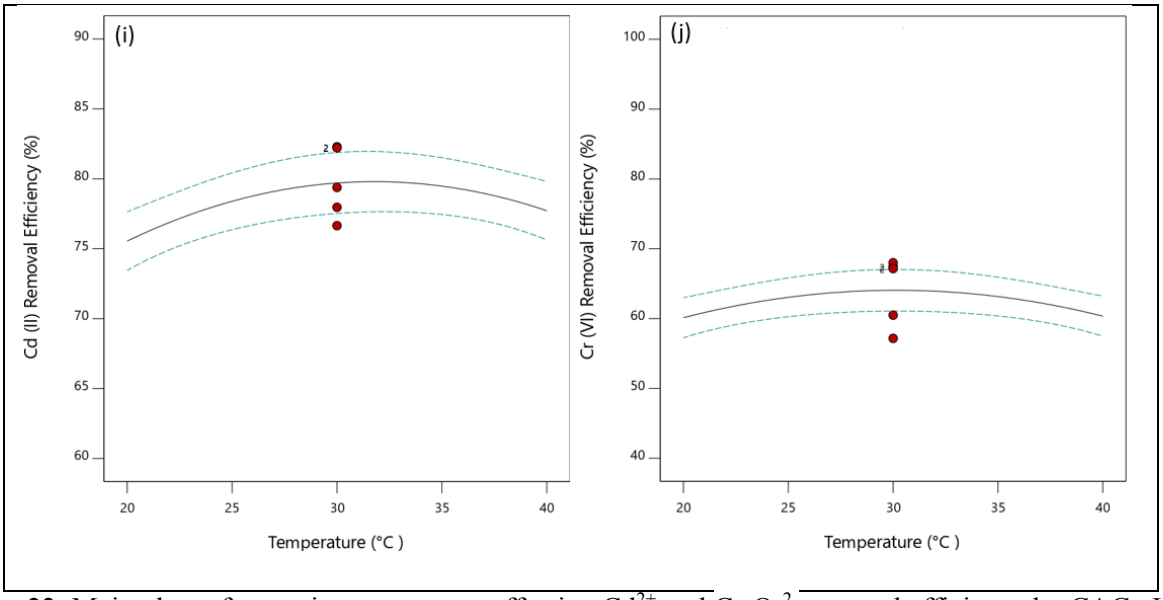

Figure 22: Main plots of operating parameters affecting Cd^{2+} and $Cr_2O_7^{2-}$ removal efficiency by CAC pH

4.2.3.2. Effect of adsorbent dosage

Fig. 22(c-d) provide insights into the influence of adsorbent dosage on Cd^{2+} and $Cr_2O_7^{2-}$ reduction. It is evident that the adsorbent dosage on the CAC has a significant effect on Cd^{2+} reduction ($p< 0.0001$) but an insignificant effect on $Cr_2O_7^{2-}$ reduction ($p=0.1217$). These findings are further supported by the results of the ANOVA analysis as presented in Table 4. Generally high adsorbent dosage is associated with high removal efficiency due to availability of more vacant site available for adsorption on the adsorbent (Kwikima et al., 2023) as is observed in Fig. 22(c) for Cd^{2+}. However, an opposite trend is observed for $Cr_2O_7^{2-}$ by CAC whereby removal efficiency is decreasing with increased adsorbent dosage (Fig. 22d). This could potentially be attributed to the increase in point of Zero Charge on CAC as the adsorbent dosage on the CAC increases, as observed and explained in Fig. 16. Conversely the observed decrease in removal efficiency for Cd^{2+} observed after 0.6g of adsorbent on CAC could be explained in terms of CAC preparation as the total surface area and active sites decrease with increasing adsorbent dosage due to overlapping adsorbent on CAC surface resulting in decreased adsorbent capacity (Kayranli, 2022).

4.2.3.3. Effect of initial metal ion concentration

The initial metal ion concentration has insignificant ($p=0.8881$) effect on the Cd^{2+} reduction but significant (<0.0001) effect on $Cr_2O_7^{2-}$ reduction by CAC (Fig. 22(e-f)). The decline in the % removal of $Cr_2O_7^{2-}$ can be attributed to the finite number of active sites present on the adsorbent, resulting in saturation at concentrations above a particular threshold (Werkneh et al., 2014). At lower initial concentrations, the ratio between the initial quantity of $Cr_2O_7^{2-}$and the accessible active

sites of the adsorbent is lower resulting in higher removal efficiency of $Cr_2O_7^{2-}$. Conversely, at higher concentrations, a greater number of residual $Cr_2O_7^{2-}$ ions persist in the aqueous solution (Emirie, 2015). Hence, the reduction of $Cr_2O_7^{2-}$ is significantly higher at low initial concentrations as there are fewer initial chromium ions relative to the number of active sites that are accessible on the adsorbent. This also explains why more residual Cr (VI) ions are left in the aqueous solution at higher initial concentrations (Gorzin & Bahri Rasht Abadi, 2018).

4.2.3.4. Effect of contact time and temperature

The influence of contact time was found to be significant to both metal ions removal but higher level of significance was observed for Cd^{2+} ($p< 0.0001$) than for $Cr_2O_7^{2-}$ ($p=0.0230$) as indicated in Table 15. In a binary component system, Cd^{2+}removal efficiency by CAC exhibited an increase with increasing contact time as shown in Fig. 22(g). On the other hand, $Cr_2O_7^{2-}$ removal efficiency demonstrated a slight decrease with contact time, attaining its maximum removal efficiency within the first 15 minutes (Fig. 22(h)). The observed pattern of increased Cd^{2+} and $Cr_2O_7^{2-}$ removal efficiencies could be due to the fact that a longer contact time allows for more dissociation of the base, APE (pH=8.0) (Jayaram & Prasad, 2009; MCP, 2012) used in the preparation of CAC. With prolonged contact time, the base dissolves in water to produce hydroxide (OH^-) ion (American Chemical Society, 2019) which in turn favors the adsorption Cd^{2+} over $Cr_2O_7^{2-}$ as observed in Fig. 22(g-h). Independently, temperature was found not to have any significant effect on both metal ions removal (Fig. 22(i-j)) in a binary component system.

4.2.4. Combined influence of operating parameters on simultaneous Cd^{2+} and $Cr_2O_7^{2-}$ removal

In this investigation, among the total of 10 potential combinations between any two operational parameters on effect on Cd^{2+} and $Cr_2O_7^{2-}$ removal efficiency established by response surface methodology, only three combinations had significant ($p\leq0.05$) effects on the removal of both metal ions i.e. pH and adsorbent dosage (AB), pH and Temperature (AE) and adsorbent dosage and contact time (BD) as already presented in Table 17. The interaction of the most significant factors for both metal ions have also been shown for any two parameters simultaneously (Fig. 23).

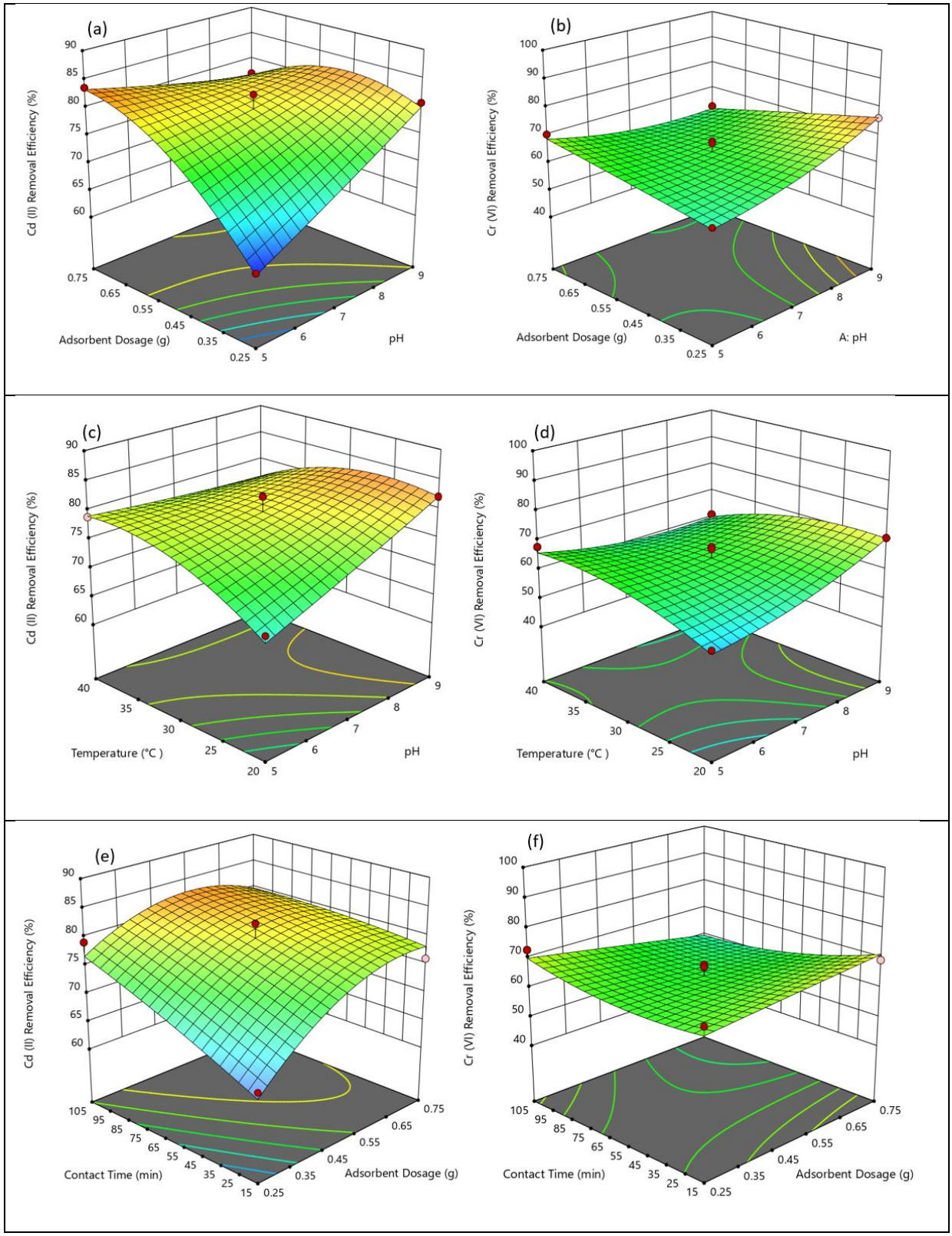

Figure 23: Response surface of experimental data showing interacting effect of most significant operating factors of CAC on Cd^{2+} and $Cr_2O_7^{2-}$ reduction.

4.2.5. CAC Cd^{2+} and $Cr_2O_7^{2-}$ simultaneous removal process optimization

The primary aim of the optimization process was to ascertain the optimal values of variables for the simultaneous removal of Cd^{2+} and $Cr_2O_7^{2-}$ using a composite adsorbent coating (CAC). This was achieved by utilizing a model derived from experimental data. The selection of the operational parameters was made with the objective of optimizing the response, i.e., both Cd^{2+} and $Cr_2O_7^{2-}$ removal efficiencies while initial pH of the sample, adsorbent dosage, initial metal ion concentration, contact time, and temperature were all left at a range. Multiple sets of experiments (100 in total) were suggested by the model but the one with high desirability score (0.808) was selected for verification and further adsorption experiments i.e. kinetics, isotherms and thermodynamics studies (Table 18).

Table 18: Some (20) of the solutions suggested and selected for preparation parameters optimization tests for Cd2+ and Cr2O72- removal by CAC

Number	pH	Adsorbent Dosage	Initial Concentration	Contact Time	Temperature	Removal Efficiency (%)		Desirability
						Cr (VI)	Cd (II)	
1	8.500	0.251	5.000	105.000	23.728	94.262	86.864	0.808
2	8.498	0.250	5.000	105.000	20.902	94.606	86.418	0.806
3	6.000	0.749	50.000	15.004	38.094	96.855	84.550	0.805
4	8.500	0.250	5.000	104.216	23.741	94.006	86.724	0.804
5	6.000	0.749	49.998	15.153	37.973	96.741	84.542	0.804
6	6.000	0.750	49.997	15.000	35.720	96.765	84.511	0.803
7	6.003	0.750	49.789	15.018	38.055	96.714	84.535	0.803
8	6.000	0.749	49.942	15.456	37.370	96.607	84.559	0.803
9	8.472	0.251	5.000	104.742	22.517	94.041	86.538	0.802
10	8.500	0.250	5.045	104.611	20.187	94.445	86.174	0.802
11	8.500	0.250	5.000	103.795	21.416	94.153	86.336	0.801
12	8.500	0.250	5.001	104.067	24.824	93.677	86.730	0.801
13	8.500	0.264	5.000	104.970	22.225	93.457	86.841	0.800
14	6.000	0.750	49.895	15.000	34.745	96.509	84.380	0.800
15	8.500	0.250	5.386	105.000	26.158	93.415	86.794	0.799
16	8.493	0.263	5.000	104.995	21.801	93.419	86.728	0.799
17	8.500	0.250	5.000	104.934	26.673	93.310	86.764	0.798
18	8.500	0.250	5.000	103.490	25.051	93.392	86.629	0.797
19	8.500	0.258	5.245	105.000	20.001	93.826	86.258	0.797
20	6.000	0.750	49.121	15.024	40.000	96.050	84.280	0.795

The optimized operation conditions (i.e. pH=8.5; Adsorbent dosage=0.25 g; initial concentration=5 mg/L, contact time=105 minutes and Temperature=23.73ºC.) predicted 86.86% and 94.26% removal for Cd^{2+} and $Cr_2O_7^{2-}$, respectively. These optimum operating conditions yielded experimental removal efficiencies of 83.98% and 58.08% for Cd^{2+} and $Cr_2O_7^{2}$, respectively, corresponding to adsorption capacities of 2.52 mg/g for Cd^{2+} and 1.74 mg/g for $Cr_2O_7^{2-}$.

4.2.6. CAC adsorption equilibrium isotherm study

Adsorption equilibrium Isotherms play a pivotal role in the design of adsorption systems due to their ability to elucidate the interaction mechanisms between pollutants and adsorbent materials. Moreover, they facilitate the prediction of adsorption parameters and enable quantitative comparisons of adsorbent behavior under different experimental conditions. (Al-Ghouti & Da'ana, 2020). As already outlined in Section 3.2.4 of the methodology, this study, employed the Langmuir, Freundlich, Dubinin–Radushkevich, and Temkin isotherm models to fit the experimental data. The derived parameter values are presented in Table 19.

Table 19: Adsorption isotherm models calculated parameters using linear regression analysis

Langmuir model			
Metal ion	q_m **[mg/g]**	K_L **[L/mg]**	R^2 **[-]**
Cd^{2+}	10.718	0.1367	0.9986
$Cr_2O_7^{2-}$	24.231	0.0549	0.9861
Freundlich model			
Metal ion	$1/n$ **[-]**	$K_{F.}$ **[(mg/g)/(L/mg)^n]**	R^2 **[-]**
Cd^{2+}	0.896	1.754	0.9933
$Cr_2O_7^{2-}$	1.278	1.266	0.9644
Dubinin-Radushkevich			
Metal ion	q_{DR} **[mg/g]**	β_{DR} **[x 10^{-8} mol^2/kJ^2]**	R^2 **[-]**
Cd^{2+}	4.167	-1.6×10^{-4}	0.8787
$Cr_2O_7^{2-}$	4.296	-4.6×10^{-5}	0.8379
Temkin			
Metal ion	K_T **[L mol-1]**	b_T **[mg/g]**	R^2 **[-]**
Cd^{2+}	0.127185	106.3501	0.8361
$Cr_2O_7^{2-}$	0.173303	84.43782	0.8288

According to the data shown in Table 19, it can be noticed that the Langmuir model had the highest correlation coefficient (R^2) values for both metal ions, specifically Cd^{2+} (R^2=0.998) and $Cr_2O_7^{2-}$ (R^2 =0.986). Similarly, Fig. 24 shows that the Langmuir model is the best-suited adsorption isotherm model for both metal ions removal by the CAC in a binary component system. Based on the above observation, it can be concluded that sorption of both metal ions onto CAC was on a monolayer and homogenous surface (Al-Ghouti & Da'ana, 2020; Gorzin & Bahri Rasht Abadi, 2018). This is

because the underlying assumption of the model is that the adsorbent sites exhibit uniformity and homogeneity, with equal amounts of energy and that the sites have an equal chance of adsorbing pollutants (Al-Ghouti & Da'ana, 2020). The present finding is consistent with the research conducted by Azha et al., (Azha et al., 2014), where they also developed an adsorbent coating layer called *Paintsorp* which was coated on a glass surface. The adsorption capabilities of this coating were then evaluated on the removal of methylene blue (MB) through a batch adsorption set-up.

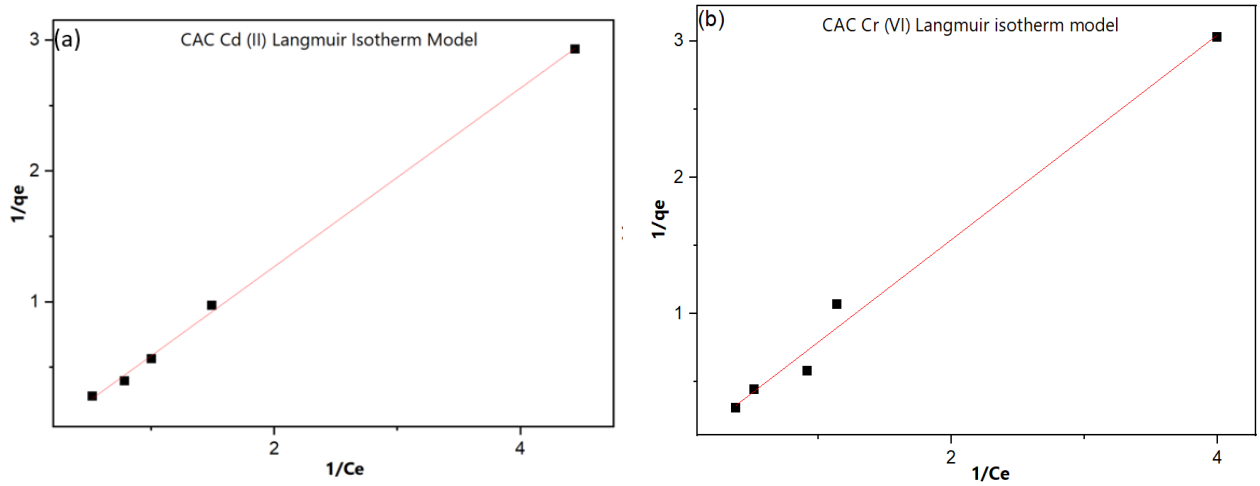

Figure 24: The best fit isotherm model for both Cd^{2+} (a) and $Cr_2O_7^{2-}$ (b) adsorption onto CAC in a binary component system

4.2.7. The kinetics of CAC Cd^{2+} and $Cr_2O_7^{2-}$ adsorption

Table 20 present the parameters of the pseudo-first order (PFO), pseudo-second order (PSO), Elovich and intra-particle diffusion (IP) as well as the findings of their validation.

Table 20: Calculated parameters of the adsorption kinetics models of the binary component system

P.F.O. model				
Metal ion	**K_1 [min^{-1}]**	**R^2 [-]**	**q_e [mg/g] (exp)**	**q_e [mg/g] (calc)**
Cd^{2+}	-0.0004	0.92301	3.5677	0.1082
$Cr_2O_7^{2-}$	-0.0006	0.5850	3.2662	1.6910
PSO model				
Metal ion	**K_2 [g mg^{-1} min^{-1}]**	**R^2 [-]**	**q_e [mg/g] (exp)**	**q_e [mg/g] (calc)**
Cd^{2+}	0.0555	0.9994	3.5677	3.6350
$Cr_2O_7^{2-}$	0.3368	0.9999	3.2662	3.2862
Elovich model				
Metal ion	**α [mg g^{-1} min^{-1}**	**β [g/mg]**	**R^2 [-]**	
Cd^{2+}	4.0209	2721.27	0.9665	
$Cr_2O_7^{2-}$	23.1107	1.9988E+29	0.9686	
I.P. model				
Metal ion0	**k_P [mg/g·h1/2]**	**C [mg/g]**	**R^2 [-]**	
Cd^{2+}	0.06285	2.82759	0.94043	
$Cr_2O_7^{2-}$	0.01106	3.14362	0.97618	

Of the four kinetic models tested, the pseudo-second-order (PSO) kinetic model showed the highest correlation values for Cd^{2+} (R^2=0.9994) and $Cr_2O_7^{2-}$ (R^2= 0.9999) as illustrated in Fig. 25. This confirms that the kinetics of both metal ions removal by CAC was regulated by PSO.

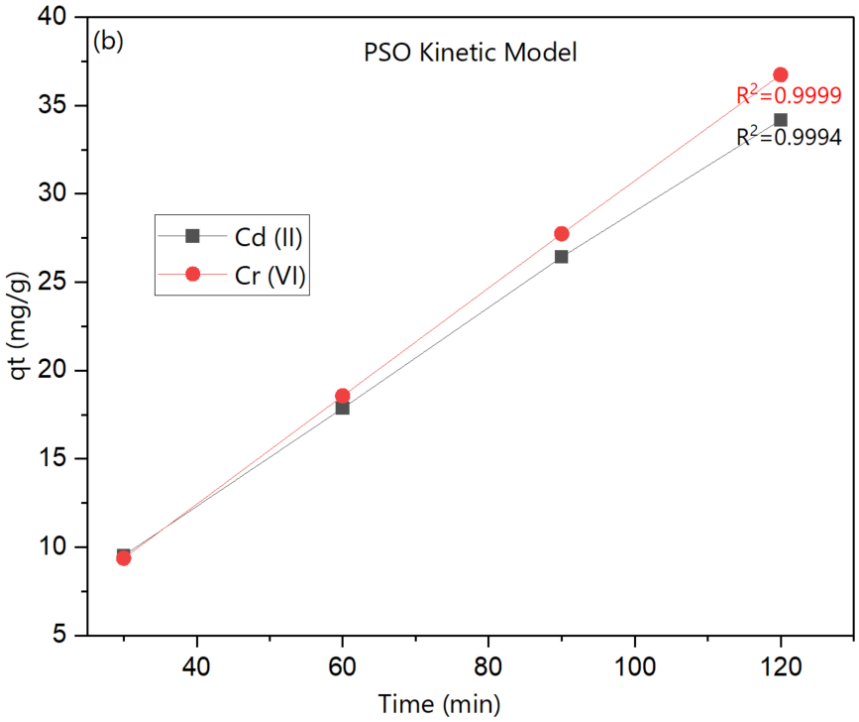

Figure 25: The best fit kinetic model for both Cd^{2+} and $Cr_2O_7^{2-}$ adsorption onto CAC in a binary component system

By conforming to the PSO model, it indicates that the CAC has abundance of active sites for the adsorption of both Cd (II) and Cr (VI) (J. Wang & Guo, 2020). The rate of Cd^{2+} and $Cr_2O_7^{2-}$ adsorption onto CAC in the present study were determined to be 0.056 g/mg/min and 0.337 g/mg/min, respectively.

4.2.8. CAC adsorption thermodynamics parameters calculation

The thermodynamic process parameters of Cd^{2+} and $Cr_2O_7^{2-}$ adsorption on CAC, i.e., enthalpy (ΔH°), entropy (ΔS°), and Gibbs free energy (ΔG°) were estimated using equations 13,14 and 15 respectively. The adsorption experiments involved thermodynamic considerations to determine the spontaneity and feasibility of such processes. The thermodynamic parameter results are summarized in Table 21.

Table 21: CAC thermodynamic parameters for Cd^{2+} and $Cr_2O_7^{2-}$ removal from aqueous solution

Metal ion	**T (K)**	**ΔG° (KJ mol-1)**	**ΔH° (KJ mol-1)**	**ΔS° (J K^{-1} mol^{-1})**	**Intercept**	**Slope**

$Cr_2O_7^{2-}$	296.15	-6.70	1.49203	27.6507	3.3258	-179.46033
	308.15	-7.02				
	318.15	-7.33				
	328.15	-7.57				
Cd (II)	296.15	-6.92	5.96698	44.1149	5.3061	-717.7025
	308.15	-8.03				
	318.15	-7.85				
	328.15	-8.50				

The negative ΔG° and positive ΔH° values in Table 21 indicate that the adsorption process is spontaneous and endothermic, respectively. While there are no specific criteria pertaining to the *ΔH°* values defining the adsorption, it is commonly assumed that heats of adsorption ranging from 20.9 to 418.4 kJ/mol, which are indicative of chemical reactions, are comparable to the heats associated with the chemisorption processes (Azha et al., 2014; Gorzin & Bahri Rasht Abadi, 2018). Conversely, low enthalpy of adsorption (5-0 kJ/mol) is associated with physisorption (Subhabrata & Gargi, 2020). Hence, based on the results of *ΔH°* values obtained for both pollutants, the study's findings suggest that the adsorption of Cd^{2+} and $Cr_2O_7^{2-}$ onto CAC proceeded via physisorption. The CAC SEM images presented and observed in Fig. 13 also conforms to this finding.

Entropy (ΔS°) is defined as a measure of randomness or disorder of a system whereby when the disorder of a system decreases it causes negative entropy (Al-Ghouti & Da'ana, 2020). Inversely a positive shift in ΔS° is indicative of the adsorbent's affinity for the adsorbate as well as an indication of increasing randomness at the solid and liquid interface. This may be accompanied by structural modifications in both the adsorbent and adsorbate (Ebelegi et al., 2020). The current investigation demonstrates that the ΔS° values for both heavy metals suggest an increase in randomness at the interface between the adsorbent and solution. This increase in randomness serves as the primary driving mechanism for the adsorption of both metal ions onto CAC.

4.3. SYNERGISTIC INTEGRATION OF IPA FOR Cd (II) REMOVAL

This chapter is based on the following published paper:

Chintokoma, G.C., Chebude. Y., & Kassahun, S.K., Demesa, A. G., & Koiranen, T. (2024). Synergistic Integration of Inclined Plate Settler (IPS) and Composite Adsorbent Coating (CAC) for the enhanced removal of Cd^{2+} from wastewater. *Applied Water Science*. https://doi.org/10.1007/s13201-024-02292-2 **(Springer)**.

The graphical abstract of this section paper is presented below:

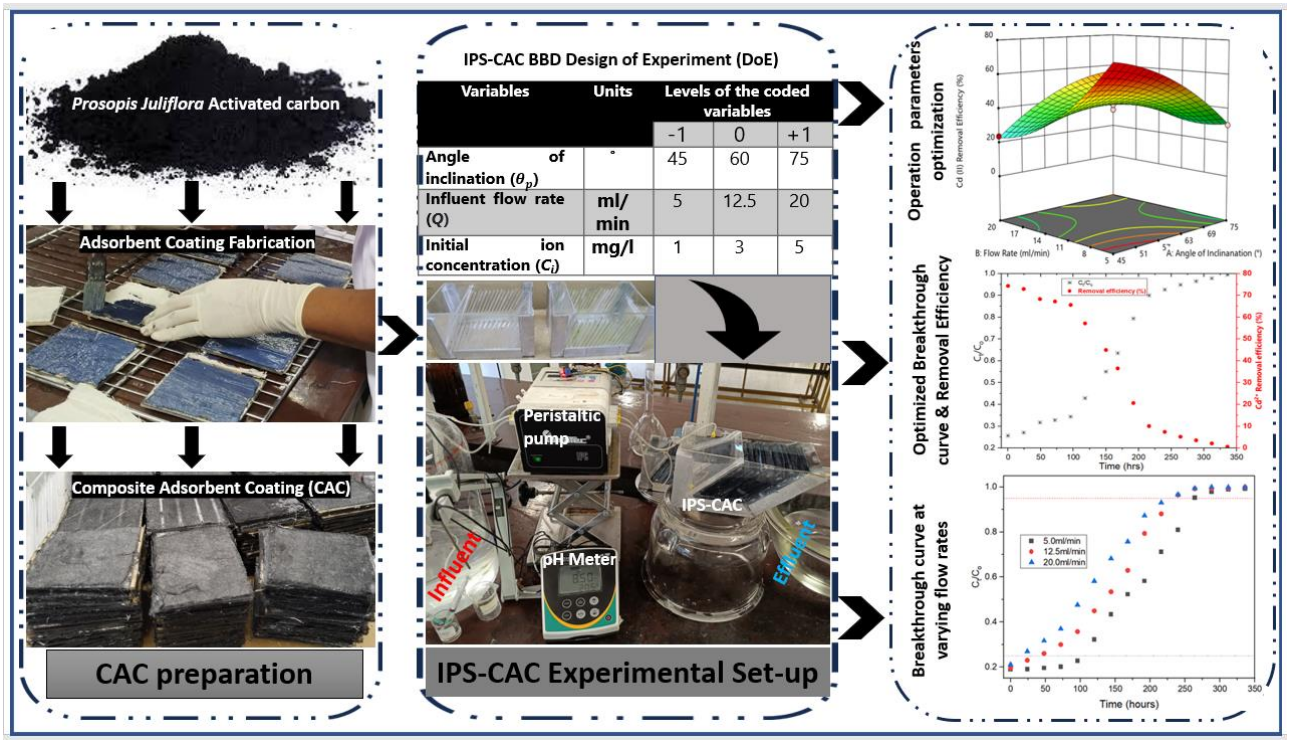

4.3.1. Evaluation of the IPA Cd^{2+} efficiency data

4.3.1.1. Regression model development and validation

The efficacy of a settling tank relies on the physical characteristics of solids and water, as well as the flow and geometric features of the tank (Sarkar et al., 2007). The variables influencing IPS efficiency are tank volume (v_p), plate length (l_p), plate surface area (A_p), plate inclination angle(θ_p), distance between plates (ω_p), number of plates (η_p), roughness of plates (ε_p), density of the particle (ρ_s), density of the water (ρ_w), size of particle (d_s), flow rate (Q), kinematic viscosity water (v_w), initial pollutant concentration (c_i), acceleration due to gravity (g) (Sarkar et al., 2007). Similarly for adsorption, operating parameters like pH, adsorbent dosage, contact time, initial pollutant concentration, temperature and their interactions affect contaminants removal efficiency from aqueous solutions (Amrutha et al., 2023). For this research, all other factors but plate inclination angle of (θ_p), flow velocity (Q), and initial pollutant concentration (c_i) (Table 1) were kept constant. Accordingly, continuous IPA adsorption experiments were performed to study the combined effect of both geometric (angle of plate inclination) and operating factors (flow rate and initial pollutant concentration) on the removal of Cd^{2+} from aqueous media using composite adsorbent coating immobilized on a substrate in an inclined plate settler.

Cd^{2+} removal efficiency was calculated using Eqn. 3. Table 22 presents the experimental findings, which shows the actual Cd^{2+} reduction by the IPA system under different combinations of operating conditions i.e. angle of plate inclination, flow rate and influent concentration. The actual values of the process variables and their variation limits were selected based on data from preliminary studies and various literature sources.

Table 22: The BBD showing actual Cd^{2+} percent removal for IPA at different operating conditions

Std	Run	Angle of Plate Inclination ($\boldsymbol{\theta_p}$)	Flow Rate (Q)	Initial Concentration ($\boldsymbol{c_i}$)	IPA Cd^{2+} Removal Efficiency
		°	ml/min	mg/L	%
7	1	45	12.5	5	14.8
13	2	60	12.5	3	45.7
1	3	45	5	3	50
6	4	75	12.5	1	35.4
4	5	75	20	3	56.5
15	6	60	12.5	3	42.3
12	7	60	20	5	25
5	8	45	12.5	1	36.3
8	9	75	12.5	5	9.5
14	10	60	12.5	3	39.5

10	11	60	20	1	46.8
2	12	75	5	3	30.4
3	13	45	20	3	23.7
9	14	60	5	1	62.5
11	15	60	5	5	35.1

The actual and coded second order polynomial equations describing the IPA Cd^{2+} removal efficiencies are given by Eqns. 33 and 34, respectively:

Actual Cd^{2+} removal %

$$= 83.17 + 1.97A + -15.83B + 11.39C + 0.17AB + -0.04AC + 0.09BC + -0.03A^2 + 0.19B^2 + -2.73C^2 \quad (33)$$

Coded Cd^{2+} removal %

$$= 42.52 + -1.91A + -6.04B + -12.08C + 18.66AB + -1.1AC + 1.4BC + -7.61A^2 + 10.79B^2 + -10.94C^2 \quad (34)$$

(where A=angle of plate Inclination (˚), B=flow Rate (ml/min), C= influent concentration (mg/L))

Table 23 presents the p-values and F-values for assessing the validity of the model prediction for IPA Cd^{2+} removal efficiency.

Table 23: Regression analysis and ANOVA results for quadratic model response surface for Cd^{2+} by IPA

Source	Sum of Squares	df	Mean Square	F-value	p-value	
Model	2932.10	9	325.79	74.37	< 0.0001	significant
A-Angle of Inclination (θ_p)	25.42	1	25.42	5.80	0.0610	not significant
B-Flow Rate (Q)	234.13	1	234.13	53.45	0.0008	Significant
C-Influent Concentration (c_i)	1166.88	1	1166.88	266.38	< 0.0001	Significant
AB	1088.93	1	1088.93	248.58	< 0.0001	significant
AC	4.80	1	4.80	1.10	0.3431	not significant
BC	7.84	1	7.84	1.79	0.2386	not significant
A^2	1162.53	1	1162.53	265.38	< 0.0001	significant
B^2	400.10	1	400.10	91.33	0.0002	significant
C^2	385.31	1	385.31	87.96	0.0002	significant
Residual	21.90	5	4.38			
Lack of Fit	2.84	3	0.9451	0.0991	0.9534	not significant
Pure Error	19.07	2	9.53			
Cor Total	2954.00	14				

R^2=0.9926; adjusted R^2=0.9762; predicted R^2=0.9700; adequate precision=31.0084

The model used for the IPA removal of Cd^{2+} shows significant high F-value of 74.37 and a low p-value of ≤0.0001. This observation suggests that there is a notable influence on the response variable from at least one of the factors included in the model (Brereton, 2019). Flow rate and influent concentration were identified as highly significant to the model, all showing low p-values ($p<0.05$) (Table 23). The interaction of angle of plate inclination and flow rate (AB) was also all found to be significant ($p< 0.0001$) for Cd^{2+} removal. Meanwhile, the square terms of all terms (A^2,

B^2, and C^2) were all highly significant ($p < 0.0001$) to the Cd^{2+}removal. The obtained lack of fit F-value of 0.099 for Cd^{2+} removal indicated that the lack of fit is not significant to the model.

The model's comparatively high regression coefficient (R^2) of 0.9926 indicate the model's capability of accurately predicting the response. The model has also demonstrated an adequate precision of 31.01, which indicate appropriateness and adequacy to navigate the design space. There is also a good agreement between predicted R^2 (0.9700) and adjusted R^2 (0.9792) as their difference (0.0092) is clearly less than 0.2. The factors added to modify the model have improved the model because the adjusted R^2 is more than the predicted R^2. Hence, the response surface model developed in this research for predicting both Cd^{2+} removal efficiency from aqueous media using IPA can be considered satisfactory.

Fig. 26(a) shows the normal percentage probability of residual against the normal plot of residuals for Cd^{2+} removal. The figure has a nearly sigmoidal pattern and forms a somewhat linear trend, indicating a strong correlation between probability and normal reduction. This confirms the assumption that the model is appropriate for estimating the efficiency of Cd^{2+} removal.

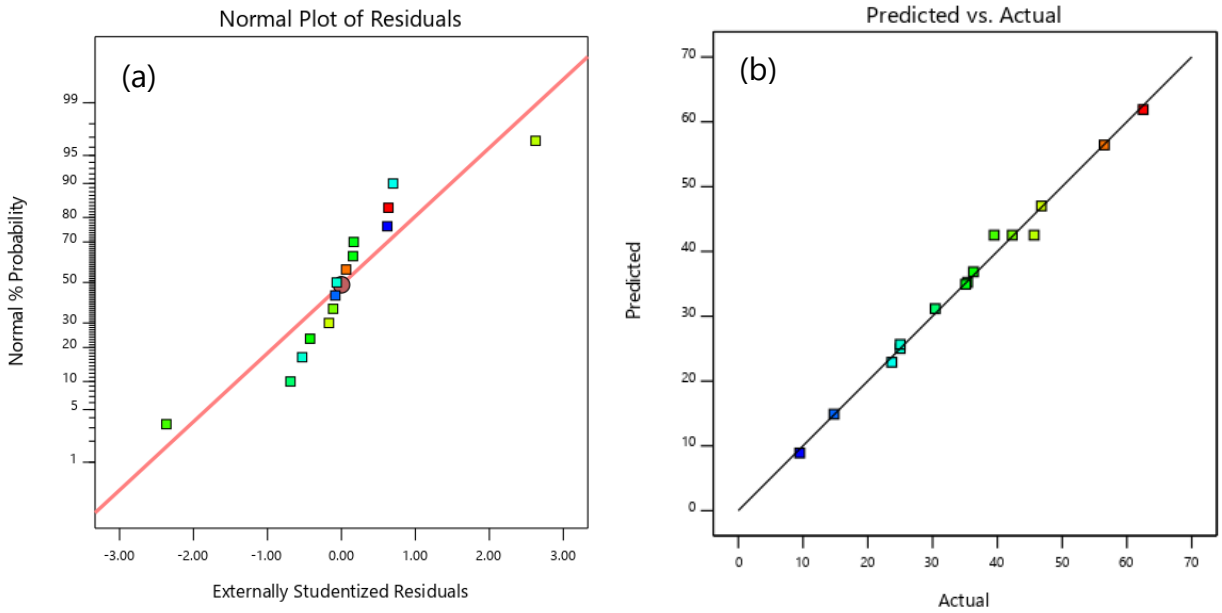

Figure 26: Normal probability plots (a) and plots for predicted against actual results (b) for Cd^{2+} reduction by IPA

In contrast, the Fig. 26(b) displays the predicted and actual plots, which corroborate the correlation between the residual and expected Cd^{2+} removal. This implies that the model is capable of accurately predicting outcomes within the specified range of both the geometric factor and the

operational parameters. Therefore, it can be concluded that the quadratic model of the response surface, which was established in this work to describe the relationship between the Cd^{2+} reduction and geometric factors and the operational parameters, is the most appropriate for accurately representing the experimental results of the innovative IPA system.

4.3.2. Effect of geometric and operating parameters on IPA Cd (II) removal efficiency

The 3D surface response graphs of experimental data showing interacting effect of IPA geometric and operating factors on Cd^{2+}reduction is shown in Fig. 27. Out of the three combinations of geometric and process factors investigated for their influence on Cd^{2+} removal using RSM, only one interaction between the angle of plate inclination and flow rate (AB) was determined to be significant ($p<0.0001$), as already presented in Table 3 and discussed above.

(a)

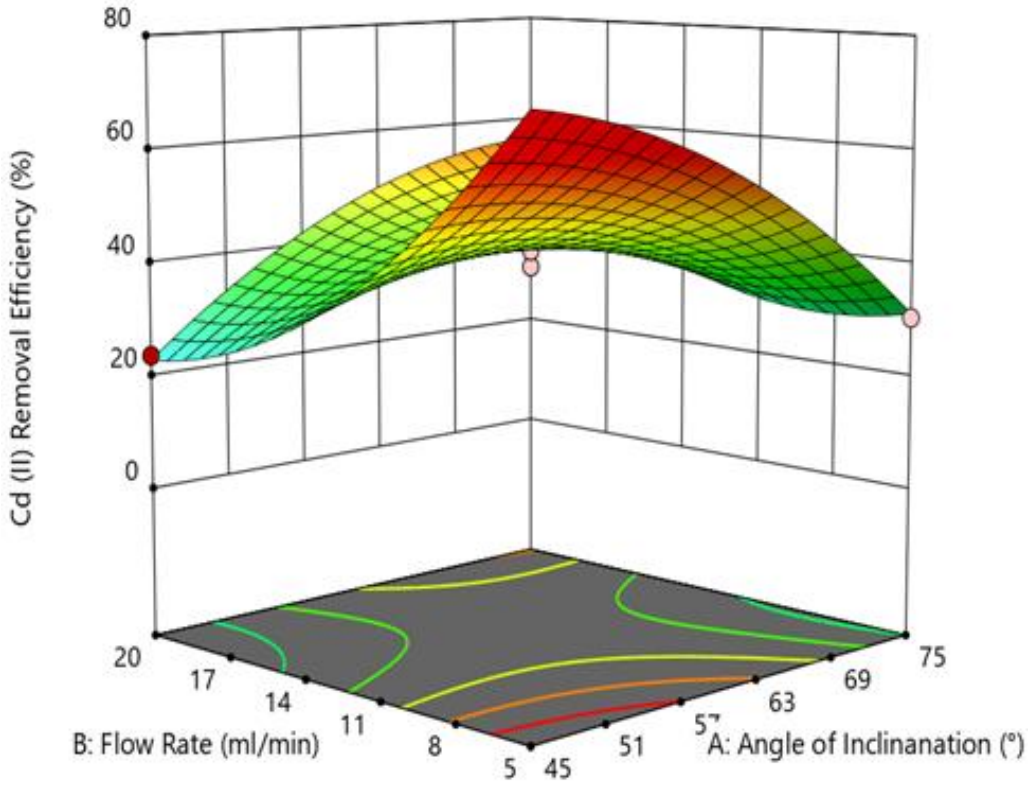

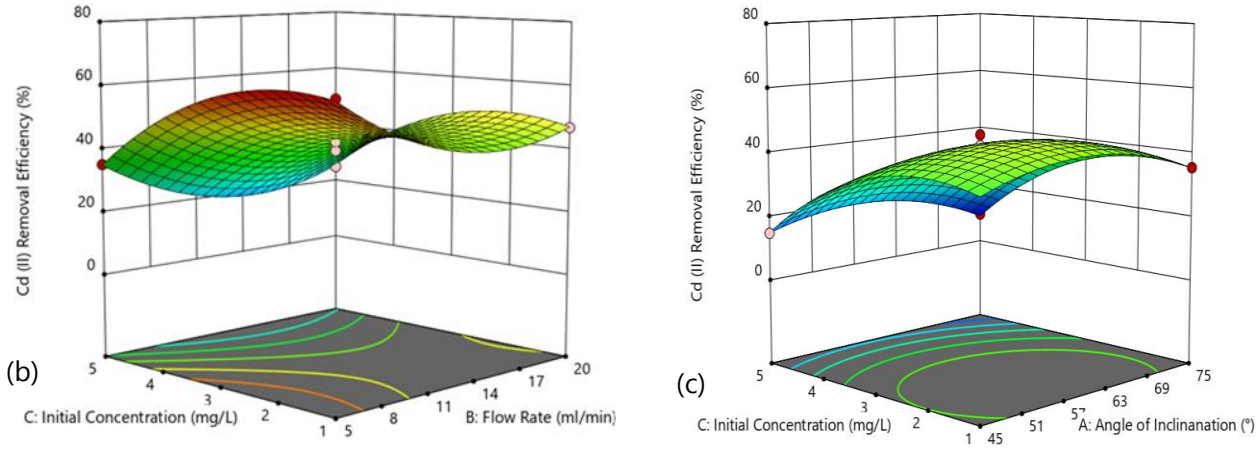

Figure 27: 3D surface response graphs of experimental data showing interacting effect of IPA operating and geometric factors on Cd^{2+}reduction.

Fig. 27a shows that Cd^{2+} removal efficiency increases with reducing both plate inclination angle of (θ_p) and flow velocity (Q). The effect of flow rate to the IPA system could be two- fold. First it relates to the CAC (adsorption) and secondly it relates to the IPA system. At low flow rates, the adsorbate had longer residence time in the IPA unit thereby increasing adsorbate-adsorbent contact time hence a high Cd^{2+} removal was achieved. Conversely, high flow rates reduce the residence or the contact time between the adsorbate and adsorbent which lead to insufficient removal of pollutants (Geleta et al., 2021). With increased angle of inclination, the adsorbate-adsorbent contact may further be minimal as the influent can move freely up the plates without contacting the CAC on the IPA plates. Furthermore, an increase in flow-rate and an increase in angle of inclination may result in the occurrence of short circuiting in the influent/adsorbate particle flow, causing an uneven distribution of the flow to the plate bundle (Chintokoma et al., 2015). Consequently, this would lead to a particular/affected CAC getting saturated faster than the rest hence allowing adsorbate to leave the treatment chamber up the collecting weir hence the low removal efficiencies at higher flow rates. Prior research has also indicated that the hydraulic performance of an inclined plate settler (IPS) decreases as the flow rate increases (Salem et al., 2011).

Table 23 and Fig. 27(b-c) show that there is insignificant interacting effect of initial Cd^{2+} concentration (c_i) and flow velocity (Q) (Fig. (2b)) and that of initial Cd^{2+} concentration (c_i) and inclination angle of (θ_p) (Figure 8c) on Cd^{2+} removal by IPA system. Nevertheless, Fig. 26 (c) indicate that the IPA Cd^{2+} removal efficiency decreases with an increase in initial Cd^{2+} concentration at any given plate inclination angle. At low concentrations, metals are absorbed by specific sites.

However, as the metal concentration increases, the specific sites become saturated and the exchange sites are filled (Mouni et al., 2012). The adsorption capacity of a given amount of adsorbent is constant, allowing for the adsorption of a finite quantity of heavy metal ions. As the initial concentration rises, the levels of heavy metal ions likewise progressively rise. The heavy metal ions will gradually occupy the surface adsorption sites and reach a state of saturation. The adsorption capacity of the adsorbent for heavy metal ions rises per unit and eventually achieves an equilibrium condition. Hence, given a certain adsorbent quantity, higher initial concentrations result in decreased removal efficiency of heavy metal ions (J. Li et al., 2022).

4.3.3. IPA Cd^{2+} removal efficiency process optimization

The main objective of the optimization method was to determine the most favorable values of variables for effectively removing Cd^{2+} utilizing the IPA hybrid. This was accomplished by employing a model generated from empirical data. The operating parameters were selected with the aim of maximizing the response (i.e., Cd^{2+} removal efficiency) while the angle of inclination, flow rate and influent concentration were all left at a range. Multiple sets of experiments (42 in total) were suggested by the model but the one with high removal efficiency (Table 24) was selected for further verification as well as breakthrough curve and comparative studies. The optimized operating conditions (i.e. angle of inclination, θ=45˚; Flow rate, Q=5 ml/min and influent concentration, C_i=1.87 mg/L) predicted 75.8% removal for Cd^{2+} with 0.76 desirability. Experimentally, the same optimum operating conditions were able to achieve 66.9±0.48% Cd^{2+} removal efficiencies.

Table 24: Some of the solutions suggested and selected for operating parameters optimization tests for Cd^{2+} removal by IPA

Number	Angle of Inclination (θ)	Flow Rate (Q)	Initial Concentration (C_i)	Cd^{2+} Removal Efficiency (%)	Desirability	
1	**45.000**	**5.000**	**1.866**	**75.798**	**0.758**	**Selected**
2	45.000	5.000	1.844	75.796	0.758	
3	45.010	5.000	1.885	75.794	0.758	
4	45.000	5.000	1.907	75.794	0.758	
5	45.001	5.000	1.816	75.790	0.758	
6	45.000	5.000	1.948	75.780	0.758	
7	45.000	5.000	2.002	75.748	0.757	
8	45.232	5.000	1.911	75.718	0.757	
9	45.000	5.000	1.675	75.696	0.757	
10	45.000	5.015	1.746	75.666	0.757	
11	45.000	5.000	1.630	75.643	0.756	
12	45.000	5.000	1.561	75.540	0.755	
13	45.000	5.000	1.490	75.407	0.754	
14	45.000	5.071	1.950	75.334	0.753	
15	45.000	5.000	2.348	75.168	0.752	
16	46.744	5.000	1.556	74.902	0.749	
17	45.000	5.000	2.490	74.740	0.747	

18	45.000	5.000	2.557	74.501	0.745	
19	45.000	5.000	2.582	74.405	0.744	
20	45.000	5.000	2.620	74.252	0.743	

4.3.4. Breakthrough curve analysis study

The primary impetus behind this study has been the necessity to develop a prototype for wastewater treatment that can be easily scalable. In this regard the utilization of mathematical modelling is essential for the successful implementation of upscaling approaches, allowing for the transfer of knowledge from laboratory studies to pilot plants and industrial sizes. The mathematical modelling serves as a powerful tool for analysing and explaining experimental data, identifying important processes, predicting the results of various operating conditions, and improving the overall efficiency of the process (de Franco et al., 2017). Breakthrough happens when the adsorbate reaches the end of the system and exits with the system effluent (Gabelman, 2017). The breakthrough curves were obtained from the continuous 336-hour IPA experimental results at the optimized conditions. The graph illustrating the relationship between adsorbate concentration and time is displayed in Fig. 28(a) which show the breakthrough curves for the sorption of Cd^{2+} on the immobilized CAC. The quantity of adsorbate that is adsorbed at a specific moment is exactly proportional to the surface area located above the breakthrough curve at that moment bounded by C_t/C_0 =1 (Gabelman, 2017) where C_t is the Cd^{2+} effluent concentration at time t, C_o is the initial of influent concentration. Where t_b is the breakthrough time, breakthrough was achieved when C_t/C_0 =0.25. C_{ex} and t_{ex} are the exhaustion/saturation concentration and time respectively when C_t/C_0=0.95 i.e. a point at which 95% of the CAC was exhausted. Hence exhaustion time (t_{ex}) was taken at exhaustion concentration C_{ex} when C_t/C_o attained a value of 0.95. The breakthrough data was effectively utilized for determination of the adsorption capacity at both breakthrough time (t_b) (C_t/C_0 =0.25) and exhaustion time (t_{ex}) (C_t/C_0 =0.95). Fig. 28(b) shows that the breakthrough and saturation times were 66.9 and 168.15 hours, respectively. Using Eqn 14, the IPA overall breakthrough adsorption capacity (q_b) was determined to be 6.17mg/g while the IPA adsorption capacity at exhaustion (q_{ex}) was calculated as 15.51mg/g. Experimentally, the optimized conditions yielded 74.3% removal at zero hours of first effluent and an average Cd^{2+} removal efficiency of 69.7% over a 96-hour period.

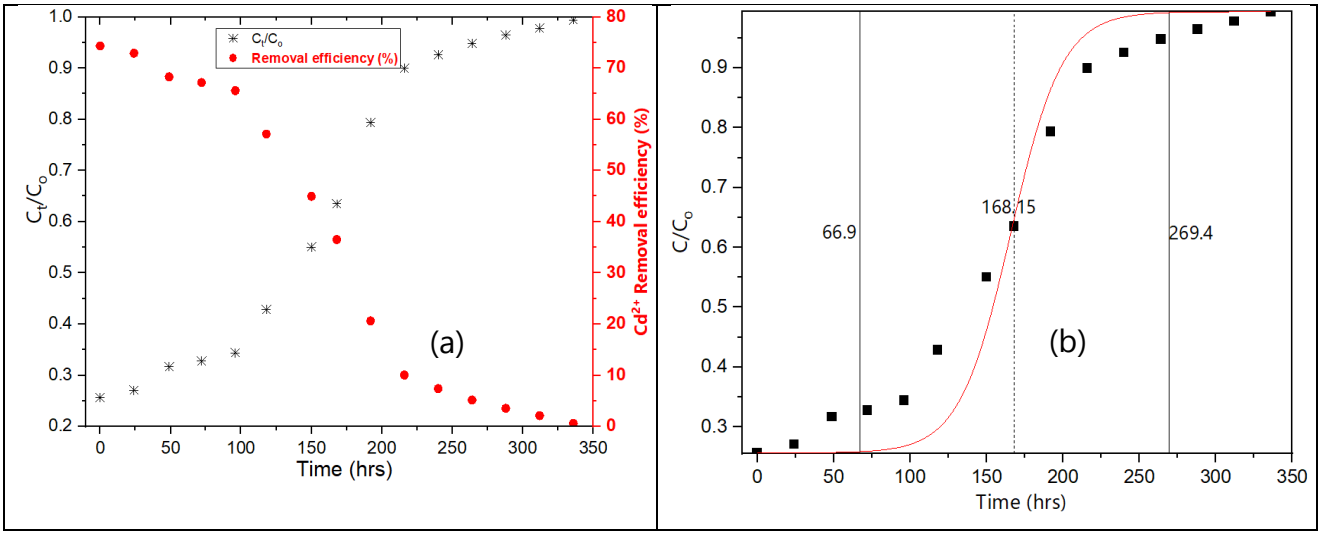

Figure 28: Optimized conditions breakthrough experimental results (a) and breakthrough curve analysis (b) of the IPA system

4.3.5. IPA Cd^{2+} adsorption dynamics

Figure 29 shows the breakthrough curves of Cd^{2+} adsorption onto IPA at different plate inclination angles, initial Cd^{2+} concentrations and flow rates. Breakthrough time, is defined as the time required to reach a specific breakthrough outlet concentration (Dorado et al., 2014). As mentioned already, the breakthrough time was reached when C_t/C_o was equal to 0.25. Similarly, saturation or exhaustion time was reached at C_t/C_o=0.95. The total IPA adsorption capacities at both breakthrough and saturation point were obtained by numerical integration of the area above the breakthrough curve up to C_t/C_o = 1 (Gómez-Avilés et al., 2022).

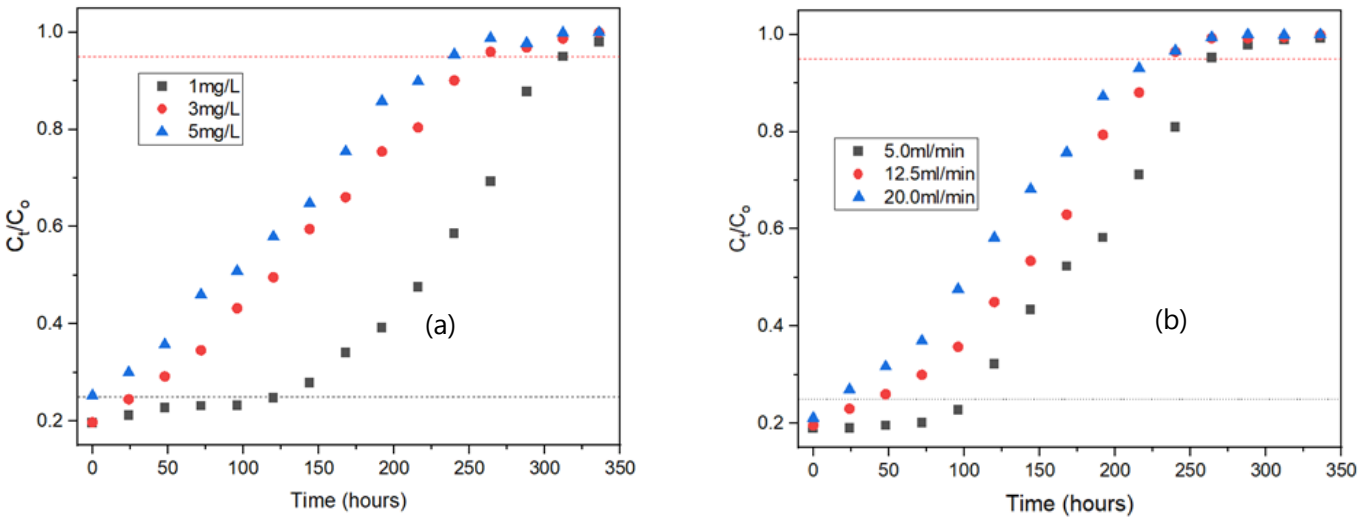

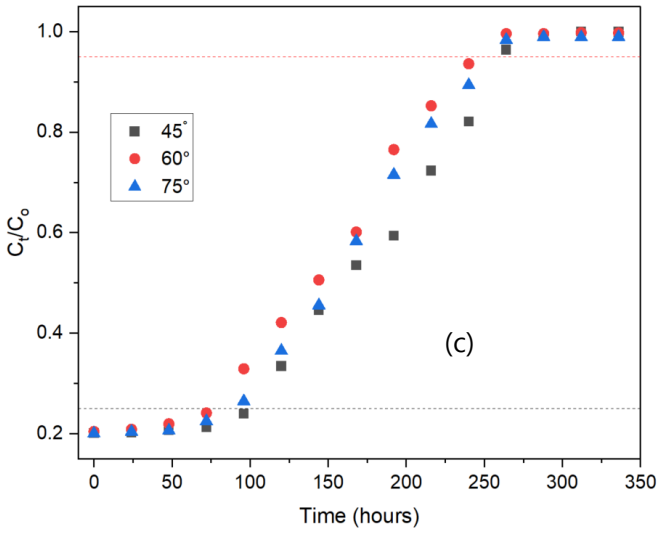

Figure 29: Breakthrough curves of Cd^{2+} onto IPA at different conditions (a) Varying initial Cd^{2+} concentration (θ=45° and Q =5ml/min), (b) Varying flow rate (θ=45° and C_o =1mg/L) and (c) Varying plate inclination angle (C_o =1mg/L and Q =5ml/min)

The Fig. 29(a) shows that the breakthrough time increases with decreasing initial Cd^{2+} concentration meaning that lower metal concentrations generates higher adsorption zone lengths (Dorado et al., 2014) there by increasing the adsorption capacity. Furthermore, it was observed that the gradient of the breakthrough curves got more steeper when the initial Cd^{2+} concentration was increased. Previous studies have attributed this to the reaction zone progressing more rapidly under higher metal concentrations (Antil et al., 2022; Dorado et al., 2014). Approximately 120 hours were required to obtain the breakthrough point for the lowest 1 mg/L influent compared with the 23.6 hours and 3 hours that was needed to reach the breakthrough point for both the 3mg/L and 5mg/L influent respectively. The breakthrough adsorption capacities at different Cd^{2+} concentrations of 1, 3 and 5 mg/L were 5.93, 3.5 and 0.74 mg/g respectively. The decline in adsorption capacity with increasing concentration observed at the breakthrough point is attributed to the saturation of adsorption sites on the CAC. Consequently, the adsorbent's surface reached saturation more rapidly at higher concentrations (Patel, 2020) leading to relatively lower adsorption capacity.

The effect of Cd^{2+} removal by IPA on varying flow rates were studied at 5, 12.5, and 20ml/min while initial influent concentration and plate inclination angle were kept constant at 1.89mg/L and 45° respectively. Both the breakthrough time and adsorption capacity decreased with an increase in flow rate (Fig. 29(b)). The breakthrough time were 118, 36, and 15.5 hours corresponding to breakthrough adsorption capacities of 5.84, 4.45, and 3.07 mg/g for the 5, 12.5 and 20 ml/min flow

rates respectively. High flow rate reduces the residence time and contact time between the adsorbate and adsorbent leading to reduced breakthrough time and relatively low adsorption capacities (Geleta et al., 2021; Ledesma et al., 2023; Mondal et al., 2018). The observed variations in the adsorption capacity and the breakthrough curve's steepness with varying flow rates may be explained by the basic principles of mass transfer (Tosun, 2019). Higher flow rates also minimizes the resistance to mass transfer caused by external coating at the adsorbent's surface, resulting in a faster rate of mass transfer and a decreased residence time (Fernandez et al., 2023).

Finally, it can be seen from Fig. 29 (c) how the breakthrough time does not vary significantly with the angle of plate inclination which agrees well with the results of the ANOVA results of the optimization experiments in Table 3 showing the insignificant (p=0.05) effect of IPC-CAC plate inclination angle on Cd^{2+} removal. The breakthrough time of the 45°, 60° and 60° IPA were 100, 80 and 60 hours respectively corresponding to adsorption capacities of 4.95, 3.96 and 2.97 mg/g respectively.

4.3.6. IPA comparative experiments and Cd (II) removal mechanism

After optimization of the IPA geometric and process factors, the IPA removal efficiency at the optimized conditions was also compared with the removal efficiencies of a tank with plain plates (IPS-PP) and a tank with no plates (IPS-NP). Fig. 30 presents results of the comparison of the percentage removal of Cd^{2+} by IPA, IPS-NP and IPS-PP, respectively. Vividly, there is a significant ($p < 0.05$) difference (Annex 3) in removal efficiencies with IPA having higher removal efficiency (66.9%) compared to IPS-PP (4.6%) and IPS-NP (2.4%). Clearly the comparative experiment results confirm that the relative higher Cd (II) removal by the IPA system was achieved due to the synergistic effect of the IPA system. The results of this experiment clearly confirm the early assumption that the dominant Cd (II) removal mechanism from the IPA system was physical adsorption. If settling/sedimentation on the IPA plate was the dominant Cd^{2+} removal mechanism from the IPA system, then the IPS-PP would have performed relatively closer to the IPA than the results shown in Fig. 30. Similarly, if precipitation was the dominant removal mechanism then the IPS-NP performance would also have been relatively higher than depicted in Fig. 30.

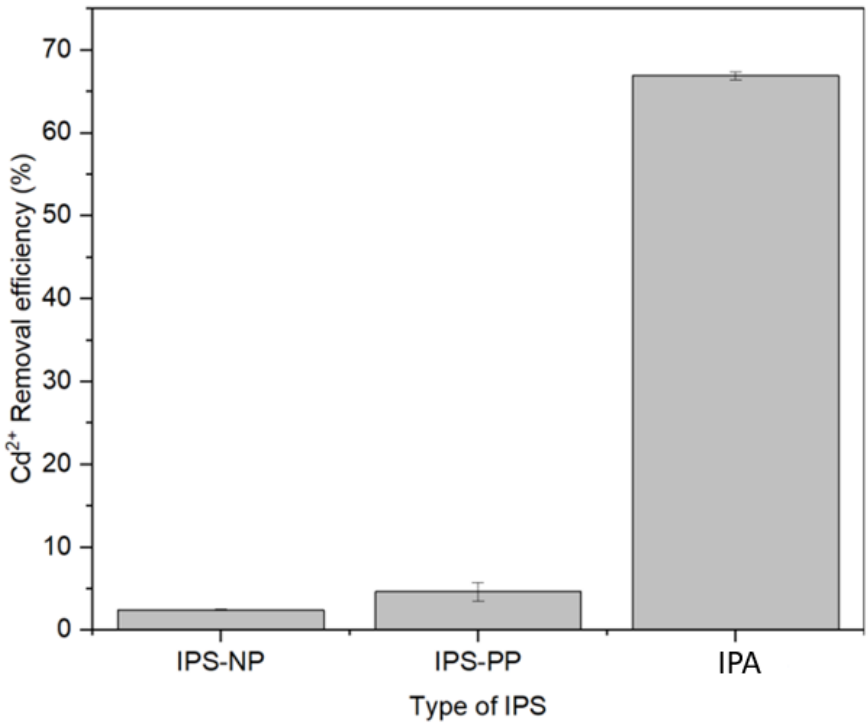

Figure 30: Optimized conditions breakthrough curve analysis results of the IPA system

With regards to Cd^{2+} removal mechanism by the IPA, there could be multiple removal mechanisms but the proposed dominant removal mechanism is physical adsorption which could have occurred through electrostatic attraction and/or pore-filling/micropore capture. Firstly the Cd^{2+} adsorption occurred at pH greater than the pH_{PZC} of the CAC (pH 6) (Chintokoma et al., 2024) ; hence, the CAC surface would gain negative charges that interact with the positive charges on the Cd^{2+} by electrostatic forces (Wu et al., 2020). Also, the Cd^{2+} ions can be entered into the CAC structure through their micropores and mesopores, and thus, they will subsequently adsorb onto the active sites. This process is known as pore-filling or micropore capture (Chowdhury, 2013).

4.4. CAC REGENERATION STUDY

4.4.1. Reusability of the pollutant loaded composite adsorbent coating (CAC)

The efficacy of a particular biomass being as adsorbent depends not only on its adsorption capability, but also on its ease of regeneration and recycling (Younas et al., 2021). The ability of the adsorbent to regenerate and be recycled is another important component of the adsorption process (Aktar, 2021). The CAC was mainly synthesized to overcome the challenges associated with leaching of adsorbents during regeneration (Azha et al., 2017a; Shamsudin & Shahadat, 2019). The Cd^{2+} desorption amount, Q_{de}, (mg/g) and desorption percentage (%) of CAC calculated using Equations 9 and 10 respectively. Fig. 31 shows that the adsorption capacity of CAC decreased only slightly after each adsorption–regeneration cycle.

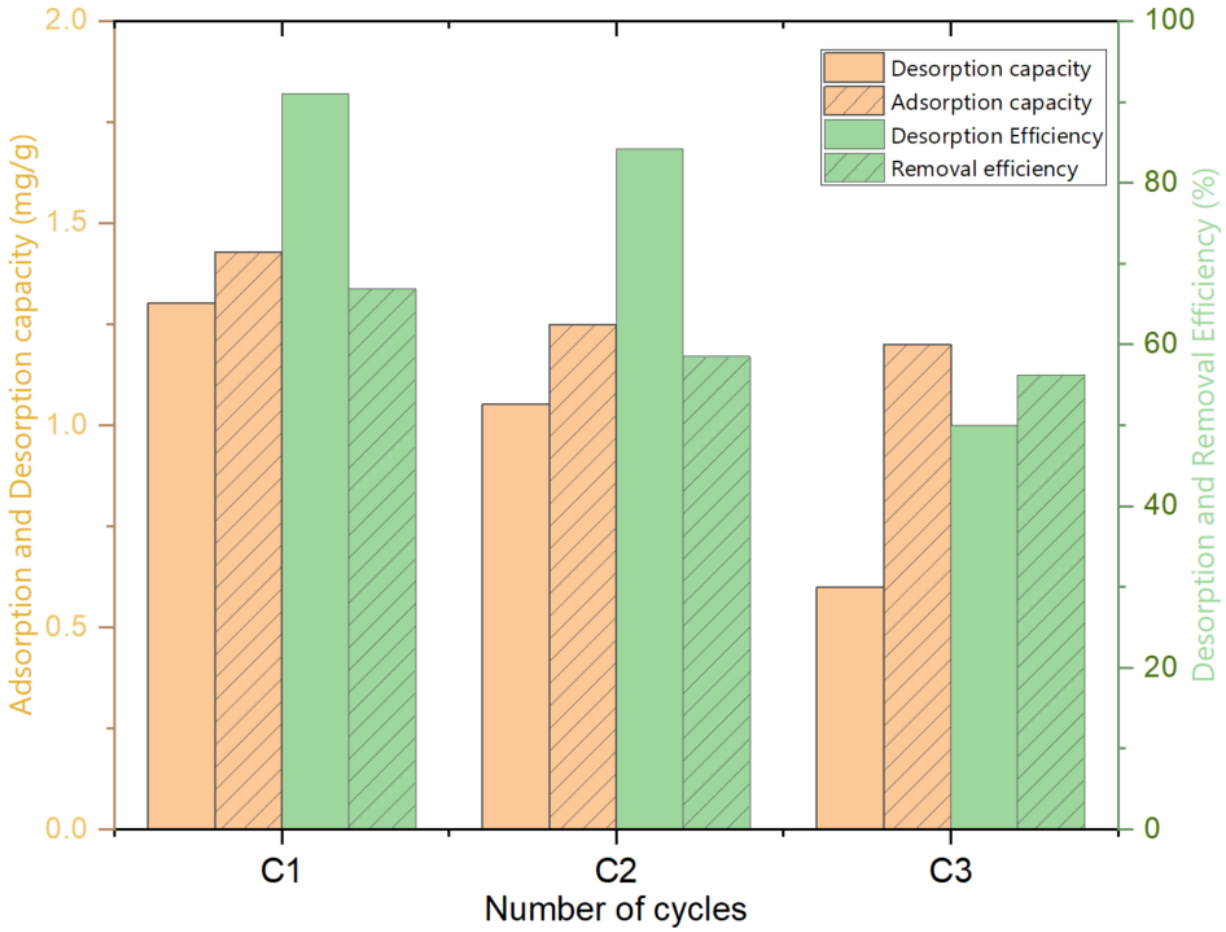

Figure 31: The CAC Cd^{2+} adsorption and desorption capacity and the Cd^{2+} desorption and removal efficiency of regenerated CAC

The regeneration study shows that the CAC lost just about 10.7% (from 66.9% to 56.2%) of its Cd^{2+} removal efficiency with a 0.1 M HCl of pH 0.3 as an eluent even after three consecutive adsorption–desorption tests. On the other hand, the desorption percentage (%) reduced from 91% to 50% following three successive cycles. This demonstrates the great stability of the CAC and its potential for three consecutive cycles of Cd^{2+} adsorption–desorption. However since the CCF used in making the CAC is basically cotton fiber composed of cellulose, accompanied by a limited number of non-cellulosic components (P. Kumar et al., 2022), the disintegration of the cotton fibers from the use of HCl as de-sorbent is evident especially after the third cycle of regeneration.

5. CONCLUSIONS AND RECOMMENDATIONS

Chapter summary

This chapter reports the conclusions and recommendations that are emanating from this study. The conclusions are generally a summary based on the research objectives, findings and discussion. The recommendations are primarily drawn from the study objectives and the conclusions made.

5.1. CONCLUSIONS

The study utilized *Prosopis Juliflora* wood material to prepare an adsorbent for the removal of heavy metals from wastewater. Initially the BBD of the RSM was effectively utilized to investigate the influence of three activated carbon preparation factors (chemical impregnation ratio, carbonization temperature, and carbonization time) on the effectiveness of Cd^{2+} removal from an aqueous solution using PJAC.

A quadratic model was developed to establish a correlation between the preparation factors and the Cd^{2+} removal efficiency by adsorption. By examining the response surfaces generated by the models, it was shown that the impregnation ratio and carbonization temperature had a significant impact on the removal of Cd^{2+} ($p=0.0003$), with carbonization temperature being the most influential factor ($p=0.0001$) among the three factors investigated.

Process optimization was conducted and the optimized predicted removal efficiency of 99.9% with 1.0 desirability was obtained for 1.8 impregnation ratio, 595 ºC carbonization temperature and 174 min activation time. Experimentally a removal efficiency of 96.7% was obtained from the PAC prepared under optimum conditions.

The optimized preparation conditions prepared PAC was characterized and the SEM images revealed a rough and porous morphological surface with an S_{BET} of 600.4m^2/g and a near neutral pH_{PZC} of 6.92. The FTIR spectrum demonstrated a well-defined difference before and after Cd^{2+} adsorption with the latter showing a reduction in both peak intensity and height. The XRD pattern also clearly indicated the amorphous nature of the prepared adsorbent with the loaded activated carbon showing some variations in the intensity of peaks as compared to that of unloaded activated carbon.

To overcome the challenges associated with PAC in wastewater treatment, CAC was synthesized using a simple sol-gel utilizing PJAC prepared under the optimized conditions, CCF, APE and DI. The synthesized CAC was characterized by FTIR (C-H, C=O and O-H stretching), pH_{PZC} (6-6.6)), SEM (Porous-rough surface) and BET surface area (10.6m^2/g) techniques.

The CAC was evaluated based on its simultaneous removal of Cd^{2+} and $Cr_2O_7^{2-}$ from simulated wastewater. ANOVA results showed that pH and contact time were significant ($p<0.0001$) for both Cd^{2+} and $Cr_2O_7^{2-}$ removal; contact time and CAC dosage were most significant ($p<0.0001$) for Cd^{2+} removal while the initial concentration was most significant ($p<0.0001$) for $Cr_2O_7^{2-}$ removal. At the optimized operating parameters (pH=8.5; adsorbent dosage=0.25g; initial concentration=5mg/L; contact time=105 minutes and temperature; 23.73°), the predicted and experimental ion removal efficiencies were 86.86% and 83.98% for Cd^{2+} and 94.26% and 58.08% for $Cr_2O_7^{2-}$, respectively.

The Langmuir adsorption isotherm was the best-suited model ($R^2>0.99$) while the metal ions removal was regulated by pseudo second order (PSO) kinetic model ($R^2>0.999$). The -ΔG°, +ΔH° and +Δ*S*° values revealed the endothermic and spontaneity of the adsorption process. The findings demonstrated the high potential of using CAC as an adsorbent for metal ions removal to circumvent the PAC challenges in wastewater treatment.

The final part of the study aimed at developing an innovative wastewater treatment prototype termed Inclined Plater Adsorber (IPA) to enable Cd^{2+} removal from aqueous solutions in a continuous adsorption set-up. The IPA system was designed, fabricated and optimized as an easily scalable novel wastewater treatment prototype for enhanced heavy metal removal. It aimed at leveraging the synergistic effect of inclined plate and coated adsorbent to enhance heavy metal removal efficiency from wastewater. The effects of angle of plate inclination (θ_p), influent flow rate (Q) and adsorbate initial concentration (C_i) on Cd^{2+} percent removal efficiency (%) was studied by again employing the BBD of the RSM.

The results showed that flow rate and initial influent concentration were the most significant ($p< 0.05$) factors on the removal of Cd^{2+} by the IPA system. It was also determined that the interaction effects of angle of plate inclination (θ) and flow rate (Q) contributes significantly to the percent reduction of Cd^{2+} ($p< 0.05$). The optimal Cd^{2+}removal by the IPA system was obtained at angle of plate inclination (θ)=45˚; Flow rate (Q)=5ml/min and influent concentration (C_i)=1.87mg/L.

With the BBD-RSM's developed optimum geometric and operational parameters, the IPA predicted a 75.8% Cd^{2+} removal efficiency while the experimentation with the same optimized conditions yielded an average of 69.7±4.67%, % removal efficiency over a 96-hour period. The optimized conditions breakthrough time (C_t/C_0 =0.25) and saturation time (C_t/C_0 =0.95) were 66.9 hours and 168.2 hours respectively each with adsorption capacity of 9.6mg/g and 15.51mg/g respectively.

Comparing IPA performance with a tank without plates and another with plain plates, the Cd^{2+} removal efficiencies were 2.4±0.1% and 4.6±1.1%, respectively confirming that adsorption (physical) was the dominant Cd^{2+} removal mechanism. The CAC is very stable for Cd^{2+} removal as only 10% decrease in its removal efficiency was observed after three adsorption-regeneration cycles. This observation indicates that the composite material has the capability of being utilized repeatedly to effectively remove Cd^{2+} ions from effluent streams.

The CAC's ability to eliminate the requirement for filtration, sedimentation, or centrifugation steps during regeneration makes it a compelling candidate for scalable and practical industrial applications. Again, the IPA system is easily scalable as it not only does it reduce treatment unit footprint, but also it can be gravity operated thereby reducing the initial and operational costs as well as the carbon footprint.

5.2.RECOMMENDATIONS

This study has provided insights of the optimized IPA system for the removal of Cd^{2+} from aqueous solutions. Nevertheless, since research frequently generates more inquiries than it resolves, at the conclusion of this comprehensive academic study endeavor, there is a list of areas in which more research is required as follows;

1) As much as this was a lab-scale experimental set-up of which ideally was supposed to be under controlled environments, however due to unavailability of appropriate equipment some parameters were not easily controlled. For example, the pH adjustment of the IPA influent was a bit challenging given the huge volume involved especially for the breakthrough curve experiments. It was noticed that much as the influent pH would be initially adjusted, but over time the pH would fluctuate. The influent pH was fluctuating because the carbon dioxide was reacting with water to form carbonic acid ($CO_2 + H_2O \Leftrightarrow H_2CO_3$) which was increasing the acidity of the system by lowering the influent pH. Perhaps sealing the influent feed container from start to finish of the experiments would be ideal as it would prevent the reaction with carbon dioxide and the consequence formation of carbonic acid. The heavy metal removal performance of a sealed IPA system needs further investigation.

2) It's possible that there could have been short-circuiting of the influent wastewater within the system which could have led to unequal distribution of the flow to the plate bundles hence allowing the easy flow of a more concentrated untreated effluent solution up the collecting weir into the effluent container. Further research should consider having a mechanism to constantly shake the influent to allow for constant adsorbate-adsorbent contact and prevent any possibility of influent short-circuiting. The constant shaking would also greatly increase the contact time between the adsorbate and adsorbent.

3) The study investigated the simultaneous reduction of Cd^{2+} and $Cr_2O_7^{2-}$ using CAC in a batch adsorption set-up. However due to time constraints, only the Cd^{2+} percent removal efficiency (%) was studied for the innovative IPA continuous set-up. Further investigation is therefore required to evaluate the removal capability of the IPA system on various contaminants in a binary system set-up.

4) Given that heavy metal ions have the ability to adhere to solid surfaces such as activated carbon, bio-sorbents, particulate matter, and clays, it is crucial to investigate the impact of the presence of suspended particles in the influent on the performance of IPA in terms of its ability to efficiently remove heavy metals. The rationale for this approach is that the pollutants would initially attach to the particulate matter, which would then settle onto the IPA plate which has the adsorbent. This process would most probably improve the efficiency of pollutant removal from wastewater hence the need for further investigation.
5) After successfully implementing the aforementioned recommendations, it would also be essential to conduct a pilot scale experimentation of the IPA design in order to have a comprehensive understanding of system performance. This would involve testing and evaluating the system in a real environment to validate and assess its design integrity under uncontrolled environmental conditions including a diverse range of feed flow-rates and influent concentrations.

REFERENCES

Abatan, O. G., Alaba, P. A., Oni, B. A., Akpojevwe, K., Efeovbokhan, V., & Abnisa, F. (2020). Performance of eggshells powder as an adsorbent for adsorption of hexavalent chromium and cadmium from wastewater. *SN Applied Sciences*, *2*(12), 1–13. https://doi.org/10.1007/S42452-020-03866-W/TABLES/7

Abdelmonem, H. A., Hassanein, T. F., Sharafeldin, H. E., Gomaa, H., Ahmed, A. S. A., Abdel-lateef, A. M., Allam, E. M., Cheira, M. F., Eissa, M. E., & Tilp, A. H. (2024). Cellulose-embedded polyacrylonitrile/amidoxime for the removal of cadmium (II) from wastewater: Adsorption performance and proposed mechanism. *Colloids and Surfaces A: Physicochemical and Engineering Aspects*, *684*, 133081.

Abdulahi, M. M., Ute, J. A., & Regasa, T. (2017). Prosopis Juliflora l: Distribution, impacts and available control methods in Ethiopia. *Tropical and Subtropical Agroecosystems*, *20*(1), 75–89. https://www.redalyc.org/pdf/939/93950595002.pdf

Abdullah, N., Yusof, N., Lau, W. J., Jaafar, J., & Ismail, A. F. (2019). Recent trends of heavy metal removal from water/wastewater by membrane technologies. *Journal of Industrial and Engineering Chemistry*, *76*, 17–38. https://doi.org/10.1016/j.jiec.2019.03.029

Abed, A., Haidar, M., Mahmood, S., & Mohammed, A. A. (2013). Removal of Cu2+, Pb2+, And Ni 2+ Ions From Simulated Waste Water By Ion Exchange Method On Zeolite And Purolite C105 Resin. *Iasj.NetAA Mohammed, HS MahmoodJournal of Engineering, 2013•iasj.Net*, *10*.

Agboola, O. D., & Benson, N. U. (2021). Physisorption and Chemisorption Mechanisms Influencing Micro (Nano) Plastics-Organic Chemical Contaminants Interactions: A Review. *Frontiers in Environmental Science*, *9*. https://doi.org/10.3389/FENVS.2021.678574/FULL

Agoro, M. A., Adeniji, A. O., Adefisoye, M. A., & Okoh, O. O. (2020). Heavy Metals in Wastewater and Sewage Sludge from Selected Municipal Treatment Plants in Eastern Cape Province, South Africa. *Water 2020, Vol. 12, Page 2746*, *12*(10), 2746. https://doi.org/10.3390/W12102746

Ahmad, A., Rehman, M. U., Wali, A. F., El-Serehy, H. A., Al-Misned, F. A., Maodaa, S. N., Aljawdah, H. M., Mir, T. M., & Ahmad, P. (2020). Box–Behnken Response Surface Design of Polysaccharide Extraction from Rhododendron arboreum and the Evaluation of Its Antioxidant Potential. *Molecules*, *25*(17). https://doi.org/10.3390/molecules25173835

Ahmad, G., Nawaz, A., Nawaz, S., Shad, N. A., Sajid, M. M., & Javed, Y. (2020). Nanomaterial-based gas sensor for environmental science and technology. *Nanofabrication for Smart Nanosensor Applications*, 229–252. https://doi.org/10.1016/B978-0-12-820702-4.00010-6

Ahmed, M. F., & Mokhtar, M. Bin. (2020). Assessing cadmium and chromium concentrations in drinking water to predict health risk in Malaysia. *International Journal of Environmental Research and Public Health*, *17*(8). https://doi.org/10.3390/ijerph17082966

Ahmed, W., Mehmood, S., Qaswar, M., Ali, S., Khan, Z. H., Ying, H., Chen, D. Y., & Núñez-Delgado, A. (2021). Oxidized biochar obtained from rice straw as adsorbent to remove uranium (VI) from aqueous solutions. *Journal of Environmental Chemical Engineering*, *9*(2), 105104. https://doi.org/10.1016/J.JECE.2021.105104

Akl, M. A., Mostafa, A. G., Abdelaal, M. Y., & Nour, M. A. K. (2023). Surfactant supported chitosan for efficient removal of Cr(VI) and anionic food stuff dyes from aquatic solutions. *Scientific Reports 2023*

13:1, *13*(1), 1–27. https://doi.org/10.1038/s41598-023-43034-9

Aktar, J. (2021). Batch adsorption process in water treatment. In *Intelligent Environmental Data Monitoring for Pollution Management*. Elsevier Inc. https://doi.org/10.1016/b978-0-12-819671-7.00001-4

Al-Ghouti, M. A., & Da'ana, D. A. (2020). Guidelines for the use and interpretation of adsorption isotherm models: A review. *Journal of Hazardous Materials*, *393*, 122383. https://doi.org/10.1016/j.jhazmat.2020.122383

Alafnan, S., Awotunde, A., Glatz, G., Adjei, S., Alrumaih, I., & Gowida, A. (2021). Langmuir adsorption isotherm in unconventional resources: Applicability and limitations. *Journal of Petroleum Science and Engineering*, *207*, 109172. https://doi.org/10.1016/J.PETROL.2021.109172

Alayu, E., & Yirgu, Z. (2018). Advanced technologies for the treatment of wastewaters from agro-processing industries and cogeneration of by-products: a case of slaughterhouse, dairy and beverage industries. *International Journal of Environmental Science and Technology*, *15*(7), 1581–1596. https://doi.org/10.1007/s13762-017-1522-9

Ali, H., Chemistry, E. K.-T. & E., & 2018, undefined. (2017). What are heavy metals? Long-standing controversy over the scientific use of the term 'heavy metals'–proposal of a comprehensive definition. *Taylor & FrancisH Ali, E KhanToxicological & Environmental Chemistry, 2018•Taylor & Francis*, *100*(1), 6–19. https://doi.org/10.1080/02772248.2017.1413652

American Chemical Society. (2019). *Chemical Reactions: Acids Donate Protons to Water Bases Accept Protons from Water*. https://www.acs.org/content/dam/acsorg/education/k-8/inquiry-in-action/fifth-grade/g5-l3.4-bkgd.pdf

Amrutha, Jeppu, G., Girish, C. R., Prabhu, B., & Mayer, K. (2023). Multi-component Adsorption Isotherms: Review and Modeling Studies. In *Environmental Processes* (Vol. 10, Issue 2). Springer International Publishing. https://doi.org/10.1007/s40710-023-00631-0

Antil, M., Singh, S., Bhagat, M., Vilvas, V., & Sundaramurthy, S. (2022). Column optimization of adsorption and evaluation of bed parameters-based on removal of arsenite ion using rice husk. *Environmental Science and Pollution Research*, *29*(48), 72279–72293. https://doi.org/10.1007/s11356-022-20580-9

APHA, A. P. H. A. (2005). Standard methods for the examination of water and wastewater. In *American Public Health Association (APHA): Washington, DC, USA*.

Arifin, E., Cha, J., & Lee, J. K. (2013). Simple and efficient synthesis of Iron oxide-coated silica gel adsorbents for arsenic removal: Adsorption isotherms and kinetic study. *Bulletin of the Korean Chemical Society*, *34*(8), 2358–2366. https://doi.org/10.5012/bkcs.2013.34.8.2358

Azha, S. F., Ahmad, A. L., & Ismail, S. (2014). Thin coated adsorbent layer: characteristics and performance study. *Desalination and Water Treatment*, *55*(4), 956–969. https://doi.org/10.1080/19443994.2014.922502

Azha, S. F., & Ismail, S. (2019). Immobilization of dye pollutants on composite adsorbent coating: Screening, efficiency and adsorption mechanism. *AIP Conference Proceedings*, *2124*(July). https://doi.org/10.1063/1.5117131

Azha, S. F., Sellaoui, L., Engku Yunus, E. H., Yee, C. J., Bonilla-Petriciolet, A., Ben Lamine, A., & Ismail, S. (2019). Iron-modified composite adsorbent coating for azo dye removal and its regeneration by photo-Fenton process: Synthesis, characterization and adsorption mechanism interpretation. *Chemical*

Engineering Journal, *361*, 31–40. https://doi.org/10.1016/j.cej.2018.12.050

Azha, S. F., Shahadat, M., & Ismail, S. (2017a). Acrylic polymer emulsion supported bentonite clay coating for the analysis of industrial dye. *Dyes and Pigments*, *145*, 550–560. https://doi.org/10.1016/j.dyepig.2017.05.009

Azha, S. F., Shahadat, M., & Ismail, S. (2017b). Acrylic polymer emulsion supported bentonite clay coating for the analysis of industrial dye. *Dyes and Pigments*, *145*, 550–560. https://doi.org/10.1016/j.dyepig.2017.05.009

Azha, S. F., Shahadat, M., Ismail, S., Ali, S. W., & Ahammad, S. Z. (2021). Prospect of clay-based flexible adsorbent coatings as cleaner production technique in wastewater treatment, challenges, and issues: A review. *Journal of the Taiwan Institute of Chemical Engineers*, *120*, 178–206. https://doi.org/10.1016/j.jtice.2021.03.018

Azimi, A., Azari, A., Rezakazemi, M., & Ansarpour, M. (2017). Removal of Heavy Metals from Industrial Wastewaters: A Review. *ChemBioEng Reviews*, *4*(1), 37–59. https://doi.org/10.1002/CBEN.201600010

Aziz, B. K., Shwan, D. M. S., & Kaufhold, S. (2020). Characterization of Tagaran natural clay and its efficiency for removal of cadmium (II) from Sulaymaniyah industrial zone sewage. *Environmental Science and Pollution Research*, *27*(31), 38384–38396. https://doi.org/10.1007/S11356-019-06995-X

Baby, R., Saifullah, B., & Hussein, M. Z. (2019). Carbon Nanomaterials for the Treatment of Heavy Metal-Contaminated Water and Environmental Remediation. *Nanoscale Research Letters 2019 14:1*, *14*(1), 1–17. https://doi.org/10.1186/S11671-019-3167-8

Bahiru, B. (2020). Determination of Heavy Metals in Wastewater and Their Toxicological Implications around Eastern Industrial Zone, Central Ethiopia. *Journal of Environmental Chemistry and Ecotoxicology*, *12*(2), 72–79. https://doi.org/10.5897/jece2019.0453

Bandara, P. C., Peña-Bahamonde, J., & Rodrigues, D. F. (2020). Redox mechanisms of conversion of Cr(VI) to Cr(III) by graphene oxide-polymer composite. *Scientific Reports 2020 10:1*, *10*(1), 1–8. https://doi.org/10.1038/s41598-020-65534-8

Barakat, M. A. (2011). New trends in removing heavy metals from industrial wastewater. *Arabian Journal of Chemistry*, *4*(4), 361–377. https://doi.org/10.1016/j.arabjc.2010.07.019

Bashir, A., Malik, L. A., Ahad, S., Manzoor, T., Bhat, M. A., Dar, G. N., & Pandith, A. H. (2018). Removal of heavy metal ions from aqueous system by ion-exchange and biosorption methods. *Environmental Chemistry Letters 2018 17:2*, *17*(2), 729–754. https://doi.org/10.1007/S10311-018-00828-Y

Bedemo, A., Chandravanshi, B. S., & Zewge, F. (2016). Removal of trivalent chromium from aqueous solution using aluminum oxide hydroxide. *SpringerPlus*, *5*(1), 1–11. https://doi.org/10.1186/S40064-016-2983-X/TABLES/3

Bhavani, K., Begum, E., & Selvakumar, S. (2016). *Chitosan-a low cost adsorbent for electroplating waste water treatment.*

Biol Sci, B. J., Adebayo Oyewole, O., Buba Adamu, B., Olalekan Oladoja, E., Nancy Balogun, A., Mary Okunlola, B., & Eguye Odiniya, E. (2018). A review on heavy metals biosorption in the environment. *Revista.Rebibio.NetOA Oyewole, BB Adamu, EO Oladoja, AN Balogun, BM Okunlola, EE OdiniyaBrazilian Journal of Biological Sciences, 2018•revista.Rebibio.Net*, *5*(10), 225–236. https://doi.org/10.21472/bjbs.051003

Bodzek, M. (2015). Membrane technologies for the removal of micropollutants in water treatment. *Advances in Membrane Technologies for Water Treatment: Materials, Processes and Applications*, 465–517. https://doi.org/10.1016/B978-1-78242-121-4.00015-0

BrbootI, D. M., AbiD, B. A., & Al-ShuwaikI, N. M. (2011). Removal of Heavy Metals Using Chemicals Precipitation. *Tech. Journal*, *29*(3). https://www.researchgate.net/publication/265490687_Removal_of_Heavy_Metals_Using_Chemicals_Precipitation

Brereton, R. G. (2019). ANOVA tables and statistical significance of models. *Journal of Chemometrics*, *33*(3), 1–5. https://doi.org/10.1002/cem.3019

Cerofolini, G. F., & Meda, L. (1998). A theory of multilayer adsorption on rough surfaces in terms of clustering and melting BET piles. *Surface Science*, *416*(3), 403–422. https://doi.org/10.1016/S0039-6028(98)00594-9

Chandrasekaran, A., Patra, C., Narayanasamy, S., & Subbiah, S. (2020). Adsorptive removal of Ciprofloxacin and Amoxicillin from single and binary aqueous systems using acid-activated carbon from Prosopis juliflora. *Environmental Research*, *188*, 109825. https://doi.org/10.1016/j.envres.2020.109825

Charkiewicz, A. E., Omeljaniuk, W. J., Nowak, K., Garley, M., & Nikliński, J. (2023). Cadmium Toxicity and Health Effects—A Brief Summary. *Molecules 2023, Vol. 28, Page 6620*, *28*(18), 6620. https://doi.org/10.3390/MOLECULES28186620

Chatterjee, S. (2011). Uptake and removal of toxic Cr (VI) by Pseudomonas aeruginosa: physico-chemical and biological evaluation. *Current Science*, *101*(6), 645–652.

Chen, C., Luo, J., Qin, W., & Tong, Z. (2014). Elemental analysis, chemical composition, cellulose crystallinity, and FT-IR spectra of Toona sinensis wood. *Monatshefte Fur Chemie*, *145*(1), 175–185. https://doi.org/10.1007/S00706-013-1077-5

Chen, X., Hossain, M. F., Duan, C., Lu, J., Tsang, Y. F., Islam, M. S., & Zhou, Y. (2022). Isotherm models for adsorption of heavy metals from water - A review. *Chemosphere*, *307*, 135545. https://doi.org/10.1016/J.CHEMOSPHERE.2022.135545

Chintokoma, G. C., Chebude, Y., Kassahun, S. K., Demesa, A. G., & Koiranen, T. (2024). Sol-gel synthesis of composite adsorbent coating from Prosopis juliflora –activated carbon for simultaneous adsorptive removal of Cd2+ and Cr2O7 CrOfrom wastewater. *AQUA — Water Infrastructure, Ecosystems and Society*, *73*(5), 945–968. https://doi.org/10.2166/aqua.2024.335

Chintokoma, G. C., Machunda, R. L., & Njau, K. N. (2015). *Optimization of Sedimentation Tank Coupled with Inclined Plate Settlers as a Pre-treatment for High Turbidity Water*. *5*(17), 11–24. https://citeseerx.ist.psu.edu/viewdoc/download?doi=10.1.1.886.3832&rep=rep1&type=pdf

Chowdhury, Z. Z. (2013). *Preparation , Characterization and Adsorption Studies of Heavy Metals Onto Activated Adsorbent Materials Derived From Agricultural Residues Thesis Submitted in Fulfilment of the Requirements for the Degree of Doctor of Philosophy Department of Chemistry F*.

Christensen, R. (2016). Chapter 8: Testing lack of fit. In *Analysis of variance, design, and regression: Linear modeling for unbalanced data* (pp. 181–201). https://doi.org/10.1201/9781315370095

Clark, S. E., Elligson, J. C., Bradley Mikula, J., Roenning, C. D., Siu, C. Y. S., & Hafera, J. M. (2007).

Inclined plate settlers to treat stormwater solids. *Restoring Our Natural Habitat - Proceedings of the 2007 World Environmental and Water Resources Congress*. https://doi.org/10.1061/40927(243)580

Costa, M., & Klein, C. B. (2006). Toxicity and Carcinogenicity of Chromium Compounds in Humans. *Critical Reviews in Toxicology*, *36*(2), 155–163. https://doi.org/10.1080/10408440500534032

Crini, G., & Lichtfouse, E. (2019). Advantages and disadvantages of techniques used for wastewater treatment. *Environmental Chemistry Letters*, *17*(1), 145–155. https://doi.org/10.1007/s10311-018-0785-9

de Borja Ojembarrena, F., Sammaraie, H., Campano, C., Blanco, A., Merayo, N., & Negro, C. (2022). Hexavalent Chromium Removal from Industrial Wastewater by Adsorption and Reduction onto Cationic Cellulose Nanocrystals. *Nanomaterials 2022, Vol. 12, Page 4172*, *12*(23), 4172. https://doi.org/10.3390/NANO12234172

de Franco, M. A. E., de Carvalho, C. B., Bonetto, M. M., Soares, R. de P., & Féris, L. A. (2017). Removal of amoxicillin from water by adsorption onto activated carbon in batch process and fixed bed column: Kinetics, isotherms, experimental design and breakthrough curves modelling. *Journal of Cleaner Production*, *161*, 947–956. https://doi.org/10.1016/j.jclepro.2017.05.197

Demim, S., Drouiche, N., Aouabed, A., Benayad, T., Dendene-Badache, O., & Semsari, S. (2013). Cadmium and nickel: Assessment of the physiological effects and heavy metal removal using a response surface approach by L. gibba. *Ecological Engineering*, *61*, 426–435. https://doi.org/10.1016/j.ecoleng.2013.10.016

Deng, H., Yang, L., Tao, G., & Dai, J. (2009). Preparation and characterization of activated carbon from cotton stalk by microwave assisted chemical activation-Application in methylene blue adsorption from aqueous solution. *Journal of Hazardous Materials*, *166*(2–3), 1514–1521. https://doi.org/10.1016/j.jhazmat.2008.12.080

Deng, Y., Wang, M., Tian, T., Lin, S., Xu, P., Zhou, L., Dai, C., Hao, Q., Wu, Y., Zhai, Z., Zhu, Y., Zhuang, G., & Dai, Z. (2019). The effect of hexavalent chromium on the incidence and mortality of human cancers: A meta-analysis based on published epidemiological cohort studies. *Frontiers in Oncology*, *9*(FEB), 434984. https://doi.org/10.3389/FONC.2019.00024/BIBTEX

Dermience, M., Lognay, G., Mathieu, F., & Goyens, P. (2015). Effects of thirty elements on bone metabolism. *Journal of Trace Elements in Medicine and Biology*, *32*, 86–106. https://doi.org/10.1016/J.JTEMB.2015.06.005

Dorado, A. D., Gamisans, X., Valderrama, C., Solé, M., & Lao, C. (2014). Cr(III) removal from aqueous solutions: A straightforward model approaching of the adsorption in a fixed-bed column. *Journal of Environmental Science and Health - Part A Toxic/Hazardous Substances and Environmental Engineering*, *49*(2), 179–186. https://doi.org/10.1080/10934529.2013.838855

Drozdova, J., Raclavska, H., Raclavsky, K., & Skrobankova, H. (2019). Heavy metals in domestic wastewater with respect to urban population in Ostrava, Czech Republic. *Water and Environment Journal*, *33*(1), 77–85. https://doi.org/10.1111/WEJ.12371

Du, P., Zhang, L., Ma, Y., Li, X., Wang, Z., Mao, K., Wang, N., Li, Y., He, J., Zhang, X., Hao, F., Li, X., Liu, M., & Wang, X. (2020). Occurrence and Fate of Heavy Metals in Municipal Wastewater in Heilongjiang Province, China: A Monthly Reconnaissance from 2015 to 2017. *Water 2020, Vol. 12, Page 728*, *12*(3), 728. https://doi.org/10.3390/W12030728

Ebelegi, A. N., Ayawei, N., & Wankasi, D. (2020). Interpretation of Adsorption Thermodynamics and Kinetics. *Open Journal of Physical Chemistry*, *10*(03), 166–182. https://doi.org/10.4236/ojpc.2020.103010

Ehis-Eriakha, C. B., & Akemu, S. E. (2022). Impact of Heavy Metal Pollution on the Biotic and Abiotic Components of the Environment. *South Asian Journal of Research in Microbiology*, 38–54. https://doi.org/10.9734/SAJRM/2022/V13I330302

Elimelech, M., science, W. P.-, & 2011, undefined. (2011). The future of seawater desalination: energy, technology, and the environment. *Science.OrgM Elimelech, WA Phillipscience, 2011•science.Org*, *333*(6043), 712–717. https://doi.org/10.1126/science.1200488

Elligson, J. C., Mikula, J. B., Clark, S. E., Roenning, C. D., Hafera, J. M., & Franklin, K. A. (2014). Inclined Plate Settlers to Treat Stormwater Solids. *Proceedings of the Water Environment Federation*, *2006*(6), 5609–5623. https://doi.org/10.2175/193864706783775711

Emirie, M. (2015). Removal of chromium hexavalent (Cr(VI) from aqueous solution using activated carbon prepared from Prosopis Juliflora Plant and find the optimal operating condition for adsorption process. In *Journal of Chemical Information and Modeling* (Issue 9). Addis Ababa University.

Fagnekar, N. A., & Mane, S. (2015). REMOVAL OF TURBIDITY USING ELECTROCOAGULATION. *IJRET: International Journal of Research in Engineering and Technology*, *04*(06), 2321–7308.

Farnane, M., Machrouhi, A., Khnifira, M., Barour, M., Elmoubarki, R., Qourzal, S., Tounsadi, H., & Barka, N. (2020). Zinc chloride activation of carob shells for heavy metals removal from water: statistical optimisation, characterisation and isotherm modelling. *International Journal of Environmental Analytical Chemistry*, *00*(00), 1–14. https://doi.org/10.1080/03067319.2020.1777290

Fernandez, R. M. D., Estrada, R. J. R., Tomon, T. R. B., Dingcong, R. G., Amparado, R. F., Capangpangan, R. Y., Malaluan, R. M., Dumancas, G. G., Lubguban, A. A., Alguno, A. C., Bacosa, H. P., & Lubguban, A. A. (2023). Experimental Design and Breakthrough Curve Modeling of Fixed-Bed Columns Utilizing a Novel 3D Coconut-Based Polyurethane-Activated Carbon Composite Adsorbent for Lead Sequestration. *Sustainability (Switzerland)*, *15*(19). https://doi.org/10.3390/su151914344

Filote, C., Ros, M., Hlihor, R. M., Cozma, P., Simion, I. M., Apostol, M., Gavrilescu, M., Gomez, M., & De Oca, M. (2021). Sustainable application of biosorption and bioaccumulation of persistent pollutants in wastewater treatment: Current practice. *Mdpi.ComC Filote, M Roșca, RM Hlihor, P Cozma, IM Simion, M Apostol, M GavrilescuProcesses, 2021•mdpi.Com*. https://doi.org/10.3390/pr9101696

Fu, F., & Wang, Q. (2011). Removal of heavy metal ions from wastewaters: A review. *Journal of Environmental Management*, *92*(3), 407–418. https://doi.org/10.1016/J.JENVMAN.2010.11.011

Gabelman, A. (2017). Adsorption basics: Part 1. *Chemical Engineering Progress*, *113*(8), 1–6. https://www.aiche.org/sites/default/files/docs/pages/adsorption_basics_part_1.pdf

Gawande, S. M., Belwalkar, N. S., & Mane, A. A. (2017). Adsorption and its Isotherm – Theory. *International Journal of Engineering Research*, *6*(6), 312. https://doi.org/10.5958/2319-6890.2017.00026.5

Geleta, W. S., Alemayehu, E., & Lennartz, B. (2021). *Enhanced Defluoridation of Water Using Zirconium — Coated Pumice in Fixed-Bed Adsorption Columns*. 1–20.

Genchi, G., Sinicropi, M. S., Lauria, G., Carocci, A., & Catalano, A. (2020). The effects of cadmium toxicity.

International Journal of Environmental Research and Public Health, *17*(11), 1–24. https://doi.org/10.3390/ijerph17113782

Goh, P. S., Lau, W. J., Othman, M. H. D., & Ismail, A. F. (2018). Membrane fouling in desalination and its mitigation strategies. *Desalination*, *425*, 130–155. https://doi.org/10.1016/J.DESAL.2017.10.018

Gómez-Avilés, A., Peñas-Garzón, M., Belver, C., Rodriguez, J. J., & Bedia, J. (2022). Equilibrium, kinetics and breakthrough curves of acetaminophen adsorption onto activated carbons from microwave-assisted FeCl3-activation of lignin. *Separation and Purification Technology*, *278*(January), 119654. https://doi.org/10.1016/j.seppur.2021.119654

Gooty, J. M., Mandala, S., Mosquera, J. A. N., Llaguno, S. N. S., & Malik, J. A. (2022). Role of biosorption technology in removing cadmium from water and soil. *Microbes and Microbial Biotechnology for Green Remediation*, 405–422. https://doi.org/10.1016/B978-0-323-90452-0.00046-3

Gopal, N., & Asaithambi, M. (2015). Adsorption of acid blue- 40 (A textile dye) using prosopis juliflora activated carbon embedded in polyaniline matrix. *Rasayan Journal of Chemistry*, *8*(3), 279–286. https://www.cabidigitallibrary.org/doi/abs/10.5555/20153444887

Gopal, N., Asaithambi, M., Sivakumar, P., & Sivakumar, V. (2014). Adsorption studies of a direct dye using polyaniline coated activated carbon prepared from Prosopis juliflora. *Journal of Water Process Engineering*, *2*, 87–95. https://doi.org/10.1016/j.jwpe.2014.05.008

Gorzin, F., & Bahri Rasht Abadi, M. M. (2018). Adsorption of Cr(VI) from aqueous solution by adsorbent prepared from paper mill sludge: Kinetics and thermodynamics studies. *Adsorption Science and Technology*, *36*(1–2), 149–169. https://doi.org/10.1177/0263617416686976

Gul, A., Ma'amor, A., Khaligh, N. G., & Muhd Julkapli, N. (2022). Recent advancements in the applications of activated carbon for the heavy metals and dyes removal. *Chemical Engineering Research and Design*, *186*, 276–299. https://doi.org/10.1016/j.cherd.2022.07.051

Gunatilake, S. K. (2015a). Methods of Removing Heavy Metals from. *Journal of Multidisciplinary Engineering Science Studies*, *1*(1), 13–18. www.jmess.org

Gunatilake, S. K. (2015b). *Methods of Removing Heavy Metals from Industrial Wastewater*. *1*(1), 12–18.

Gupta, A., Sharma, V., Sharma, K., Kumar, V., Choudhary, S., Mankotia, P., Kumar, B., Mishra, H., Moulick, A., Ekielski, A., & Mishra, P. K. (2021). A review of adsorbents for heavy metal decontamination: Growing approach to wastewater treatment. *Materials*, *14*(16), 1–45. https://doi.org/10.3390/ma14164702

Gupta, R., Khan, F., Alqahtani, F. M., Hashem, M., & Ahmad, F. (2024). Plant growth--promoting Rhizobacteria (PGPR) assisted bioremediation of Heavy Metal Toxicity. *Applied Biochemistry and Biotechnology*, *196*(5), 2928–2956.

Gupta, S., Sireesha, S., Sreedhar, I., Patel, C. M., & Anitha, K. L. (2020). Latest trends in heavy metal removal from wastewater by biochar based sorbents. *Journal of Water Process Engineering*, *38*, 101561. https://doi.org/10.1016/J.JWPE.2020.101561

Habashi, F. (2015). Mineral resources and geo-engineering. *International Journal of Mining and Geo-Engineering*, *49*(2), 221–233. https://doi.org/10.22059/IJMGE.2015.56108

Habineza, A., Zhai, J., Ntakirutimana, T., Ping Qiu, F., Li, X., & Wang, Q. (2017). *+86) 17783490217; email: 1054402911@qq.com (F.P. Qiu), Tel. (+86) 15736244421; A. Habineza et al. / Desalination and*

Water Treatment. *78*, 192–214. https://doi.org/10.5004/dwt.2017.20581

Heidmann, I., & Calmano, W. (2008). Removal of Cr(VI) from model wastewaters by electrocoagulation with Fe electrodes. *Separation and Purification Technology*, *61*(1), 15–21. https://doi.org/10.1016/J.SEPPUR.2007.09.011

Hossini, H., Shafie, B., Niri, A. D., Nazari, M., Esfahlan, A. J., Ahmadpour, M., Nazmara, Z., Ahmadimanesh, M., Makhdoumi, P., Mirzaei, N., & Hoseinzadeh, E. (2022). A comprehensive review on human health effects of chromium: insights on induced toxicity. *Environmental Science and Pollution Research 2022 29:47*, *29*(47), 70686–70705. https://doi.org/10.1007/S11356-022-22705-6

Hsu, L. Y., & Teng, H. (2000). Influence of different chemical reagents on the preparation of activated carbons from bituminous coal. *Fuel Processing Technology*, *64*(1), 155–166. https://doi.org/10.1016/S0378-3820(00)00071-0

Hu, J., Chen, J., Liu, F., An, S., Shi, Y., Luan, Z., Xiao, J., & Zhang, B. (2022). Enhancing oil removal from wastewater by combining inclined plate settler and electrocoagulation. *Separation Science and Technology (Philadelphia)*, *57*(17), 2824–2835. https://doi.org/10.1080/01496395.2021.1993258

Hussain, A., Madan, S., & Madan, R. (2012). Heavy Metals-Their Environmental Impacts and Mitigation. In *IntechOpen* (pp. 1–24). IntechOpen. http://dx.doi.org/10.1039/C7RA00172J%0Ahttps://www.intechopen.com/books/advanced-biometric-technologies/liveness-detection-in-biometrics%0Ahttp://dx.doi.org/10.1016/j.colsurfa.2011.12.014

Hussain, A., Madan, S., & Madan, R. (2021). Removal of Heavy Metals from Wastewater by Adsorption. In *Heavy Metals - Their Environmental Impacts and Mitigation* (Vol. 32, Issue Environmental Engineering, pp. 137–144). https://www.intechopen.com/books/advanced-biometric-technologies/liveness-detection-in-biometrics

Hyun, K., & Kang, Y. (2023). Performance of Inclined-Plate Settler and Activated Carbon Sponge-Cube Media Filter for the Treatment of Urban Stormwater Runoff from an Industrial Complexs. *KSCE Journal of Civil Engineering*, *27*(9), 3686–3693. https://doi.org/10.1007/s12205-023-2307-y

Irshad, M. A., Nawaz, R., Wojciechowska, E., Mohsin, M., Nawrot, N., Nasim, I., & Hussain, F. (2023). Application of Nanomaterials for Cadmium Adsorption for Sustainable Treatment of Wastewater: a Review. *Water, Air, and Soil Pollution*, *234*(1). https://doi.org/10.1007/S11270-023-06064-7

Islam, M. M., Mohana, A. A., Rahman, M. A., Rahman, M., Naidu, R., & Rahman, M. M. (2023). A Comprehensive Review of the Current Progress of Chromium Removal Methods from Aqueous Solution. *Toxics 2023, Vol. 11, Page 252*, *11*(3), 252. https://doi.org/10.3390/TOXICS11030252

Iwuozor, K. O. (2019). Prospects and Challenges of Using Coagulation-Flocculation Method in the Treatment of Effluents. *Advanced Journal of Chemistry-Section A*, *2*(2), 105–127.

Jain, M., Garg, V. K., Kadirvelu, K., & Sillanpää, M. (2016). Adsorption of heavy metals from multi-metal aqueous solution by sunflower plant biomass-based carbons. *International Journal of Environmental Science and Technology*, *13*(2), 493–500. https://doi.org/10.1007/s13762-015-0855-5

Jayaram, K., & Prasad, M. N. V. (2009). Removal of Pb(II) from aqueous solution by seed powder of Prosopis juliflora DC. *Journal of Hazardous Materials*, *169*(1–3), 991–997. https://doi.org/10.1016/j.jhazmat.2009.04.048

Jeyakumar, P., Debnath, C., Vijayaraghavan, R., & Muthuraj, M. (2023). Trends in Bioremediation of Heavy

Metal Contaminations. *Environ. Eng. Res*, *28*(4), 220631. https://doi.org/10.4491/eer.2021.631

Joshi, H. K., Vishwakarma, M. C., Kumar, R., Sharma, H., Joshi, S. K., & Bhandari, N. S. (2022). Adsorption of Cd2+ from synthetic wastewater by modified leaves of Eupatorium adenophorum and Acer oblongum: thermodynamics, kinetics and equilibrium studies. *Discover Water 2022 2:1*, *2*(1), 1–16. https://doi.org/10.1007/S43832-022-00018-6

Kadirvelu, K., Goel, J., & Rajagopal, C. (2008). Sorption of lead, mercury and cadmium ions in multi-component system using carbon aerogel as adsorbent. *Journal of Hazardous Materials*, *153*(1–2), 502–507. https://doi.org/10.1016/j.jhazmat.2007.08.082

Kalinowska, A., Szopí Nska, M., Chmiel, S., Kó Nczak, M., Polkowska, Z., Artichowicz, W., Jankowska, K., Nowak, A., & Łuczkiewicz, A. (2020). Heavy metals in a high arctic fiord and their introduction with the wastewater: A case study of adventfjorden-longyearbyen system, svalbard. *Mdpi.ComA Kalinowska, M Szopińska, S Chmiel, M Kończak, Ż Polkowska, W ArtichowiczWater, 2020•mdpi.Com*. https://doi.org/10.3390/w12030794

Kasenene, A. J., Machunda, R. L., & Njau, K. N. (2021). Performance of inclined plates settler integrated with constructed wetland for high turbidity water treatment. *Water Practice and Technology*, *16*(2), 516–529. https://doi.org/10.2166/wpt.2021.009

Kaur, B., Kalra, P., & Kaur, N. (2022). Prosopis Juliflora (Kikar) pods as adsorbent for removal of Cd(II) ions from aqueous streams. *Materials Today: Proceedings*, *xxxx*. https://doi.org/10.1016/j.matpr.2022.06.177

Kaur, G., Singh, N., & Rajor, A. (2021). RSM-CCD optimized Prosopis juliflora activated carbon for the Adsorptive uptake of Ofloxacin and disposal studies. *Environmental Technology & Innovation*, *25*, 102176. https://doi.org/10.1016/j.eti.2021.102176

Kavand, M., Eslami, P., & Razeh, L. (2020). The adsorption of cadmium and lead ions from the synthesis wastewater with the activated carbon: Optimization of the single and binary systems. *Journal of Water Process Engineering*, *34*, 101151. https://doi.org/10.1016/J.JWPE.2020.101151

Kayranli, B. (2022). Cadmium removal mechanisms from aqueous solution by using recycled lignocelluloses. *Alexandria Engineering Journal*, *61*(1), 443–457. https://doi.org/10.1016/j.aej.2021.06.036

Keerthivasan, K. C., Vivekanandan, S., & Suresh, R. (2019). Performance of four stroke compression ignition engine operated on dual fuel mode with producer gas and diesel. *International Journal of Innovative Technology and Exploring Engineering*, *8*(11), 83–88. https://doi.org/10.35940/ijitee.J9952.0981119

Kerur, S. S., Bandekar, S., Hanagadakar, M. S., Nandi, S. S., Ratnamala, G. M., & Hegde, P. G. (2020). Removal of hexavalent Chromium-Industry treated water and Wastewater: A review. *Materials Today: Proceedings*, *42*, 1112–1121. https://doi.org/10.1016/J.MATPR.2020.12.492

Kerur, S. S., Bandekar, S., Hanagadakar, M. S., Nandi, S. S., Ratnamala, G. M., & Hegde, P. G. (2021). Removal of hexavalent Chromium-Industry treated water and Wastewater: A review. *Materials Today: Proceedings*, *42*, 1112–1121. https://doi.org/10.1016/J.MATPR.2020.12.492

Khan, S., Ahmad, I., Shah, M. T., Rehman, S., & Khaliq, A. (2009). Use of constructed wetland for the removal of heavy metals from industrial wastewater. *Journal of Environmental Management*, *90*(11), 3451–3457. https://doi.org/10.1016/j.jenvman.2009.05.026

Khatun, M., Kobir, M. M., Miah, M. A. R., Sarkar, A. K., Alam, M. A., & others. (2024). Technologies for remediation of heavy metals in environment and ecosystem: A critical overview of comparison study. *Asian Journal of Environment \& Ecology*, *23*(4), 61–80.

Khedmati, M., Khodaii, A., & Haghshenas, H. F. (2017). A study on moisture susceptibility of stone matrix warm mix asphalt. *Construction and Building Materials*, *144*, 42–49. https://doi.org/10.1016/j.conbuildmat.2017.03.121

Khoshraftar, Z., Masoumi, H., & Ghaemi, A. (2023). Experimental, response surface methodology (RSM) and mass transfer modeling of heavy metals elimination using dolomite powder as an economical adsorbent. *Case Studies in Chemical and Environmental Engineering*, *7*(January), 100329. https://doi.org/10.1016/j.cscee.2023.100329

Kinuthia, G. K., Ngure, V., Beti, D., Lugalia, R., Wangila, A., & Kamau, L. (2020). Levels of heavy metals in wastewater and soil samples from open drainage channels in Nairobi, Kenya: community health implication. *Scientific Reports*, *10*(1), 1–13. https://doi.org/10.1038/s41598-020-65359-5

Kobya, M., Demirbas, E., Parlak, N. U., & Yigit, S. (2010). Treatment of cadmium and nickel electroplating rinse water by electrocoagulation. *Environmental Technology*, *31*(13), 1471–1481. https://doi.org/10.1080/09593331003713693

Korak, J. A., Huggins, R., & Arias-Paic, M. (2017). Regeneration of pilot-scale ion exchange columns for hexavalent chromium removal. *Water Research*, *118*, 141–151. https://doi.org/10.1016/J.WATRES.2017.03.018

Kotaś, J., & Stasicka, Z. (2000). Chromium occurrence in the environment and methods of its speciation. *Environmental Pollution*, *107*(3), 263–283. https://doi.org/10.1016/S0269-7491(99)00168-2

Krystynik, P., & Tito, D. N. (2017). Key process parameters affecting performance of electro-coagulation. *Chemical Engineering and Processing: Process Intensification*, *117*, 106–112. https://doi.org/10.1016/J.CEP.2017.03.022

Kumar, A., & Jena, H. M. (2016). Preparation and characterization of high surface area activated carbon from Fox nut (Euryale ferox) shell by chemical activation with H3PO4. *Results in Physics*, *6*(September), 651–658. https://doi.org/10.1016/j.rinp.2016.09.012

Kumar Joshi, H., Chandra Vishwakarma, M., Kumar, R., Sharma, H., Kumar Joshi, S., & Singh Bhandari, N. (2022). Adsorption of Cd2+ from synthetic wastewater by modified leaves of Eupatorium adenophorum and Acer oblongum: thermodynamics, kinetics and equilibrium. *SpringerHK Joshi, MC Vishwakarma, R Kumar, H Sharma, SK Joshi, NS BhandariDiscover Water, 2022•Springer*, *2*(1), 9. https://doi.org/10.1007/s43832-022-00018-6

Kumar, M., & Tamilarasan, R. (2017). Kinetics, equilibrium data and modeling studies for the sorption of chromium by Prosopis juliflora bark carbon. *Arabian Journal of Chemistry*, *10*, S1567–S1577. https://doi.org/10.1016/j.arabjc.2013.05.025

Kumar, P., Sai Ram, C., Srivastava, J. P., Behura, A. K., & Kumar, A. (2022). Synthesis of Cotton Fiber and Its Structure. *Natural and Synthetic Fiber Reinforced Composites*, *February*, 17–36. https://doi.org/10.1002/9783527832996.ch2

Kumar, R., & Chawla, J. (2014). Removal of Cadmium Ion from Water/Wastewater by Nano-metal Oxides: A Review. *Water Quality, Exposure and Health*, *5*(4), 215–226. https://doi.org/10.1007/S12403-013-0100-8

Kumar, S., & Sharma, A. (2019). Cadmium toxicity: effects on human reproduction and fertility. *Reviews on Environmental Health*, *34*(4), 327–338. https://doi.org/10.1515/REVEH-2019-0016/MACHINEREADABLECITATION/RIS

Kurkura, K., Aynalem, Z., Bheemalingeswara, K., Kinfe, A., Solomon, G., & Kassa, A. (2012). Mineralogical and Geochemical Characterization of Clay and Lacustrine Deposits of Lake Ashenge Basin, Northern Ethiopia: Implication for Industrial Applications. *Momona Ethiopian Journal of Science*, *4*(2), 111. https://doi.org/10.4314/mejs.v4i2.80120

Kurniawan, T. A., Chan, G. Y. S., Lo, W. H., & Babel, S. (2006). Physico–chemical treatment techniques for wastewater laden with heavy metals. *Chemical Engineering Journal*, *118*(1–2), 83–98. https://doi.org/10.1016/J.CEJ.2006.01.015

Kwikima, M. M., Chebude, Y., & Meshesha, B. T. (2022a). Kinetics, adsorption isotherms, thermodynamics, and desorption studies of cadmium removal from aqueous solutions using bamboo sawdust/rice husk biochar. *Biomass Conversion and Biorefinery*, *0123456789*. https://doi.org/10.1007/s13399-022-03472-3

Kwikima, M. M., Chebude, Y., & Meshesha, B. T. (2022b). Process Optimization of Cadmium Adsorption on Blended Bamboo Saw Dust/Rice-Husk from Aqueous Solution Using the Response Surface Methodology. *Chemistry Africa*, *5*(2), 279–292. https://doi.org/10.1007/s42250-022-00317-4

Kwikima, M. M., Chebude, Y., & Meshesha, B. T. (2023). Cadmium removal from aqueous solution by blended bamboo sawdust/rice-husk biochar; optimization of influencing parameters. *International Journal of Phytoremediation*, *25*(11), 1397–1412. https://doi.org/10.1080/15226514.2022.2159318

Kyzas, G. Z., & Kostoglou, M. (2014a). Green adsorbents for wastewaters: A critical review. *Materials*, *7*(1), 333–364. https://doi.org/10.3390/ma7010333

Kyzas, G. Z., & Kostoglou, M. (2014b). Green Adsorbents for Wastewaters: A Critical Review. *Materials 2014, Vol. 7, Pages 333-364*, *7*(1), 333–364. https://doi.org/10.3390/MA7010333

Ledesma, B., Sabio, E., González-García, C. M., Román, S., Fernandez, M. E., Bonelli, P., & Cukierman, A. L. (2023). Batch and Continuous Column Adsorption of p-Nitrophenol onto Activated Carbons with Different Particle Sizes. *Processes*, *11*(7), 1–22. https://doi.org/10.3390/pr11072045

Lega Muhammd, B. (2018). Determination of Cadmium, Chromium and Lead from Industrial Wastewater in Kombolcha Town, Ethiopia Using FAAS. *Journal of Environmental Analytical Chemistry*, *05*(03), 8–12. https://doi.org/10.4172/2380-2391.1000243

Leung, W. F., & Probsteln, R. F. (1983). Lamella and Tube Settlers. 1. Model and Operation. *Industrial and Engineering Chemistry Process Design and Development*, *22*(1), 58–67. https://doi.org/10.1021/i200020a011

Li, J., Dong, X., Liu, X., Xu, X., Duan, W., Park, J., Gao, L., & Lu, Y. (2022). Comparative Study on the Adsorption Characteristics of Heavy Metal Ions by Activated Carbon and Selected Natural Adsorbents. *MDPI*. https://www.mdpi.com/2071-1050/14/23/15579

Li, Z., Han, Q., Zong, Z. F., Xu, Q., & Wang, K. W. (2020). Exploring on the optimal preparation conditions of activated carbon produced from solid waste produced from sugar industry and Chinese medicine factory. *Waste Disposal and Sustainable Energy*, *2*(1), 65–77. https://doi.org/10.1007/s42768-019-00032-w

Liu, L., Sun, P., Chen, Y., Li, X., & Zheng, X. (2023). Distinct chromium removal mechanisms by iron-modified biochar under varying pH: Role of iron and chromium speciation. *Chemosphere*, *331*, 138796. https://doi.org/10.1016/J.CHEMOSPHERE.2023.138796

Lunk, H. J. (2015). Discovery, properties and applications of chromium and its compounds. *ChemTexts*, *1*(1), 1–17. https://doi.org/10.1007/S40828-015-0007-Z/FIGURES/33

Luo, B., Xiao, C., Liu, Y., Li, L., Peng, L., Zeng, Q., & Luo, S. (2022). Activation of cadmium under simulated solar illumination and its impact on the mobility of Cd in flooded soils. *Environmental Science and Pollution Research*, *29*(35), 52367–52377. https://doi.org/10.1007/S11356-022-19567-3/METRICS

Lv, Y., Cheng, K., Gao, J., Sun, W., Luo, Q., Li, Y., Deng, Z., Lai, R., Wu, W., Dai, Z., & others. (2024). Corrosion resistance of Nb and NbTi alloy predicted by hydrogen evolution reaction models modified with Langmuir isotherm adsorption theory. *Materials Chemistry and Physics*, *319*, 129386.

Mahajan, G. V, Femina, A., Begum, S. M., & Anantharaman, N. (2017). Preparation and characterization of micro porous activated carbon prepared from Prosopis Juliflora with chemical ... *Research Journal of Engineering Sciences*, *6*(1), 5–11. https://www.researchgate.net/publication/313029630_Preparation_and_characterization_of_micro_porous_activated_carbon_prepared_from_Prosopis_Juliflora_with_chemical_and_thermal_activation

Mahdi, R. K., Naji, N. M., Al-Mamoori, S. O. H., Al-Rifaie, Z. I., & Ali, R. N. (2021). Effect Cadmium on living organisms. *IOP Conference Series: Earth and Environmental Science*, *735*(1), 0–3. https://doi.org/10.1088/1755-1315/735/1/012035

Mahmood, S. W., Seyala, N. N., & Algamal, Z. Y. (2020). Adjusted R2 - type measures for beta regression model. *Electronic Journal of Applied Statistical Analysis*, *13*(2), 350–357. https://doi.org/10.1285/i20705948v13n2p350

Mahmoud, A. E. D., & Mostafa, E. (2023). Nanofiltration Membranes for the Removal of Heavy Metals from Aqueous Solutions: Preparations and Applications. *Membranes 2023, Vol. 13, Page 789*, *13*(9), 789. https://doi.org/10.3390/MEMBRANES13090789

Mallard Creek Polymers. (2019). *Ecronova ® RA 127 Acrylic Emulsion*. https://www.matweb.com/search/datasheet.aspx?matguid=b71ebe9b5e344432b644f71415e04bd3&ckck=1

Mandal, S., Calderon, J., Marpu, S. B., Omary, M. A., & Shi, S. Q. (2021). Mesoporous activated carbon as a green adsorbent for the removal of heavy metals and Congo red: Characterization, adsorption kinetics, and isotherm studies. *Journal of Contaminant Hydrology*, *243*(August), 103869. https://doi.org/10.1016/j.jconhyd.2021.103869

Manjunath, S. V., & Kumar, M. (2018). Evaluation of single-component and multi-component adsorption of metronidazole, phosphate and nitrate on activated carbon from Prosopıs julıflora. *Chemical Engineering Journal*, *346*, 525–534. https://doi.org/10.1016/j.cej.2018.04.013

Mariana, M., Abdul, A. K., Mistar, E. M., Yahya, E. B., Alfatah, T., Danish, M., & Amayreh, M. (2021). Recent advances in activated carbon modification techniques for enhanced heavy metal adsorption. *Journal of Water Process Engineering*, *43*(July), 102221. https://doi.org/10.1016/j.jwpe.2021.102221

Massányi, P., Massányi, M., Madeddu, R., Stawarz, R., & Lukáč, N. (2020). Effects of Cadmium, Lead, and Mercury on the Structure and Function of Reproductive Organs. *Toxics 2020, Vol. 8, Page 94*, *8*(4), 94.

https://doi.org/10.3390/TOXICS8040094

Mbarki, F., Selmi, T., Kesraoui, A., & Seffen, M. (2022). Low-cost activated carbon preparation from Corn stigmata fibers chemically activated using H3PO4, ZnCl2 and KOH: Study of methylene blue adsorption, stochastic isotherm and fractal kinetic. *Industrial Crops and Products*, *178*(December 2021), 114546. https://doi.org/10.1016/j.indcrop.2022.114546

MCP. (2012). *Ecronova® RA 127 Acrylic Emulsion*. Mallard Creek Polymers. https://doi.org/10.1016/j.actamat.2010.10.053

Meng, Q., Nan, J., Wang, Z., Ji, X., Wu, F., Liu, B., & Xiao, Q. (2019). Study on the efficiency of ultrafiltration technology in dealing with sudden cadmium pollution in surface water and ultrafiltration membrane fouling. *Environmental Science and Pollution Research*, *26*(16), 16641–16651. https://doi.org/10.1007/S11356-019-04691-4

Mishra, S., & Bharagava, R. N. (2016). Toxic and genotoxic effects of hexavalent chromium in environment and its bioremediation strategies. *Journal of Environmental Science and Health, Part C*, *34*(1), 1–32. https://doi.org/10.1080/10590501.2015.1096883

Mitsui, H., Nakai, O., Shibayama, K., & -, S. S. (2019). Chromium-containing water treatment method. *US Patents*, *10*, 442–715.

Mohamed, H. S., Soliman, N. K., Abdelrheem, D. A., Ramadan, A. A., Elghandour, A. H., Ahmed, S. A., & Adsorption, S. A. A. (2019). Adsorption of Cd2+ and Cr3+ ions from aqueous solutions by using residue of Padina gymnospora waste as promising low-cost adsorbent. *Cell.ComHS Mohamed, NK Soliman, DA Abdelrheem, AA Ramadan, AH Elghandour, SA AhmedHeliyon, 2019•cell.Com*, *5*, e01287. https://doi.org/10.1016/j.heliyon.2019

Mohan, D., & Singh, K. P. (2002). Single- and multi-component adsorption of cadmium and zinc using activated carbon derived from bagasse - An agricultural waste. *Water Research*, *36*(9), 2304–2318. https://doi.org/10.1016/S0043-1354(01)00447-X

Mollah, M. Y. A., Morkovsky, P., Gomes, J. A. G., Kesmez, M., Parga, J., & Cocke, D. L. (2004). Fundamentals, present and future perspectives of electrocoagulation. *Journal of Hazardous Materials*, *114*(1–3), 199–210. https://doi.org/10.1016/J.JHAZMAT.2004.08.009

Mondal, P., Mehta, D., Saharan, V. K., & George, S. (2018). Continuous Column Studies for Water Defluoridation Using Synthesized Magnesium-incorporated Hydroxyapatite Pellets: Experimental and Modeling Studies. *Environmental Processes*, *5*(2), 261–285. https://doi.org/10.1007/s40710-018-0287-6

Monga, A., Fulke, A. B., & Dasgupta, D. (2022). Recent developments in essentiality of trivalent chromium and toxicity of hexavalent chromium: Implications on human health and remediation strategies. *Journal of Hazardous Materials Advances*, *7*, 100113. https://doi.org/10.1016/J.HAZADV.2022.100113

Montgomery, D. C. (2017). *Design and analysis of experiments*. Wiley. https://books.google.com/books?hl=en&lr=&id=Py7bDgAAQBAJ&oi=fnd&pg=PA1&ots=X8q2m-PV15&sig=vwvEecmU6O15WfdL78p77cwYN_k

Mouni, L., Merabet, D., Bouzaza, K., & Belkhiri, L. (2012). Removal of Pb2 + and Zn2 + from the aqueous solutions by activated carbon prepared from Dates stone Removal of Pb 2 + and Zn 2 + from the aqueous solutions by activated carbon prepared from Dates stone. *Desalination and Water Treatment*, *June 2014*. https://doi.org/10.5004/dwt.2010.1106

Murithi, G., Onindo, C., & Wambu, E. (2014). Removal of cadmium (II) ions from water by adsorption using water hyacinth (Eichhornia crassipes) biomass. *BiioResources*, *9*(2), 3613–3651.

Najmi, S., Hatamipour, M. S., Sadeh, P., Najafipour, I., & Mehranfar, F. (2020). Activated carbon produced from Glycyrrhiza glabra residue for the adsorption of nitrate and phosphate: batch and fixed-bed column studies. *SN Applied Sciences*, *2*(4), 1–22. https://doi.org/10.1007/s42452-020-2585-7

Ng, K. C., Thu, K., Kim, Y., Chakraborty, A., & Amy, G. (2013). Adsorption desalination: An emerging low-cost thermal desalination method. *Desalination*, *308*, 161–179. https://doi.org/10.1016/j.desal.2012.07.030

Nur-E-Alam, M., Mia, M. A. S., Ahmad, F., & Rahman, M. M. (2020). An overview of chromium removal techniques from tannery effluent. *Applied Water Science*, *10*(9), 1–22. https://doi.org/10.1007/s13201-020-01286-0

Nyangi, M. J., Chebude, Y., & Kilulya, K. F. (2020). Fluoride removal efficiencies of Al-EC and Fe-EC reactors: process optimization using Box–Behnken design of the surface response methodology. *Applied Water Science*, *10*(9), 1–11. https://doi.org/10.1007/s13201-020-01297-x

Obayomi, K. S., Bello, J. O., Yahya, M. D., Chukwunedum, E., & Adeoye, J. B. (2020). Statistical analyses on effective removal of cadmium and hexavalent chromium ions by multiwall carbon nanotubes (MWCNTs). *Heliyon*, *6*(6), e04174. https://doi.org/10.1016/j.heliyon.2020.e04174

Ojedokun, A. T., & Bello, O. S. (2016). Sequestering heavy metals from wastewater using cow dung. *Water Resources and Industry*, *13*, 7–13. https://doi.org/10.1016/j.wri.2016.02.002

Oke, M. A., Sonibare, J. A., Onakpohor, A., Odunlami, O. A., Akeredolu, F. A., & Elehinafe, F. B. (2022). Proximate analysis of some common charcoal in Southwestern Nigeria. *Results in Engineering*, *15*(April), 100454. https://doi.org/10.1016/j.rineng.2022.100454

Olorundare, O. F., Msagati, T. A. M., Krause, R. W. M., Okonkwo, J. O., & Mamba, B. B. (2014). Activated carbon from lignocellulosic waste residues: Effect of activating agent on porosity characteristics and use as adsorbents for organic species. *Water, Air, and Soil Pollution*, *225*(3). https://doi.org/10.1007/s11270-014-1876-2

Padmavathy, K. S., Madhu, G., & Haseena, P. V. (2016). A study on Effects of pH, Adsorbent Dosage, Time, Initial Concentration and Adsorption Isotherm Study for the Removal of Hexavalent Chromium (Cr (VI)) from Wastewater by Magnetite Nanoparticles. *Procedia Technology*, *24*, 585–594. https://doi.org/10.1016/j.protcy.2016.05.127

Patel, H. (2020). Batch and continuous fixed bed adsorption of heavy metals removal using activated charcoal from neem (Azadirachta indica) leaf powder. *Scientific Reports*, *10*(1), 1–12. https://doi.org/10.1038/s41598-020-72583-6

Pathania, D., & Srivastava, A. K. (2020). Advances in nanoparticles tailored lignocellulosic biochars for removal of heavy metals with special reference to cadmium (II) and chromium (VI). *Environmental Sustainability 2020 4:2*, *4*(2), 201–214. https://doi.org/10.1007/S42398-020-00142-W

Patnaik, P., Abbasi, T., & Abbasi, S. A. (2017). Prosopis (Prosopis juliflora): Blessing and bane. *Tropical Ecology*, *58*(3), 455–483. https://www.academia.edu/35753856/Prosopis_Prosopis_juliflora_blessing_and_bane

Pavia, D., Lampman, G., & Kriz, G. (2009). Introduction to Spectroscopy; A guide for students of organic

chemistry. In *Thomson Learning* (Third Edit). Thomson Learning. https://doi.org/10.1520/stp37187s

Peng, H., Leng, Y., sciences, J. G.-A., & 2019, undefined. (2019). Electrochemical removal of chromium (VI) from wastewater. *Mdpi.ComH Peng, Y Leng, J GuoApplied Sciences, 2019•mdpi.Com*. https://doi.org/10.3390/app9061156

Poljsak, B., Pócsi, I., & Pesti, M. (2011). Interference of Chromium with Cellular Functions. *Cellular Effects of Heavy Metals*, 59–86. https://doi.org/10.1007/978-94-007-0428-2_3

Poustie, A., Yang, Y., Verburg, P., Pagilla, K., & Hanigan, D. (2020). Reclaimed wastewater as a viable water source for agricultural irrigation: A review of food crop growth inhibition and promotion in the context of environmental change. *Science of the Total Environment*, *739*, 1–43. https://doi.org/10.1016/j.scitotenv.2020.139756

Prauchner, M. J., & Rodríguez-Reinoso, F. (2012). Chemical versus physical activation of coconut shell: A comparative study. *Microporous and Mesoporous Materials*, *152*(March), 163–171. https://doi.org/10.1016/j.micromeso.2011.11.040

Pyrzynska, K. (2019). Removal of cadmium from wastewaters with low-cost adsorbents. *Journal of Environmental Chemical Engineering*, *7*(1), 102795. https://doi.org/10.1016/J.JECE.2018.11.040

Qasaimeh, A., AlSharie, H., & Masoud, T. (2015). A Review on Constructed Wetlands Components and Heavy Metal Removal from Wastewater. *Journal of Environmental Protection*, *06*(07), 710–718. https://doi.org/10.4236/jep.2015.67064

Qasem, N. A. A., Mohammed, R. H., & Lawal, D. U. (2021). Removal of heavy metal ions from wastewater: a comprehensive and critical review. *Npj Clean Water*, *4*(1). https://doi.org/10.1038/s41545-021-00127-0

Qian, Q., MacHida, M., Aikawa, M., & Tatsumoto, H. (2008). Effect of ZnCl2 impregnation ratio on pore structure of activated carbons prepared from cattle manure compost: Application of N 2 adsorption-desorption isotherms. *Journal of Material Cycles and Waste Management*, *10*(1), 53–61. https://doi.org/10.1007/s10163-007-0185-x

Quiñones, I., & Guiochon, G. (1998). Extension of a Jovanovic–Freundlich isotherm model to multicomponent adsorption on heterogeneous surfaces. *Journal of Chromatography A*, *796*(1), 15–40. https://doi.org/10.1016/S0021-9673(97)01096-0

Rahimzadeh, M. R., Rahimzadeh, M. R., Kazemi, S., & Moghadamnia, A. A. (2017). Cadmium toxicity and treatment: An update. *Caspian Journal of Internal Medicine*, *8*(3), 135. https://doi.org/10.22088/CJIM.8.3.135

Rangabhashiyam, S., Anu, N., Giri Nandagopal, M. S., & Selvaraju, N. (2014). Relevance of isotherm models in biosorption of pollutants by agricultural byproducts. *Journal of Environmental Chemical Engineering*, *2*(1), 398–414. https://doi.org/10.1016/J.JECE.2014.01.014

Rashid, R., Shafiq, I., Akhter, P., Iqbal, M. J., & Hussain, M. (2021). A state-of-the-art review on wastewater treatment techniques: the effectiveness of adsorption method. *Environmental Science and Pollution Research*, *28*(8), 9050–9066. https://doi.org/10.1007/s11356-021-12395-x

Ray, S. S., Gusain, R., & Kumar, N. (2020). Effect of reaction parameters on the adsorption. *Carbon Nanomaterial-Based Adsorbents for Water Purification*, 119–135. https://doi.org/10.1016/b978-0-12-821959-1.00006-4

Reddy, N. A., Lakshmipathy, R., & Sarada, N. C. (2014). Application of Citrullus lanatus rind as biosorbent for removal of trivalent chromium from aqueous solution. *Alexandria Engineering Journal*, *53*(4), 969–975. https://doi.org/10.1016/j.aej.2014.07.006

Rehman, K. K., Fatima, F. F., & Waheed, I. I. (2018). *Prevalence of exposure of heavy metals and their impact on health consequences.*

Renu, Agarwal, M., & Singh, K. (2023). Simultaneous removal of heavy metals and dye from wastewater: modelling and experimental study. *Water Science and Technology*, *87*(1), 193–217. https://doi.org/10.2166/wst.2022.410

Roy, A., & Bharadvaja, N. (2021). Efficient removal of heavy metals from artificial wastewater using biochar. *Environmental Nanotechnology, Monitoring and Management*, *16*(August), 100602. https://doi.org/10.1016/j.enmm.2021.100602

Rubalcaba, A., Suárez-Ojeda, M. E., Stüber, F., Fortuny, A., Bengoa, C., Metcalfe, I., Font, J., Carrera, J., & Fabregat, A. (2007). Phenol wastewater remediation: Advanced oxidation processes coupled to a biological treatment. *Water Science and Technology*, *55*(12), 221–227. https://doi.org/10.2166/wst.2007.412

Rzig, B., Guesmi, F., … M. S.-W. S. and, & 2021, undefined. (2006). Modelling and optimization of hexavalent chromium removal from aqueous solution by adsorption on low-cost agricultural waste biomass using response surface. *Iwaponline.ComB Rzig, F Guesmi, M Sillanpää, B HamrouniWater Science and Technology, 2021•iwaponline.Com*, *84*, 552. https://doi.org/10.2166/wst.2021.233

Sabzehmeidani, M. M., Mahnaee, S., Ghaedi, M., Heidari, H., & Roy, V. A. L. (2021). Carbon based materials: a review of adsorbents for inorganic and organic compounds. In *Materials Advances* (Vol. 2, Issue 2, pp. 598–627). https://doi.org/10.1039/d0ma00087f

Saeed, M. U., Hussain, N., Sumrin, A., Shahbaz, A., Noor, S., Bilal, M., Aleya, L., & Iqbal, H. M. N. (2022). Microbial bioremediation strategies with wastewater treatment potentialities – A review. *Science of The Total Environment*, *818*, 151754. https://doi.org/10.1016/J.SCITOTENV.2021.151754

Saha, P., & Paul, B. (2019). Assessment of heavy metal toxicity related with human health risk in the surface water of an industrialized area by a novel technique. *Human and Ecological Risk Assessment: An International Journal*, *25*(4), 966–987. https://doi.org/10.1080/10807039.2018.1458595

Saha, R., Nandi, R., & Saha, B. (2011). Sources and toxicity of hexavalent chromium. *Journal of Coordination Chemistry*, *64*(10), 1782–1806. https://doi.org/10.1080/00958972.2011.583646

Saini, S., Katnoria, J. K., & Kaur, I. (2019). A comparative study for removal of cadmium(II) ions using unmodified and NTA-modified Dendrocalamus strictus charcoal powder. *Journal of Environmental Health Science and Engineering*, *17*(1), 259–272. https://doi.org/10.1007/s40201-019-00345-2

Salam, A., Zambrano, M. C., Venditti, R. A., & Pawlak, J. J. (2021). Hemicellulose and Starch Citrate Chitosan Foam Adsorbents for Removal of Arsenic and Other Heavy Metals from Contaminated Water. *BioResources,Raleigh*, *16*(3), 5628–5645.

Salem, A. I., Okoth, G., & Tho, J. (2011). An approach to improve the separation of solid e liquid suspensions in inclined plate settlers : CFD simulation and experimental validation. *Water Research*, *5*, 1–9. https://doi.org/10.1016/j.watres.2011.04.019

Sarkar, S., Kamilya, D., & Mal, B. C. (2007). Effect of geometric and process variables on the performance

of inclined plate settlers in treating aquacultural waste. *Water Research*, *41*(5), 993–1000. https://doi.org/10.1016/j.watres.2006.12.015

Sattar Ali Khan, A., & Sattar Ali KHAN, A. (2012). Theory of adsorption equilibria analysis based on general equilibrium constant expression. *Turkish Journal of Chemistry*, *36*(2), 219–231. https://doi.org/10.3906/kim-1110-6

Scheufele, F. B., Módenes, A. N., Borba, C. E., Ribeiro, C., Espinoza-Quiñones, F. R., Bergamasco, R., & Pereira, N. C. (2016). Monolayer–multilayer adsorption phenomenological model: Kinetics, equilibrium and thermodynamics. *Chemical Engineering Journal*, *284*, 1328–1341. https://doi.org/10.1016/J.CEJ.2015.09.085

Schmickler, W., & Santos, E. (2010). Adsorption on metal electrodes: principles. *Interfacial Electrochemistry*, 51–65. https://doi.org/10.1007/978-3-642-04937-8_6

Shahid, M. M., Abbas, S. Z., Maqbool, F., Ramirez-Solis, S., Dupont, V., & Mahmud, T. (2021). Modeling of sorption enhanced steam methane reforming in an adiabatic packed bed reactor using various CO2 sorbents. *Journal of Environmental Chemical Engineering*, *9*(5), 105863. https://doi.org/10.1016/J.JECE.2021.105863

Shaji, A., & Zachariah, A. K. (2017). Surface Area Analysis of Nanomaterials. *Thermal and Rheological Measurement Techniques for Nanomaterials Characterization*, *3*, 197–231. https://doi.org/10.1016/B978-0-323-46139-9.00009-8

Shamsudin, M. S., & Shahadat, M. (2019). Cellulose/bentonite-zeolite composite adsorbent material coating for treatment of N-based antiseptic cationic dye from water. *Journal of Water Process Engineering*, *29*(August), 100764. https://doi.org/10.1016/j.jwpe.2019.02.004

Shanmugam, S., & Arabi Mohammed Saleh, M. A. (2016). An overview of research trends in remediation of heavy metal ion from polluted water. *International Journal of PharmTech Research*, *9*(1), 90–96.

Sharma, N., Sodhi, K. K., Kumar, M., & Singh, D. K. (2021). Heavy metal pollution: Insights into chromium eco-toxicity and recent advancement in its remediation. *Environmental Nanotechnology, Monitoring & Management*, *15*, 100388. https://doi.org/10.1016/J.ENMM.2020.100388

Shiel, A. E., Weis, D., & Orians, K. J. (2010). Evaluation of zinc, cadmium and lead isotope fractionation during smelting and refining. *Science of The Total Environment*, *408*(11), 2357–2368. https://doi.org/10.1016/J.SCITOTENV.2010.02.016

Shiferaw, H., Bewket, W., Alamirew, T., Zeleke, G., Teketay, D., Bekele, K., Schaffner, U., & Eckert, S. (2019). Implications of land use/land cover dynamics and Prosopis invasion on ecosystem service values in Afar Region, Ethiopia. *Science of the Total Environment*, *675*, 354–366. https://doi.org/10.1016/j.scitotenv.2019.04.220

Shrestha, R., Ban, S., Devkota, S., Sharma, S., Joshi, R., Tiwari, A. P., Kim, H. Y., & Joshi, M. K. (2021). Technological trends in heavy metals removal from industrial wastewater: A review. *Journal of Environmental Chemical Engineering*, *9*(4). https://doi.org/10.1016/j.jece.2021.105688

Singh Thakur, L., Baghel, R., Sharma, A., Sharma, S., verma, S., Parmar, H., Kumar Varma, A., & Mondal, P. (2023). Simultaneous removal of lead, chromium and cadmium from synthetic water by electrocoagulation: Optimization through response surface methodology. *Materials Today: Proceedings*, *72*, 2697–2704. https://doi.org/10.1016/j.matpr.2022.09.031

Singh, V., Pant, N., Sharma, R. K., Padalia, D., Rawat, P. S., Goswami, R., Singh, P., Kumar, A., Bhandari, P., Tabish, A., & Deifalla, A. M. (2023). Adsorption Studies of Pb(II) and Cd(II) Heavy Metal Ions from Aqueous Solutions Using a Magnetic Biochar Composite Material. *Separations*, *10*(7). https://doi.org/10.3390/separations10070389

Sintayehu, D. W., Dalle, G., & Bobasa, A. F. (2020). Impacts of climate change on current and future invasion of Prosopis juliflora in Ethiopia: environmental and socio-economic implications. *Heliyon*, *6*(8), e04596. https://doi.org/10.1016/j.heliyon.2020.e04596

Smith, B. C. (2011). *Fundamentals of FTIR*. https://ds.amu.edu.et/xmlui/bitstream/handle/123456789/7157/%5BBrian_C._Smith%5D_Fundamentals_of_Fourier_Transform%28BookZZ.org%29.pdf?sequence=1&isAllowed=y

Somma, S., Reverchon, E., & Baldino, L. (2021). Water purification of classical and emerging organic pollutants: An extensive review. *ChemEngineering*, *5*(3). https://doi.org/10.3390/chemengineering5030047

Somyanonthanakun, W., Ahmed, R., Krongtong, V., & Thongmee, S. (2023). Studies on the adsorption of Pb(II) from aqueous solutions using sugarcane bagasse-based modified activated carbon with nitric acid: Kinetic, isotherm and desorption. *Chemical Physics Impact*, *6*(December 2022), 100181. https://doi.org/10.1016/j.chphi.2023.100181

Song, L., Feng, Y., Zhu, C., Liu, F., & Li, A. (2020). Enhanced synergistic removal of Cr(VI) and Cd(II) with bi-functional biomass-based composites. *Journal of Hazardous Materials*, *388*(Vi), 121776. https://doi.org/10.1016/j.jhazmat.2019.121776

Sörme, L. (2002). Sources of heavy metals in urban wastewater in Stockholm. *ElsevierL Sörme, R LagerkvistScience of the Total Environment, 2002•Elsevier*.

Sreedhar, I., & Reddy, N. S. (2019). Heavy metal removal from industrial effluent using bio-sorbent blends. *SN Applied Sciences*, *1*(9), 1–15. https://doi.org/10.1007/s42452-019-1057-4

Subhabrata, R., & Gargi, D. (2020). Adsorption. In *Process Equipment and Plant Design* (pp. 351–384). Elsevier. https://doi.org/10.1016/B978-0-12-814885-3.00012-9

Subramani, A., & Jacangelo, J. G. (2015). Emerging desalination technologies for water treatment: A critical review. *Water Research*, *75*, 164–187. https://doi.org/10.1016/J.WATRES.2015.02.032

Sud, D. (2012). Chelating Ion Exchangers: Theory and Applications. *Ion Exchange Technology I: Theory and Materials*, 373–401. https://doi.org/10.1007/978-94-007-1700-8_10

Swenson, H., Stadie, N. P., & Stadie, N. P. (2019). Langmuir's theory of adsorption: A centennial review. *ACS PublicationsH Swenson, NP StadieLangmuir, 2019•ACS Publications*, *35*(16), 5409–5426. https://doi.org/10.1021/acs.langmuir.9b00154

Taha, M. H., Masoud, A. M., Khawassek, Y. M., Hussein, A. E. M., Aly, H. F., & Guibal, E. (2020). Cadmium and iron removal from phosphoric acid using commercial resins for purification purpose. *Environmental Science and Pollution Research*, *27*(25), 31278–31288. https://doi.org/10.1007/S11356-020-09342-7

Takata, K., & Kurose, R. (2017). Influence of density flow on treated water turbidity in a sedimentation basin with inclined plate settler. *Water Supply*, *17*(4), 1140–1148. https://doi.org/10.2166/WS.2017.012

Teklay, A. (2016). Physiological Effect of Chromium Exposure: A Review. *Int J Food Sci Nutr Diet*, *7*, 1–11.

https://doi.org/10.19070/2326-3350-SI07001

Teng, H., & Yeh, T. S. (1998). Preparation of Activated Carbons from Bituminous Coals with Zinc Chloride Activation. *Industrial and Engineering Chemistry Research*, *37*(1), 58–65. https://doi.org/10.1021/ie970534h

Thanh Nguyen, T., My Loan Phan Thi, T., Nguyen Thi, T., Thich Le, T., Tien Nguyen Thi, C., Huy Nguyen, N., Chi Minh City, H., Trung Ward, L., & Duc District, T. (2023). Adsorption Optimization for the Removal of Cadmium in Water by Aluminum (Hydr)oxide on Cation Exchange Resin. *Current Applied Science and Technology*, *23*(2). https://doi.org/10.55003/cast.2022.02.23.012

Thévenod, F., & Lee, W. K. (2013). Toxicology of Cadmium and Its Damage to Mammalian Organs. *Metal Ions in Life Sciences*, *11*, 415–490. https://doi.org/10.1007/978-94-007-5179-8_14

Tian, Y., Yu, T., Shen, J., Zheng, G., Li, H., & Zhao, W. (2022). Cr release after Cr(III) and Cr(VI) enrichment from different layers of cast iron corrosion scales in drinking water distribution systems: the impact of pH, temperature, sulfate, and chloride. *Environmental Science and Pollution Research*, *29*(13), 18778–18792. https://doi.org/10.1007/s11356-021-15754-w

Tony, M. A. (2022). Low-cost adsorbents for environmental pollution control: a concise systematic review from the prospective of principles, mechanism and their applications. *Journal of Dispersion Science and Technology*, *43*(11), 1612–1633. https://doi.org/10.1080/01932691.2021.1878037

Tosun, I. (2019). Fundamental Mass Transfer Concepts in Engineering Applications. In *Fundamental Mass Transfer Concepts in Engineering Applications*. Taylor & Francis Group. https://doi.org/10.1201/b22432

Touzani, I., El Machrafi, I., Harboul, K., Boudouch, O., Alouiz, I., Hammani, K., Flouchi, R., & Fikri-Benbrahim, K. (2024). Evaluation of Activated Carbons Prepared from Bioprecursors for the Removal of Cadmium and Chromium (VI). *Applied and Environmental Soil Science*, *2024*(1), 8663114.

Tran, H. N., Nguyen, H. C., Woo, S. H., Nguyen, T. V., Vigneswaran, S., Hosseini-Bandegharaei, A., Rinklebe, J., Kumar Sarmah, A., Ivanets, A., Dotto, G. L., Bui, T. T., Juang, R. S., & Chao, H. P. (2019). Removal of various contaminants from water by renewable lignocellulose-derived biosorbents: a comprehensive and critical review. *Critical Reviews in Environmental Science and Technology*, *49*(23), 2155–2219. https://doi.org/10.1080/10643389.2019.1607442

Ugwu, E. I., Othmani, A., & Nnaji, C. C. (2022). A review on zeolites as cost-effective adsorbents for removal of heavy metals from aqueous environment. *International Journal of Environmental Science and Technology*, *19*(8), 8061–8084. https://doi.org/10.1007/S13762-021-03560-3

Ugwu, E. I., Tursunov, O., Kodirov, D., Shaker, L. M., Al-Amiery, A. A., Yangibaeva, I., & Shavkarov, F. (2020). Adsorption mechanisms for heavy metal removal using low cost adsorbents: A review. *IOP Conference Series: Earth and Environmental Science*, *614*(1). https://doi.org/10.1088/1755-1315/614/1/012166

Ukah, B., Egbueri, J., … C. U.-I. J. of, & 2019, undefined. (2019). Extent of heavy metals pollution and health risk assessment of groundwater in a densely populated industrial area, Lagos, Nigeria. *SpringerBU Ukah, JC Egbueri, CO Unigwe, OE UbidoInternational Journal of Energy and Water Resources, 2019•Springer*, *3*(4), 291–303. https://doi.org/10.1007/s42108-019-00039-3

Ukanwa, K. S., Patchigolla, K., Sakrabani, R., & Anthony, E. (2020). Preparation and Characterisation of Activated Carbon from Palm Mixed Waste Treated with Trona Ore. *Molecules (Basel, Switzerland)*,

25(21). https://doi.org/10.3390/MOLECULES25215028

Vázquez-Guerrero, A., Cortés-Martínez, R., Alfaro-Cuevas-villanueva, R., Rivera-Muñoz, E. M., & Huirache-Acuña, R. (2021). CD(II) and PB(II) adsorption using a composite obtained from moringa oleifera lam. cellulose nanofibrils impregnated with iron nanoparticles. *Water (Switzerland)*, *13*(1). https://doi.org/10.3390/w13010089

Vunain, E., Mishra, A. K., & Mamba, B. B. (2016). Dendrimers, mesoporous silicas and chitosan-based nanosorbents for the removal of heavy-metal ions: A review. *International Journal of Biological Macromolecules*, *86*, 570–586. https://doi.org/10.1016/j.ijbiomac.2016.02.005

Wang, H., Zhou, Y., Hu, X., Guo, Y., Cai, X., Liu, C., Wang, P., & Liu, Y. (2020). Optimization of Cadmium Adsorption by Magnetic Graphene Oxide Using a Fractional Factorial Design. *International Journal of Environmental Research and Public Health 2020, Vol. 17, Page 6648*, *17*(18), 6648. https://doi.org/10.3390/IJERPH17186648

Wang, J., & Guo, X. (2020). Adsorption kinetic models: Physical meanings, applications, and solving methods. *Journal of Hazardous Materials*, *390*, 122156.

Werkneh, A. A., Haftu, N. G., & Beyene, H. D. (2014). *Removal of hexavalent chromium from tannery wastewater using activated carbon primed from sugarcane bagasse : Adsorption / desorption studies*. *2*(6), 128–135. https://doi.org/10.11648/j.ajac.20140206.16

WHO. (2011). Water quality for drinking: WHO guidelines. In *World Health Organization*. https://doi.org/10.1007/978-1-4020-4410-6_184

Wise, S. S., Holmes, A. L., & Wise, J. P. (2008). Hexavalent chromium-induced DNA damage and repair mechanisms. *Reviews on Environmental Health*, *23*(1), 39–57. https://doi.org/10.1515/REVEH.2008.23.1.39/MACHINEREADABLECITATION/RIS

Wisniewski, E. (2014). Sedimentation tank design for rural communities in the hilly regions of Nepal. *Journal of Humanitarian Engineering*, *2*(1), 43–54. https://doi.org/10.36479/jhe.v2i1.15

Wu, Z., Ye, X., Liu, H., Zhang, H., Liu, Z., Guo, M., Li, Q., & Li, J. (2020). Interactions between adsorbents and adsorbates in aqueous solutions. *Pure and Applied Chemistry*, *92*(10), 1655–1662. https://doi.org/10.1515/pac-2019-1110

Xu, C., Feng, Y., Li, H., Wu, R., Ju, J., Liu, S., Yang, Y., & Wang, B. (2022). Adsorption of heavy metal ions by iron tailings: Behavior, mechanism, evaluation and new perspectives. *Journal of Cleaner Production*, *344*, 131065. https://doi.org/10.1016/J.JCLEPRO.2022.131065

Y. Bai, B. B. (2009). Removal of Cadmium from Wastewater Using Ion Exchange Resin Amberjet 1200H Columns. *Polish Journal of Environmental Studies*, *18*(6), 1191–1195.

Yang, X., Wan, Y., Zheng, Y., He, F., Yu, Z., Huang, J., Wang, H., Ok, Y. S., Jiang, Y., & Gao, B. (2019). Surface functional groups of carbon-based adsorbents and their roles in the removal of heavy metals from aqueous solutions: A critical review. *Chemical Engineering Journal*, *366*(352), 608–621. https://doi.org/10.1016/j.cej.2019.02.119

Younas, F., Mustafa, A., Ur, Z., Farooqi, R., Wang, X., Younas, S., Mohy-ud-din, W., Hameed, M. A., Abrar, M. M., Maitlo, A. A., Noreen, S., & Hussain, M. M. (2021). Current and Emerging Adsorbent Technologies for Wastewater Treatment: Trends, Limitations, and Environmental Implications. *Water*, *13*(215), 1–25. https://www.mdpi.com/2073-4441/13/2/215/pdf

Youness, E. R., Mohammed, N. A., & Morsy, F. A. (2012). Cadmium impact and osteoporosis: mechanism of action. *Toxicology Mechanisms and Methods*, *22*(7), 560–567. https://doi.org/10.3109/15376516.2012.702796

Zahoor, A., & Rehman, A. (2009). Isolation of Cr(VI) reducing bacteria from industrial effluents and their potential use in bioremediation of chromium containing wastewater. *Journal of Environmental Sciences*, *21*(6), 814–820. https://doi.org/10.1016/S1001-0742(08)62346-3

Zhang, H., Zheng, S., Zhang, X., Duan, S., & Li, S. (2020). Optimizing the inclined plate settler for a high-rate microaerobic activated sludge process for domestic wastewater treatment: A theoretical model and experimental validation. *International Biodeterioration and Biodegradation*, *154*(May), 105060. https://doi.org/10.1016/j.ibiod.2020.105060

Zhao, M., Xu, Y., Zhang, C., Rong, H., & Zeng, G. (2016). New trends in removing heavy metals from wastewater. *Applied Microbiology and Biotechnology*, *100*(15), 6509–6518. https://doi.org/10.1007/S00253-016-7646-X

Zhao, X., Zhang, B., Liu, H., & Qu, J. (2010). Removal of arsenite by simultaneous electro-oxidation and electro-coagulation process. *Journal of Hazardous Materials*, *184*(1–3), 472–476. https://doi.org/10.1016/J.JHAZMAT.2010.08.058

LIST OF PUBLICATIONS

Chintokoma, G.C., Chebude. Y., & Kassahun, S.K (2024). Cd^{2+} removal efficiency of activated carbon from *Prosopis Juliflora*: Optimization of preparation parameters by the Box-Behnken Design of Response Surface Methodology. *Heliyon.* 10(10). https://doi.org/10.1016/j.heliyon.2024.e31357 **(Elsevier)**.

Chintokoma, G.C., Chebude. Y., & Kassahun, S.K., Demesa, A. G., & Koiranen, T. (2024). Sol-gel synthesis of composite adsorbent coating from Prosopis juliflora –activated carbon for simultaneous adsorptive removal of Cd^{2+} and $Cr_2O_7^{2-}$ from wastewater. *AQUA — Water Infrastructure, Ecosystems and Society*, *73*(5), 945–968. https://doi.org/10.2166/aqua.2024.335 **(IWA Publishing)**.

Chintokoma, G.C., Chebude. Y., & Kassahun, S.K., Demesa, A. G., & Koiranen, T. (2024). Synergistic Integration of Inclined Plate Settler (IPS) and Composite Adsorbent Coating (CAC) for the enhanced removal of Cd^{2+} from wastewater. Applied Water Science. **Accepted for Publication (12 September, 2024**. **(Springer)**.

LIST OF CONFERENCES/WORKSHOPS ATTENDED

- Water-Energy-Food (WEF) Nexus Master Class for Southern Africa, Water Net in collaboration with the University of KwaZulu-Natal, July 27-29, 2021, Open online course
- Groundwater: making the invisible visible, World Water Day 2022, Africa Centre of Excellence for Water Management, 22 March 2022, Addis Ababa University Campus, Addis Ababa, Ethiopia
- Research Writing in the Sciences (2022), International Network for Advancing Science and Policy (inasp), 5 April – 16 May 2022, On-line Course
- Water-Energy-Food (WEF) Nexus Winter School for Southern Africa, Water Net in collaboration with the University of KwaZulu-Natal, August 08-12, 2022, Future Africa Campus University of Pretoria, Pretoria, South Africa
- Practice Oriented Research Grant Writing for Early Stage Researchers in Ethiopia (PrO-ReGEStaR), Virtual Seminar, June-October 2022
- Climate Change and Technology Innovation in Hydro-Environmental Engineering, ACEWM, 03 July 2023, Capital Hotel, Addis Ababa Ethiopia
- Workshop on the World Water Day 2024, organized by the Africa Centre of Excellence for Water Management, 22 March 2024, Addis Ababa University Campus, Addis Ababa, Ethiopia
- AfDB Integrated Safeguards System (2023) orientation for the Environmental and Social Safeguards Specialists, African Development Bank (AfDB), 14-19 May 2023, Zanzibar, Tanzania.

LIST OF AWARDS RECEIVED

- Second best Rank in the 4th PhD. Candidates Research Poster exhibition and presentation during the National Workshop and Exhibition for the World Water Day 2024 organized by the ACEWM, 22 March 2024

ANNEXES

ANNEX 1: Published papers

Chintokoma, G.C., Chebude. Y., & Kassahun, S.K (2024). Cd^{2+} removal efficiency of activated carbon from *Prosopis Juliflora*: Optimization of preparation parameters by the Box-Behnken Design of Response Surface Methodology. *Heliyon.* 10(10). https://doi.org/10.1016/j.heliyon.2024.e31357 **(Elsevier)**.

Chintokoma, G.C., Chebude. Y., & Kassahun, S.K., Demesa, A. G., & Koiranen, T. (2024). Sol-gel synthesis of composite adsorbent coating from Prosopis juliflora –activated carbon for simultaneous adsorptive removal of Cd^{2+} and $Cr_2O_7^{2-}$ from wastewater. *AQUA — Water Infrastructure, Ecosystems and Society*, *73*(5), 945–968. https://doi.org/10.2166/aqua.2024.335 **(IWA Publishing)**.

Chintokoma, G.C., Chebude. Y., & Kassahun, S.K., Demesa, A. G., & Koiranen, T. (2024). Synergistic Integration of Inclined Plate Settler (IPS) and Composite Adsorbent Coating (CAC) for the enhanced removal of Cd^{2+} from wastewater. *Applied Water Science*. https://doi.org/10.1007/s13201-024-02292-2 **(Springer Nature)**.

ANNEX 2: Inclined plate settler drawings

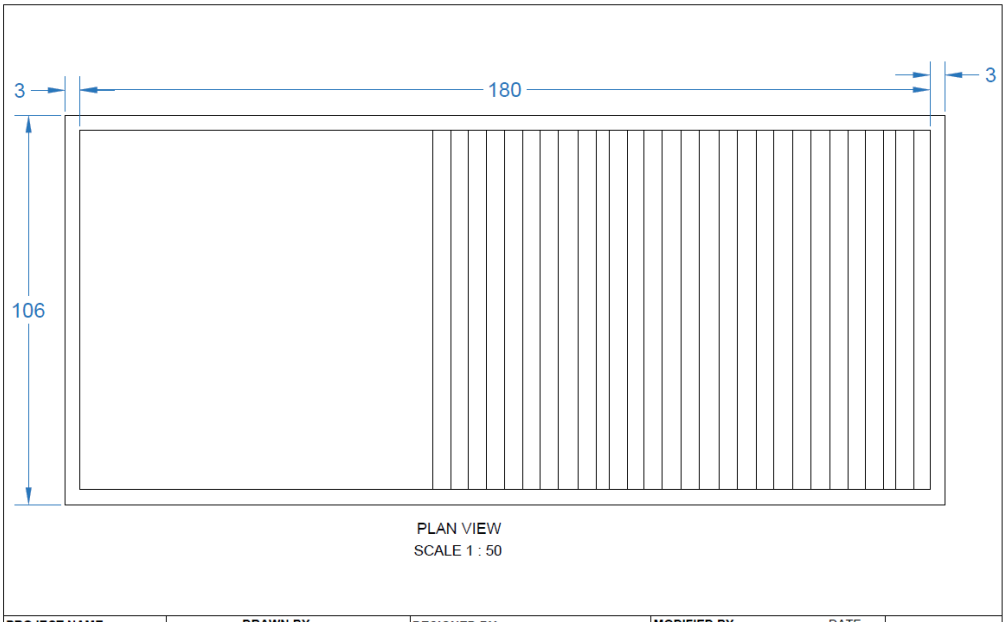

PROJECT NAME SEDIMENTATION TANK 75°	**DRAWN BY** GILBERT CHINTOKOMA	**DESIGNED BY** GILBERT CHINTOKOMA	**MODIFIED BY**	DATE
DRAWING NAME **PLAN VIEW**	**DATE;** 10th JUNE,2023	**DRAWING ID** PTS2023/T.S/2D_A3	**CHECKED BY**	DATE
SCALE : **AS INDICATED**	DRAWING STATUS **FINAL**	**BASE UNIT** MILLIMETER		
SHEET NO; **02**				

Plan view of the 75° angle inclined plate settler

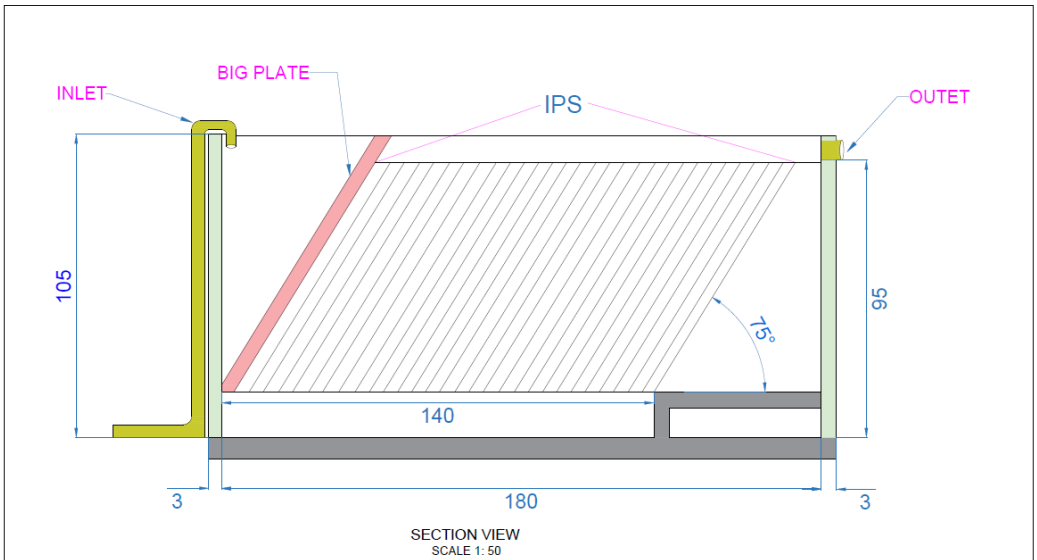

PROJECT NAME SEDIMENTATION TANK 75°	**DRAWN BY** GILBERT CHINTOKOMA	**DESIGNED BY** GILBERT CHINTOKOMA	**MODIFIED BY**	DATE
DRAWING NAME **SECTION VIEW**	**DATE;** 10th JUNE,2023	**DRAWING ID** PTS2023/S.V/2D_A3	**CHECKED BY**	DATE
SCALE : **AS INDICATED**	DRAWING STATUS **FINAL**	**BASE UNIT** MILLIMETER		
SHEET NO; **03**				

Section view of the 75° angle inclined plate settler

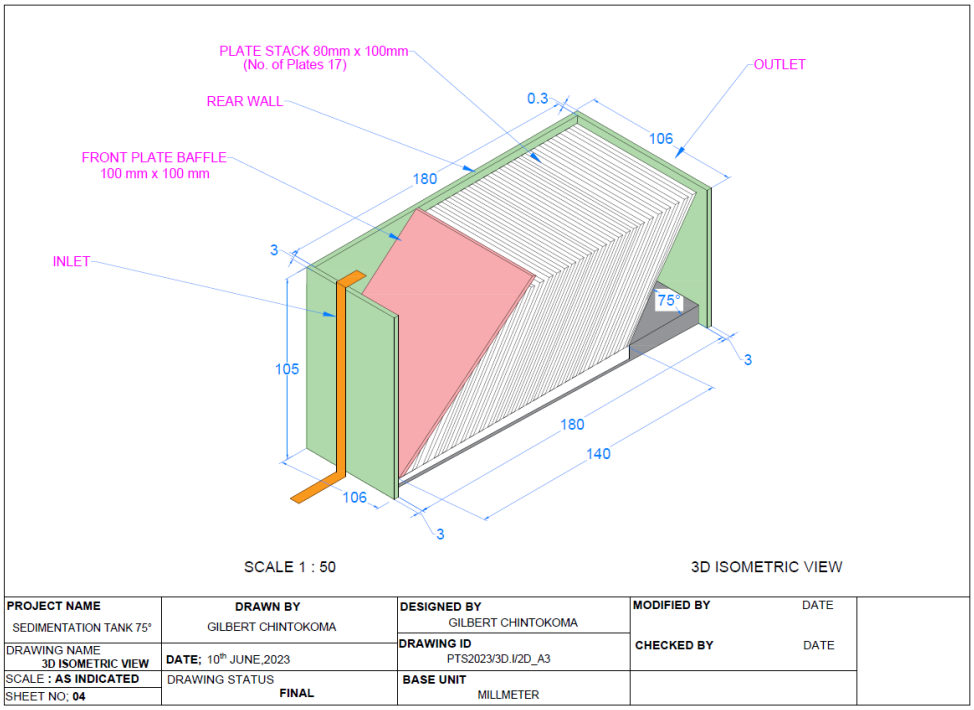

PROJECT NAME SEDIMENTATION TANK 75°	**DRAWN BY** GILBERT CHINTOKOMA	**DESIGNED BY** GILBERT CHINTOKOMA	**MODIFIED BY**	DATE
DRAWING NAME **3D ISOMETRIC VIEW**	**DATE;** 10th JUNE,2023	**DRAWING ID** PTS2023/3D.I/2D_A3	**CHECKED BY**	DATE
SCALE : **AS INDICATED**	DRAWING STATUS **FINAL**	**BASE UNIT** MILLMETER		
SHEET NO; **04**				

3D isometric view of the 75° angle inclined plate settler

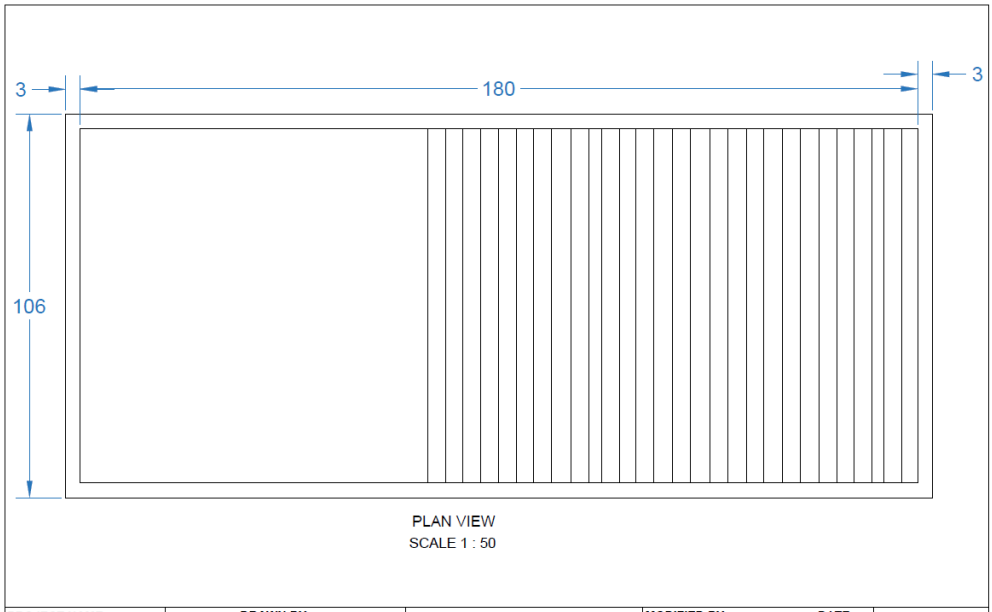

PROJECT NAME SEDIMENTATION TANK 60°	**DRAWN BY** GILBERT CHINTOKOMA	**DESIGNED BY** GILBERT CHINTOKOMA	**MODIFIED BY**	DATE
DRAWING NAME **PLAN VIEW**	**DATE;** 10th JUNE,2023	**DRAWING ID** PTS2023/T.S/2D_A3	**CHECKED BY**	DATE
SCALE : **AS INDICATED**	DRAWING STATUS **FINAL**	**BASE UNIT** MILLIMETER		
SHEET NO; **02**				

Figure 32: Plan view of the 60° angle inclined plate settler

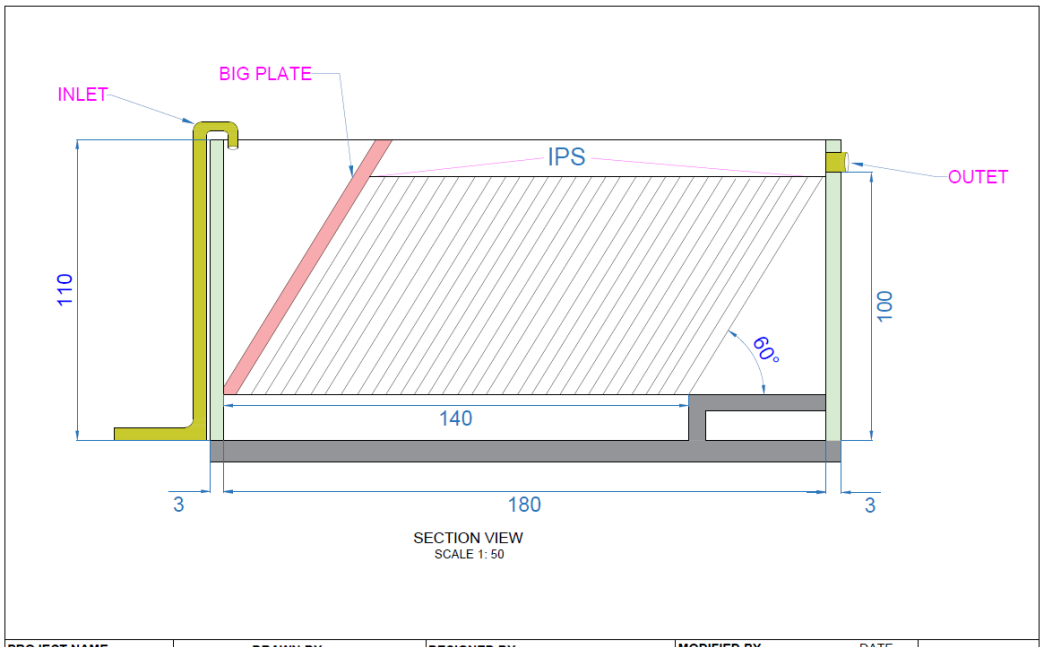

PROJECT NAME SEDIMENTATION TANK 60°	**DRAWN BY** GILBERT CHINTOKOMA	**DESIGNED BY** GILBERT CHINTOKOMA	**MODIFIED BY**	DATE
DRAWING NAME **SECTION VIEW**	**DATE;** 10th JUNE,2023	**DRAWING ID** PTS2023/S.V/2D_A3	**CHECKED BY**	DATE
SCALE : **AS INDICATED**	DRAWING STATUS **FINAL**	**BASE UNIT** MILLIMETER		
SHEET NO; **03**				

Section view of the 60° angle inclined plate settler

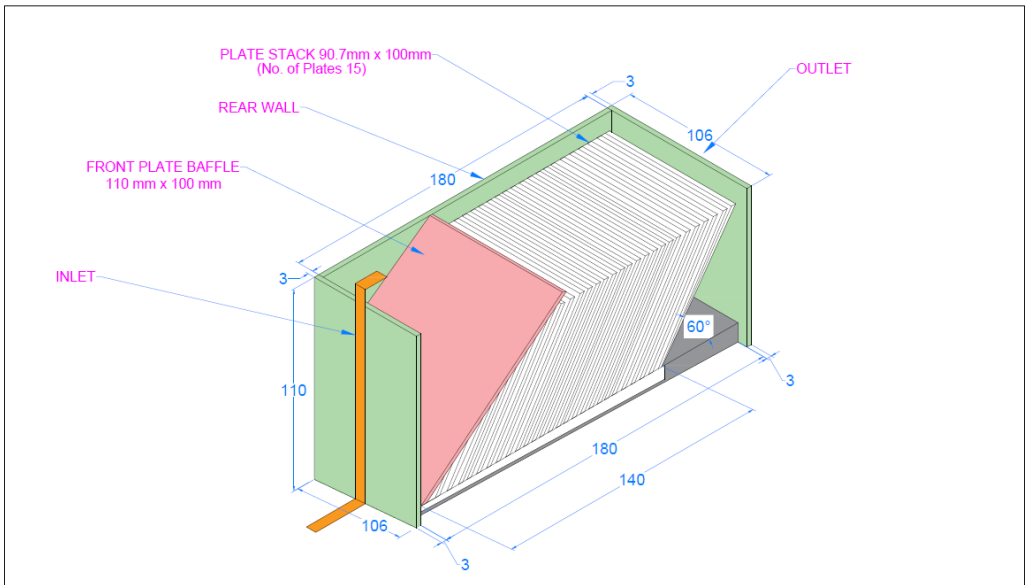

PROJECT NAME SEDIMENTATION TANK 60°	**DRAWN BY** GILBERT CHINTOKOMA	**DESIGNED BY** GILBERT CHINTOKOMA	**MODIFIED BY**	DATE
DRAWING NAME **3D ISOMETRIC VIEW**	**DATE;** 10th JUNE,2023	**DRAWING ID** PTS2023/3D.I/2D_A3	**CHECKED BY**	DATE
SCALE : **AS INDICATED**	DRAWING STATUS **FINAL**	**BASE UNIT** MILLIMETER		
SHEET NO; **04**				

3D isometric view of the 60° angle inclined plate settler

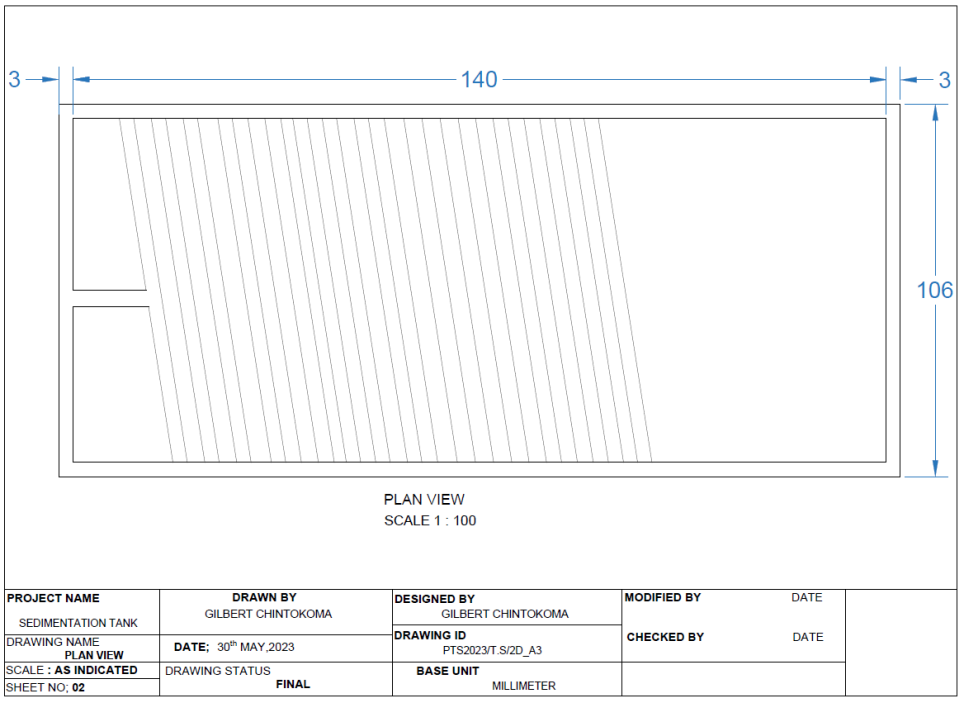

Plan view of the 45° angle inclined plate settler

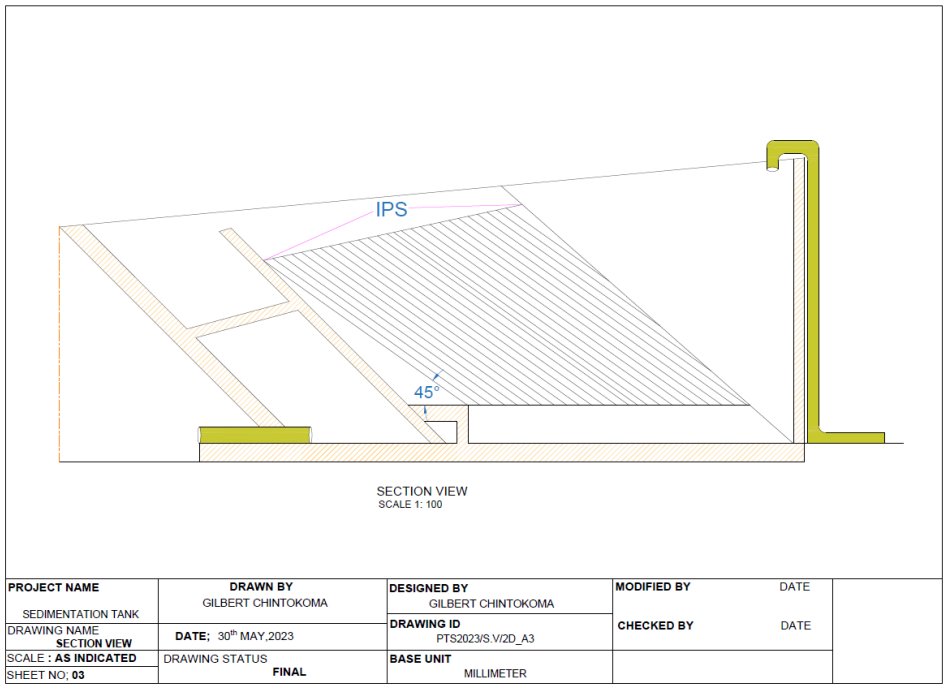

Section view of the 45° angle inclined plate settler

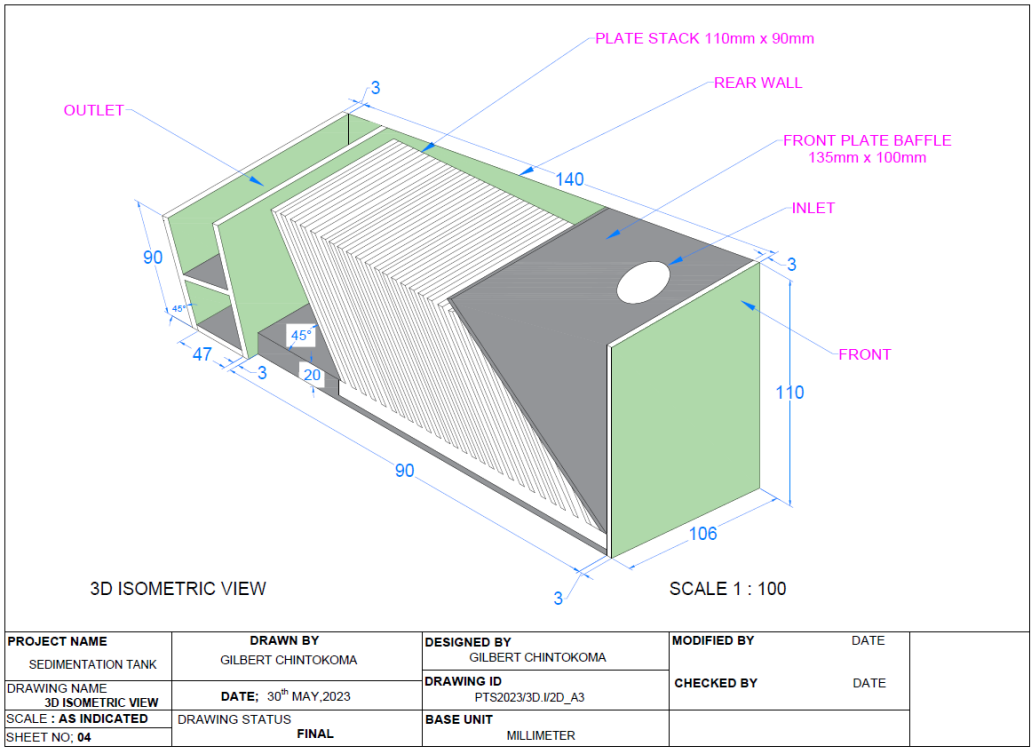

3D isometric view of the 45° angle inclined plate settler

ANNEX 3: Comparative experiment ANOVA results

Notes

Input Data

Descriptive Statistics

	N Analysis	N Missing	Mean	Standard Deviation	SE of Mean
No plane	3	0	2.43333	0.05774	0.03333
Plain plate	3	0	4.63333	0.9815	0.56667
CAC	3	0	66.9	0.1	0.05774

One Way ANOVA

Overall ANOVA

	DF	Sum of Squares	Mean Square	F Value	Prob>F
Model	2	8037.92889	4018.96444	12344.94198	<0.0001
Error	6	1.95333	0.32556		
Total	8	8039.88222			

Null Hypothesis: The means of all levels are equal.
Alternative Hypothesis: The means of one or more levels are different.
At the 0.05 level, the population means are significantly different.

Fit Statistics

R-Square	Coeff Var	Root MSE	Data Mean
0.99976	0.02314	0.57057	24.65556